

**MFN 10-310**

**Enclosure 2**

**ESBWR Licensing Topical Report**

**NEDO-33083 Supplement 2-A Revision 2**

**TRACG APPLICATION FOR ESBWR ANTICIPATED  
TRANSIENT WITHOUT SCRAM ANALYSES**

**Non-Proprietary Version**



**HITACHI**

GE Hitachi Nuclear Energy

NEDO-33083 Supplement 2-A

Revision 2

Class I

DRF 0000-00107-3339

October 2010

**TRACG APPLICATION FOR ESBWR ANTICIPATED  
TRANSIENT WITHOUT SCRAM ANALYSES**

*Copyright 2009 - 2010 GE-Hitachi Nuclear Energy Americas LLC*

*All Rights Reserved*

## **Public Information Notice**

This is a public version of NEDE-33083 Supplement 2P-A, Revision 2, from which the proprietary information has been removed. Portions of the document that have been removed are indicated by white space within double square brackets, as shown here [[ ]].

### **IMPORTANT NOTICE REGARDING CONTENTS OF THIS REPORT**

#### **Please read carefully**

The information contained in this document is furnished as reference to the NRC Staff for the purpose of obtaining NRC approval of the ESBWR Certification and implementation. The only undertakings of GE Hitachi Nuclear Energy (GEH) with respect to information in this document are contained in contracts between GEH and participating utilities, and nothing contained in this document shall be construed as changing those contracts. The use of this information by anyone other than for which it is intended is not authorized; and with respect to any unauthorized use, GEH makes no representation or warranty, and assumes no liability as to the completeness, accuracy, or usefulness of the information contained in this document.

NEDO-33083 Supplement 2-A, Rev. 2

Summary of Changes (NED-33083 Supp 2-A, Rev 2 vs. NED-33083 Supp 2, Rev 2)

Item	Location	Change
1	Cover page	Updated including document number correction
2	Cover page	Author names deleted
3	Acknowledgments page	Page deleted
4	All	“-A” is added to the document number for this revision denoting NRC acceptance of this revision for ESBWR design certification.
5	Attachment 1	Added the NRC letter describing the acceptance of Revision 2 of this Licensing Topical Report . The NRC letter as well as the Final Safety Evaluation for this Licensing Topical Report, has been added to the end of this document.

**SUMMARY OF CHANGES (NED-33083 SUPP 2, REV 2 VS. REV 1)**

Item	Location	Change
1	Cover page	Updated
2	Sections 5.1, 8.1 and 10.0	Updated in response to RAI 21.6-120
3	Tables 3-1, 4.1-1 and 4.2-1	Table headings and Phenomena descriptions updated to be consistent with each other and PIRT rankings updated to be consistent with AOO methodology
4	Sections 8.1, 8.2, and 8.3	MSIV Closure baseline and uncertainty analysis updated to be consistent with latest ESBWR design
4 (a)	Figure 8.1-1b	Added to be consistent with latest MSIVC analysis
4 (b)	Figure 8.1-2b	Added to be consistent with latest MSIVC analysis
4 (c)	Figure 8.1-3b	Added to be consistent with latest MSIVC analysis
4 (d)	Table 8.1-1b	Added to be consistent with latest MSIVC analysis
4 (e)	Figure 8.2-1b	Added to be consistent with latest MSIVC analysis
4 (f)	Tables 8.2-2 and 8.2-3	Updated to be consistent with latest MSIVC analysis
4 (g)	Figures 8.3-1, 8.3-2, 8.3-3 and 8.3-4 Tables 8.3-2, 8.3-3, and 8.3-4	Updated to be consistent with latest MSIVC analysis
5	Table 8.1-3	Updated to be consistent with ESBWR DCD Rev. 6, add dual units, units correction and clarification
6	Section 8.2.3 and Figure 8.2-2	ATWS Stability replaced by ESBWR DCD Rev. 6 analysis
7	Appendix 2	Added a note under title for clarity

**SUMMARY OF CHANGES (NED-33083 SUPP 2, REV 1 VS. REV 0)**

<b>Item</b>	<b>Location</b>	<b>Change</b>	<b>Comment</b>
1	Cover page	Updated	
2	Proprietary Statement	Updated	
3	Acronyms	Added, deleted, and updated	ESBWR deleted as an Acronym.
4	Section 2.8	Added heading for Table 2.8-1. Added comment to the Inadvertent Isolation Condenser Initiation	Editorial change
5	Section 5 and Section 8	Replaced the word GE14 with GE14E in the text	
6	Section 5.1	Boron mixing and transport theoretical analysis moved to Appendix 1	Appendix 1 is new
7	Section 8	<ul style="list-style-type: none"> <li>a) Incorporated ESBWR design changes e.g. increased SRV capacity.</li> <li>b) Corrected analysis input error in feedwater runback modeling related to level setpoint adder Function table in the ATWS TRACG basedecks.</li> <li>c) Analyzed the ATWS LTR cases for the limiting core exposure EOC state point.</li> <li>d) Updated the wetwell and drywell volumes in analysis to be consistent with DCD Tier 2.</li> <li>e) Updated, and larger IC Drain tank inputs used in analysis (consistent with DCD Tier 2).</li> <li>f) Used consistent definition of inputs to define the nominal cases.</li> <li>g) Used appropriate definition of Bounding case: CPR <math>\leq</math>1.2, LHGR <math>&gt;</math>13.4.</li> <li>h) Used appropriate definition of Nominal case: CPR <math>\leq</math>1.3, LHGR <math>&gt;</math>13.4.</li> </ul>	

Item	Location	Change	Comment
8	Section 8.1	<ul style="list-style-type: none"> <li>a) Updated Table 8.1-1 for EOC core exposure. Radial peaking for channel groups changed.</li> <li>b) In Figure 8.1-1 updated axial elevations for Levels 6, 7, and 8 to be consistent with the ATWS basedecks</li> <li>c) Updated Figure 8.1-2 to provide TRACG sector-average bundle power for GE14E EOC core exposure point used in ATWS nominal and bounding analysis.</li> </ul>	<p>Change due to EOC</p> <p>Minor change</p> <p>Updated for EOC</p>
9	Section 8.1.1	<ul style="list-style-type: none"> <li>a) In Table 8.1-2 updated the values for Dome Pressure and Steam/Feed Flow. Added a row for the initial CPR.</li> <li>b) Updated Table 8.1-3 using similar Table in DCD Tier 2, Section 15.5.4. Added a row for the feedwater runback time used in nominal analysis.</li> <li>c) SLCS Delay: total transportation and signal delay time increased to 11 seconds in addition to the 180 seconds timer delay.</li> <li>d) Added a sentence before the MSIVC Summary Table 8.1-5 that the lower PCT results from using initial CPR of 1.3.</li> </ul>	
10	Section 8.1.2	<ul style="list-style-type: none"> <li>a) In Table 8.1-6, LCV Sequence of Events Table, updated timings of ATWS high-pressure signal, feedwater runback initiation, and sorted the rows by event time.</li> <li>b) Added a sentence before the LCV Summary Table 8.1-7 that the lower PCT results from using initial CPR of 1.3.</li> </ul>	
11	Section 8.1.3	<ul style="list-style-type: none"> <li>a) Updated ATWS Performance Requirements, Table 8.1-3.</li> <li>b) The content for Section 8.1.3 has been replaced with the same as that in DCD Tier 2, Section 15.5.4, Loss of Feedwater Heating analysis.</li> </ul>	<p>Incorporates most recent DCD analysis</p>

Item	Location	Change	Comment
12	Section 8.1.4	Revised ATWS depressurization results. The content for Section 8.1.4 came from the verified response to RAI 21.6-4 S01 for MSIV Closure Depressurization, ATWS baseline analysis.	ATWS Depressurization
13	Section 8.2.1, Section 8.2.2	Deleted “% change” in results, as it was unclear (e.g. PCT % change not adding value, and can be derived from the information provided in this Section). Replaced with value of the change.	
14	Section 8.2.3	The content for Section 8.2.3 ATWS Stability Study has been replaced with the limiting stability analysis of Turbine Trip with Full Bypass ATWS with 30% perturbation on void reactivity coefficient for more conservatism. This is consistent with verified and released response to RAI 21.6-51.	ATWS Stability
15	Section 8.3.3	Added Section 8.3.3 to summarize plant parameter sensitivities.  Changed the number of significant digits displayed in Tables 8.3-1, 8.3-2, 8.3-3, and 8.3-4.	New Section 8.3.3
16	Section 9	Expanded and updated the conclusions	
17	Appendix 1	See the row for Section 5.1 above	Appendix 1 is new
18	Appendix 2	Contains responses to NRC RAI 21.6-8 and 21.6-41 (MFN 07-255)	Appendix 2 is new

## ACRONYMS AND ABBREVIATIONS

ABWR	Advanced Boiling Water Reactor
AL	Analytical Limit
AOO	Anticipated Operational Occurrence
ARI	Alternate Rod Insertion
ASME	American Society of Mechanical Engineers
ATWS	Anticipated Transients Without Scram
BOC	Beginning of Cycle
BWR	Boiling Water Reactor
CHF	Critical Heat Flux
CPR	Critical Power Ratio
CSAU	Code Scaling, Applicability, and Uncertainty
CTR	Customer Technical Requirement
DCD	Design Control Document
DCIS	Distributed Control & Information System
dP	Differential Pressure
EBWR	Experimental Boiling Water Reactor
EOC	End of Cycle
EOP	Emergency Operating Procedures
FAPCS	Fuel and Auxiliary Pool Cooling System
FMCRD	Fine Motion Control Rod Drive
FW	Feedwater
FWRB	Feedwater Runback
GE	General Electric Company
GEH	GE Hitachi Nuclear Energy
GE13	GE fuel product line 13
GE14E	GE fuel product line 14E
GESTR	General Electric Stress and Thermal Analysis of Fuel Rods
GEXL	GE Critical Quality Boiling Length Correlation
HCTL	Heat Capacity Temperature Limit
HP CRD	High Pressure Control Rod Drive
IC	Isolation Condenser

LCV	Loss of Condenser Vacuum ATWS Event
LFWH	Loss of Feedwater Heating ATWS Event
LOCA	Loss of Coolant Accident
LTP	Lower Tie Plate
LTR	Licensing Topical Report
MCNP	Monte Carlo Neutral Particle Transport Code
MOC	Middle of Cycle
MSIV	Main Steam Isolation Valve
MSIVC	MSIV Closure ATWS Event
MWth	Mega-Watt Thermal
NRC	United States Nuclear Regulatory Commission
ODYN	One-Dimensional Reactor Dynamics Code
PANAC11	Three-Dimensional BWR Core Steady State Simulator Code, version 11
PANACEA	Three-Dimensional BWR Core Steady State Simulator Code
PCCS	Passive Containment Cooling System
PCT	Peak Cladding Temperature
PDF	Probability Density Function
PIRT	Phenomena Identification and Ranking Table
RCPB	Reactor Coolant Pressure Boundary
RHR	Residual Heat Removal
RMS	Root Mean Square
RPS	Reactor Protection System
RPT	Recirculation Pump Trip
RPV	Reactor Pressure Vessel
RWCU/SDC	Reactor Water Cleanup/Shutdown Cooling System
S/RV	Safety/Relief Valve
SCRRI	Select Control Rod Run-In
SEO	Side Entry Orifice
SER	Safety Evaluation Report
SLCS	Standby Liquid Control System
SRV	Safety Relief Valve
TAF	Top of Active Fuel
TASC	Single Channel Transient Analysis Code

NEDO-33083 Supplement 2-A, Rev. 2

TCV	Turbine Control Valve
TGBLA	Lattice Physics Design Code
TRACG	GEH version of the Transient Reactor Analysis Code

## CONTENTS

<b>1. Introduction.....</b>	<b>1</b>
1.1 Background.....	1
1.2 Summary.....	1
1.3 Scope of Review.....	1
<b>2. Licensing Requirements and Scope of Application .....</b>	<b>2</b>
2.1 10 CFR 50 Appendix A .....	2
2.2 10 CFR 50.62.....	2
2.3 Standard Review Plan Guidelines (NUREG 800).....	3
2.4 Current Implementation and Practices.....	3
2.5 Proposed Application Methodology .....	3
2.5.1 Conformance with CSAU Methodology.....	3
2.5.2 Advantages of TRACG Compared to the Current Process.....	4
2.6 Implementation Requirements.....	4
2.7 Review Requirements For Updates .....	4
2.7.1 Updates to TRACG Code .....	4
2.7.2 Updates to TRACG Model Uncertainties .....	5
2.7.3 Updates to TRACG Application Method.....	5
2.8 ATWS Scenario Specification.....	5
2.9 Nuclear Power Plant Selection.....	8
<b>3. Phenomena Identification and Ranking Tables (PIRT).....</b>	<b>9</b>
<b>4. Applicability of TRACG to ATWS Analyses .....</b>	<b>20</b>
4.1 Model Capability .....	20
4.2 Model Assessment Matrix .....	25
<b>5. Model Uncertainties and Biases.....</b>	<b>37</b>
5.1 Model Parameters and Uncertainties .....	37
5.2 Effects of Nodalization .....	66
5.2.1 Vessel Nodalization for ESBWR ATWS Analysis.....	66
5.2.2 Channel Grouping for ATWS Applications.....	66
5.3 Effects of Scale .....	67
5.3.1 Full Scale Test Coverage .....	67
5.3.2 Operating Plant Data.....	68
5.4 Sensitivity Analysis .....	68
<b>6. Application Uncertainties and Biases.....</b>	<b>69</b>
6.1 Input.....	69

6.2 Initial Conditions .....	69
6.3 Plant Parameters.....	70
<b>7. COMBINATION OF UNCERTAINTIES.....</b>	<b>71</b>
7.1 Approaches for Combining Uncertainties .....	71
7.2 Statistical Analysis for Qualification Events .....	73
<b>8. Demonstration Analysis.....</b>	<b>74</b>
8.1 Baseline Analysis.....	74
8.1.1 MSIV Closure ATWS (MSIVC) Baseline Analysis.....	86
8.1.2 Loss of Condenser Vacuum ATWS (LCV) Baseline Analysis .....	94
8.1.3 Loss of Feedwater Heating ATWS (LFWH) Baseline Analysis .....	100
8.1.4 MSIV Closure Depressurization ATWS Baseline Analysis.....	106
8.2 Initial Condition and Plant Parameter Review.....	113
8.2.1 Initial Conditions.....	113
8.2.1.1 Initial Conditions Sensitivity Results .....	114
8.2.2 Plant Parameters.....	117
8.2.2.1 Plant Parameter Sensitivity Results .....	119
8.2.3 ATWS Stability Study .....	121
8.2.4 Summary of Initial Conditions, Plant Parameters and Stability .....	122
8.2.5 Sensitivity to Azimuthal Sector Size for Boron Injection (RAI 21.6-8).....	122
8.2.6 Sensitivity to Finer Nodalization of the Peripheral Bypass Region (RAI 21.6-41).....	122
8.3 Uncertainty Analysis for Licensing Events .....	123
8.3.1 Uncertainty Screening.....	123
8.3.2 Overall Uncertainty.....	128
8.3.3 Summary of Plant Parameter Sensitivity Study.....	130
<b>9. Conclusions.....</b>	<b>133</b>
<b>10. References.....</b>	<b>133</b>
<b>Appendix 1.....</b>	<b>136</b>
<b>Appendix 2.....</b>	<b>149</b>

**LIST OF FIGURES**

Figure 5.1-1. TGBLA06 Void Coefficient Relative Bias and Relative Standard Deviation for Various Exposures (GWd/MT)..... 41

Figure 5.1-2. Void Fraction Deviations for Toshiba Tests ..... 44

Figure 5.1-3. Sensitivity of TRACG Prediction of Toshiba Void Fraction to PIRT Multiplier on ( $C_o-1$ )..... 45

Figure 5.1-4. Sensitivity of TRACG Prediction of Toshiba Void Fraction to PIRT Multiplier on Entrainment Coefficient,  $\eta$ ..... 45

Figure 5.1-5. Lognormal Probability Distribution for PIRT22 and PIRT52 ..... 46

Figure 5.1-6. FRIGG OF64 Void Fraction Data – Subcooled Boiling..... 48

Figure 5.1-7. Void Fraction Sensitivity to PIRT23..... 48

Figure 5.1-8. Sensitivity of Fuel Center to Fluid Temperature Difference for 8x8 Fuel..... 50

Figure 5.1-9. Sensitivity of Fuel Center to Fluid Temperature Difference for 9x9 Fuel..... 50

Figure 5.1-10. Fractional Error in Modified Zuber Critical Heat Flux Correlation ..... 53

Figure 5.1-11. Fractional Error in Wall Temperature Calculated with the Dittus-Boelter Heat Transfer Coefficient..... 57

Figure 5.1-12. Void Fraction Deviations for Tests Applicable to Regions with Large Hydraulic Diameter..... 60

Figure 5.1-13. Sensitivity of TRACG Prediction of Average Void Fraction in EBWR Test Facility to PIRT Multiplier on Interfacial Drag Coefficient..... 61

Figure 5.1-14. Probability Distribution for Multiplier on Interfacial Drag Coefficient ..... 61

Figure 8.1-1a. TRACG ESBWR Vessel R-Z Modeling..... 76

Figure 8.1-1b. TRACG ESBWR Vessel R-Z Modeling..... 77

Figure 8.1-2a. TRACG Core Map with Sector Average Bundle Power..... 78

Figure 8.1-2b. TRACG Core Map with Sector Average Bundle Power ..... 79

Figure 8.1-3a. TRACG Channel Grouping for ESBWR Core ..... 80

Figure 8.1-3b. TRACG Channel Grouping for ESBWR Core ..... 81

Figure 8.1-4. SR/V Discharge Line and Suppression Pool Nodalization ..... 82

Figure 8.1-5. MSIVC Neutron Flux, Feedwater Flow, and Steam Flow..... 90

Figure 8.1-6. MSIVC Steam and Feedwater Flow, and SRV Flow..... 90

Figure 8.1-7. MSIVC Water Levels..... 91

Figure 8.1-8. MSIVC Dome Pressure and Pool Temperature ..... 91

Figure 8.1-9. MSIVC Neutron Flux and Core Flow..... 92

Figure 8.1-10. MSIVC Reactivity Feedback and Boron Concentration..... 92

Figure 8.1-11. MSIVC HCTL and Pool Temperature Response..... 93

Figure 8.1-12. MSIVC Neutron Flux and Core Average Void.....	93
Figure 8.1-13. LCV Neutron Flux , Feedwater Flow, and Steam Flow .....	96
Figure 8.1-14. LCV Steam and Feedwater Flow, and SRV Flow .....	96
Figure 8.1-15. LCV Water Levels .....	97
Figure 8.1-16. LCV Dome Pressure and Pool Temperature.....	97
Figure 8.1-17. LCV Neutron Flux and Core Flow.....	98
Figure 8.1-18. LCV Reactivity Feedback and Boron Concentration.....	98
Figure 8.1-19. LCV HCTL and Pool Temperature Response .....	99
Figure 8.1-20. LCV Neutron Flux and Core Average Void .....	99
Figure 8.1-21. Loss of Feedwater Heating Neutron Flux, Feedwater Flow, and Steam Flow .....	102
Figure 8.1-22. Loss of Feedwater Heating Steam and Feedwater Flow, and SRV Flow .....	102
Figure 8.1-23. Loss of Feedwater Heating Water Levels .....	103
Figure 8.1-24. Loss of Feedwater Heating Dome Pressure and Pool Temperature.....	103
Figure 8.1-25. Loss of Feedwater Heating Neutron Flux and Core Flow .....	104
Figure 8.1-26. Loss of Feedwater Heating Reactivity Feedback and Boron Concentration .....	104
Figure 8.1-27. Loss of Feedwater Heating HCTL and Pool Temperature Response .....	105
Figure 8.1-28. Loss of Feedwater Heating Neutron Flux and Core Average Void .....	105
Figure 8.1-29a. MSIVC Depressurization Neutron Flux, Feedwater Flow, and Steam Flow .....	109
Figure 8.1-29b. MSIVC Depressurization Steam and Feedwater Flow, and SRV Flow.....	109
Figure 8.1-30. MSIVC Depressurization Water Levels.....	110
Figure 8.1-31. MSIVC Depressurization Dome Pressure and Pool Temperature .....	110
Figure 8.1-32. MSIVC Depressurization Neutron Flux and Core Flow.....	111
Figure 8.1-33. MSIVC Depressurization Reactivity Feedback and Boron Concentration.....	111
Figure 8.1-34. MSIVC Depressurization HCTL and Pool Temperature Response.....	112
Figure 8.1-35. MSIVC Depressurization Neutron Flux and Core Average Void .....	112
Figure 8.2-1a. Relative Axial Power Distribution for Three Exposure State Points .....	115
Figure 8.2-1b. Relative Axial Power Distribution for Three Exposure State Points.....	115
Figure 8.2-2. Core Stability During Turbine Trip with Full Bypass ATWS Event.....	121
Figure 8.3-1. MSIVC –Peak Power Sensitivity .....	124
Figure 8.3-2. MSIVC –Peak Vessel Bottom Pressure Sensitivity .....	125
Figure 8.3-3. MSIVC –Peak Cladding Temperature Sensitivity .....	126
Figure 8.3-4. MSIVC –Peak Pool Temperature Sensitivity .....	127
Figure A1-1. Overall geometry of Injected jets and peripheral Bypass .....	143
Figure A1-2. Channel Geometry and Jet Properties in Cross-section of Injection Locations.....	144

Figure A1-3. Downward Plumes in Annular Space..... 145

Figure A1-4: Boron settling in guide tubes and lower plenum..... 146

Figure A1-5: Liquid temperatures calculated in the bypass region by TRACG at Level 7 (above injection elevation) ..... 147

Figure A1-6. Liquid temperatures calculated in the bypass region by TRACG at Level 5 (Injection Elevation)..... 148

**LIST OF TABLES**

Table 2-1. ESBWR ATWS Categorization ..... 6

Table 3-1. Phenomena That Govern ESBWR ATWS Response..... 12

Table 4.1-1. ESBWR Phenomena and TRACG Model Capability Matrix ..... 21

Table 4.2-1. Qualification Assessment Matrix for ESBWR ATWS Phenomena..... 26

Table 5.1-1. Error Measures for Wall Temperature [Reference 33] and Dittus-Boelter Heat Transfer Coefficient (Estimated)..... 55

Table 5.1-2. Bias and Uncertainty for High Ranked ATWS Model Parameters..... 64

Table 7.1-1 Methods for Combining Uncertainty..... 71

Table 7.1-2 Comparisons of Methods for Combining Uncertainties..... 72

Table 8.1-1a. TRACG Channel Grouping (EOC) ..... 83

Table 8.1-1b. TRACG Channel Grouping (EOC) ..... 84

Table 8.1-2. ATWS Initial Operating Conditions and Initial CPR for Nominal Case ..... 86

Table 8.1-3. ATWS Equipment Performance Characteristics ..... 87

Table 8.1-4. Sequence of Events for MSIVC ..... 88

Table 8.1-5. Key Results from MSIVC ..... 89

Table 8.1-6 Sequence of Events for LCV ..... 94

Table 8.1-7. Key Results from LCV ..... 95

Table 8.1-8. Sequence of Events for Loss of Feedwater Heating..... 100

Table 8.1-9. Key Results from Loss of Feedwater Heating..... 101

Table 8.1-10. Sequence of Events for MSIVC Depressurization ..... 107

Table 8.1-11. Key Results from MSIVC Depressurization ..... 108

Table 8.2-1. Initial Conditions Sensitivity Analysis..... 113

Table 8.2-2. MSIVC Allowable Operating Range Results: Change from Base Case ..... 116

Table 8.2-3. MSIVC Initial Conditions Characterizations ..... 117

Table 8.2-4. MSIVC Plant Parameters ..... 118

Table 8.2-5. MSIVC Plant Parameter Sensitivity Study, Change from Base Case ..... 120

Table 8.3-1. Main Features of the Nominal, and Bounding Cases ..... 129

Table 8.3-2. Nominal and Bounding Cases: Summary..... 130

Table 8.3-3. Summary of Uncertainty Analyses..... 131

Table 8.3-4. Final Results ..... 132

## **ABSTRACT**

This report discusses the application of TRACG, the GE Hitachi (GEH) proprietary version of the Transient Reactor Analysis Code, to analyses of Anticipated Transient Without Scram (ATWS) for ESBWRs. Realistic calculations with TRACG can be used to support licensing evaluations for these transient events. The information presented in this report is an extension to the information submitted for TRACG Application to ESBWR Stability, Anticipated Operational Occurrences (AOOs), Loss Of Coolant Accidents (LOCA) and Containment analysis.

## 1. INTRODUCTION

### 1.1 BACKGROUND

Anticipated operational occurrences are those conditions of normal operation that are expected to occur one or more times during the life of the nuclear power unit. An Anticipated Transient Without Scram (ATWS) is an Anticipated Operational Occurrence (AOO), followed by the failure of the reactor trip portion of the protection system.

GEH ATWS analysis of jet pump BWRs has been performed with ODYN in accordance with Reference 5. The ODYN code along with the TASC code [Reference 9] is used to determine peak vessel pressure and Peak Cladding Temperature (PCT) [Reference 3]. For the suppression pool heat-up, the method includes an energy balance on the suppression pool, considering the Safety/Relief Valve (S/RV) steam flow, Residual Heat Removal (RHR) heat exchanger capacity, initial suppression pool conditions, and service water temperature. The NRC approved the use of TRACG for calculation of ATWS peak vessel pressure in accordance with Reference 8.

Reference 1 provides the licensing basis for the TRACG application to ESBWR LOCA ECCS and Containment Analysis. The U. S. Nuclear Regulatory Commission (NRC) Safety Evaluation Report (SER) for Reference 1 explicitly excluded ATWS and stability from the scope of evaluation.

This report describes an application methodology for ATWS analysis of ESBWR vessel pressure, clad temperature and suppression pool temperature using TRACG consistent with References 1, 8 and 12. As much as possible, this reports references or follows analysis models, nodalization, procedures, tests and qualification, which have previously been submitted or approved by the NRC.

Some areas of ATWS analysis involve phenomena or models that have not been reviewed in the NRC's review of prior TRACG applications. Justification is provided that TRACG can model these phenomena or that the application methodology bounds the phenomenon and the models are qualified by comparisons to tests or alternate methods.

### 1.2 SUMMARY

This document demonstrates the acceptable use of TRACG analysis results for licensing ESBWR power plants within the applicable licensing bases. GEH has provided information to support the use of TRACG as a method of analyzing ESBWR ATWS to provide reasonable assurance that applicable licensing limits are not exceeded.

[[

]]

### 1.3 SCOPE OF REVIEW

GEH requests that the NRC approve TRACG for use in analysis of ESBWR ATWS transients.

## 2. LICENSING REQUIREMENTS AND SCOPE OF APPLICATION

### 2.1 10 CFR 50 APPENDIX A

*Anticipated Transient Without Scram (ATWS)* means an Anticipated Operational Occurrence (AOO) as defined in Appendix A, followed by the failure of the reactor trip portion of the protection system specified in General Design Criterion 20 of Appendix A of 10 CFR 50.

### 2.2 10 CFR 50.62

This section specifies the features required in a BWR to mitigate ATWS. It requires the BWR to have:

- (1) An alternate rod insertion (ARI) system that utilizes sensors and logic which are diverse and independent of the reactor protection system (RPS),
- (2) An automatic standby liquid control system (SLCS) with a minimum capacity equivalent to  $5.42E-3$  m<sup>3</sup>/sec (86 gpm) of 13 weight percent sodium pentaborate decahydrate solution at the natural boron-10 isotope abundance into a 251-inch inside diameter reactor pressure vessel,
- (3) Automatic recirculation pump trip (RPT)

Information must be provided to the NRC to demonstrate that these items are adequate.

ATWS prevention/mitigation features of ESBWR include:

- (1) An ARI system that utilizes sensors and logic which are diverse and independent of the RPS,
- (2) An automatic standby liquid control system (SLCS) with a minimum capacity equivalent to  $5.42E-3$  m<sup>3</sup>/sec (86 gpm) of 13 weight percent sodium pentaborate decahydrate solution at the natural boron-10 isotope abundance into a 251-inch inside diameter reactor pressure vessel,
- (3) Electrical insertion of fine motion control rod drives (FMCRDs) that also utilize sensors and logic which are diverse and independent of the RPS, and
- (4) Automatic feedwater runback under conditions indicative of an ATWS.

10 CFR 50.62 prescribes hardware requirements, rather than acceptance criteria. BWR performance with the required hardware had been shown to meet specific acceptance criteria in Reference 3. Since the ESBWR uses natural circulation, there are no recirculation pumps to be tripped. Hence, no RPT logic is implemented in the ESBWR. Two additional mitigation features are provided, electrical insertion of control rods, which is diverse from the hydraulic scram and ARI, and an ATWS automatic feedwater runback feature.

The purpose of ESBWR ATWS analysis is to demonstrate that the ESBWR mitigation features are adequate with respect to the same criteria used to evaluate the 10 CFR 50.46 hardware requirements for forced recirculation plants in Reference 3. Those criteria are:

Fuel Integrity - The long term core cooling capacity is assured by meeting the cladding temperature and oxidation criteria of 10 CFR 50.46 (i.e. peak cladding temperature not exceeding 1200°C (2200°F), and the local oxidation of the cladding not exceeding 17% of the total cladding thickness).

Primary System – Reactor Pressure Vessel integrity is assured by limiting the maximum primary stress within the reactor coolant pressure boundary (RCPB) to the emergency limits as defined in the ASME Code, Section III.

Containment Integrity - The long term containment capability is assured by limiting the maximum containment pressure to the design pressure of the containment structure and the suppression pool temperature to the wetwell design temperature.

Long-Term Shutdown Cooling - Subsequent to an ATWS event, the reactor shall be brought to a safe shutdown condition, and be cooled down and maintained in a cold shutdown condition.

### **2.3 STANDARD REVIEW PLAN GUIDELINES (NUREG 800)**

The guidelines provided in the Standard Review Plan 15.8, ATWS [Reference 2] predate 10 CFR 50.62.

### **2.4 CURRENT IMPLEMENTATION AND PRACTICES**

The licensing basis analysis of AOs must be performed with an approved model and analysis assumptions. The ODYN code [Reference 5] is accepted by the NRC for use in ATWS analysis. TRACG has model capabilities that exceed those in ODYN and has been qualified against a wider range of data.

NRC Staff Report for ATWS events is described in NUREG-0460 [Reference 10].

[[

]]

### **2.5 PROPOSED APPLICATION METHODOLOGY**

#### **2.5.1 Conformance with CSAU Methodology**

The proposed application methodology using TRACG for ATWS transient analyses considers the elements of the NRC-developed CSAU evaluation methodology [Reference 6]. The code scaling, applicability, and uncertainty (CSAU) report describes a rigorous process for evaluating the total model and plant parameter uncertainty for a nuclear power plant calculation. The rigorous process for applying realistic codes and quantifying the overall model and plant parameter uncertainties

appears to represent the best available practice. While the CSAU methodology was developed for application to Loss-Of-Coolant Accidents (LOCAs), there are no technical reasons that prevent CSAU methodology from being applied to other event scenarios such as ATWS.

[[

]]

### **2.5.2 Advantages of TRACG Compared to the Current Process**

The primary advantage of TRACG over the current process used for ATWS transient analyses is:

[[

]]

## **2.6 IMPLEMENTATION REQUIREMENTS**

The implementation of TRACG into actual licensing analysis is contingent on completion of the following implementation requirements:

- Review and approval by the NRC of the process for analyzing ATWS events described in Section 6, 7 and 8.

## **2.7 REVIEW REQUIREMENTS FOR UPDATES**

In order to effectively manage the future viability of TRACG for ATWS licensing calculations, GEH proposes the following requirements for upgrades to the code to define changes that (1) require NRC review and approval and (2) are on a notification basis only.

### **2.7.1 Updates to TRACG Code**

Modifications to the basic models described in Reference 14 may not be used for ATWS licensing calculations without NRC review and approval.

Updates to the TRACG nuclear methods to ensure compatibility with the NRC-approved steady-state nuclear methods (e.g., PANAC11) may be used for ATWS licensing calculations without NRC review and approval as long as the peak vessel pressure, fuel temperature and suppression pool temperature shows less than 1 sigma deviation difference compared to the method presented in this LTR. A typical ATWS in each of the event scenarios is compared and the result from the comparison is transmitted for information.

Changes in the numerical methods to improve code convergence may be used in ATWS licensing calculations without NRC review and approval.

Features that support effective code input/output may be added without NRC review and approval.

### **2.7.2 Updates to TRACG Model Uncertainties**

New data may become available with which the specific model uncertainties described in Section 5 may be reassessed. If the reassessment results in a need to change specific model uncertainty, the specific model uncertainty may be revised for ATWS licensing calculations without NRC review and approval as long as the process for determining the uncertainty is unchanged.

The nuclear uncertainties (void coefficient and Doppler coefficient) may be revised without review and approval as long as the process for determining the uncertainty is unchanged. The revised uncertainties are used to confirm the conservatism of the calculation. In all cases, changes to model uncertainties made without review and approval is transmitted for information.

### **2.7.3 Updates to TRACG Application Method**

Revisions to the TRACG application method described in Section 7 may not be used for ATWS licensing calculations without NRC review and approval.

## **2.8 ATWS SCENARIO SPECIFICATION**

The events that must be considered for ATWS analysis are the Anticipated Operational Occurrences (AOOs). AOO transient events include:

- (1) Pressurization events, including: turbine trip, load rejection, main steam line isolation valve closure.
- (2) Depressurization events, including: opening of one control or turbine bypass valve.
- (3) Cold water events, including: loss of feedwater heating and inadvertent Isolation Condenser injection.
- (4) Level transient events such as partial or complete loss of feedwater.

Core flow transients do not apply to ESBWR, since the initiating event does not apply to a natural circulation BWR.

The preliminary list of AOOs for ESBWR in Table 4 Reference 20 is considered for determining the limiting ATWS scenario. This list is finalized in the ESBWR Design Control Document (DCD), and is used for the ATWS section of the DCD. Any additions that may affect the limiting ATWS scenarios are considered in the DCD. The ESBWR AOO events are considered in a screening process, to select the most limiting ATWS scenarios. The scenarios are grouped into three categories. The first category includes events that demonstrate ATWS mitigation for the most severe and limiting cases. The uncertainties involved in the analysis of these events are quantified.

The second category has events that are less severe. Results are provided in the safety analysis to demonstrate they are bounded by the category I events, and show the sensitivity of key ATWS parameters. If a category II event is determined to be more severe than a category I event, an additional uncertainty evaluation is provided.

The third category covers the cases that have only minor impact to the reactor vessel and containment. They are discussed briefly in the safety analysis report to justify that they do not significantly influence the design of ATWS mitigation. No calculations are performed for events in the third category. The ATWS scenarios in each category are given below:

**Table 2-1. ESBWR ATWS Categorization**

<b>Abnormal Operational Occurrence</b>	<b>ATWS Severity</b>	<b>Category</b>
Loss of Feedwater Heating	In ESBWR this event is mitigated with Select Control Rod Run-In (SCRRI). Consistent with ATWS failure to scram, this event is evaluated with no SCRRI. This event is included in category I, to determine whether it is limiting for peak clad temperature. Because the turbine bypass valves are available, it is not limiting for vessel pressure or suppression pool temperature.	I
Closure of One Turbine Control Valve	Because other turbine control valves (TCVs) and the bypass valves are available, the pressurization rate is less severe than MSIVC, and the energy addition to the pool is less severe than MSIVC.	III
Generator Load Rejection with Bypass	Because the bypass valves are available, the pressurization rate is less severe than MSIVC. The FW temperature change is similar to MSIVC and the energy addition to the pool is less severe than MSIVC.	III
Generator Load Rejection with a Single Failure in the Turbine Bypass System	Because half of the bypass valves are available, the pressurization rate is less severe than MSIVC, the feedwater (FW) temperature change is similar to MSIVC and the energy addition to the pool is less severe than MSIVC.	II
Turbine Trip with Bypass	Because the bypass valves are available, the pressurization rate is less severe than MSIVC, the FW temperature change is similar to MSIVC and the energy addition to the pool is less severe than MSIVC.	III

<b>Abnormal Operational Occurrence</b>	<b>ATWS Severity</b>	<b>Category</b>
Turbine Trip with a Single Failure in the Turbine Bypass System	Because half of the bypass valves are available, the pressurization rate is less severe than MSIVC, the FW temperature change is similar to MSIVC and the energy addition to the pool is less severe than MSIVC. Because the Generator Load Rejection event with a single failure in the bypass system is similar and a category II, it's evaluation addresses the severity of turbine trip with a single failure in the turbine bypass, and the turbine trip event can be category III.	III
Closure of One Main Steam Isolation Valve	Because three main steam lines are available, the pressurization rate is less severe than MSIVC, and the energy addition to the pool is less severe than MSIVC.	III
Closure of All Main Steam Isolation Valves (MSIVC)	Generic studies have shown that this transient produces high neutron flux, heat flux, vessel pressure, peak cladding temperature, and suppression pool temperature. The maximum values from this event are, in most cases, bounding of all events considered.	I
Loss of Condenser Vacuum	The turbine trips on low condenser vacuum. The bypass valves are available for a short period, and then close on low condenser vacuum. Depending on detailed balance of plant performance the pressurization rate and the energy addition to the pool may be as severe as MSIVC. This event is included in category I to assure the short-term peak vessel pressure and clad temperature remain within limits.	I
Loss of Shutdown Cooling Function of reactor water clean up/shutdown cooling (RWCU/SDC) System	When the reactor is at power, other heat sinks besides RWCU/SDC are available. Loss of RWCU/SDC is only a concern when the reactor is subcritical.	III
Inadvertent Isolation Condenser Initiation	Spurious initiation of the isolation condensers causes a moderator temperature decrease and a slow insertion of positive reactivity into the core. During power operation, the system settles at a new steady state.	III (This is similar/bounded by loss of feedwater heating)

Abnormal Operational Occurrence	ATWS Severity	Category
Runout of One Feedwater Pump	The other FW pumps reduce flow to compensate for the runout pump. This event is expected to be bounded by Loss of Feedwater Heating with SCRRRI failure.	III
Opening of One Control or Turbine Bypass Valve	This event assumes a hydraulic system failure that causes a mild decrease in pressure, which is compensated by the control system closing other valves. The ATWS response is not limiting.	III
Loss of Unit Auxiliary Transformer	The event is expected to result in a fast transfer of the buses and no scram or pressurization.	III
Loss of Grid Connection	The response is similar to Load Rejection with bypass.	II
Loss of All Feedwater Flow	Initially this will cause a reduction in reactor power and pressure. This transient is less severe than the category I events, because the initiating event is one of the ESBWR ATWS mitigation features, FW reduction, which reduces core power. Following MSIVC closure at low water level, there is pressurization that is bounded by the MSIVC ATWS. The energy addition to the pool is less severe than MSIVC, because of the initial power reduction. It is the only event that is mitigated by ARI or FMCRD run-in initiated from the low level signals. It is analyzed in the DCD to show that the low level trips are capable of mitigating the event.	II

[[

]]

A detailed description of these three events is given in Section 8.

## 2.9 NUCLEAR POWER PLANT SELECTION

The included plant type is ESBWR.

### 3. PHENOMENA IDENTIFICATION AND RANKING TABLES (PIRT)

The critical safety parameters, for ESBWR ATWS analyses, are reactor pressure vessel (RPV) pressure, peak fuel clad temperature (PCT), containment pressure and suppression pool temperature. These are the criteria used to judge the performance of the safety systems and the margins in the design. The values of the critical safety parameters are determined by the governing physical phenomena. To delineate the important physical phenomena, it is customary to develop phenomena identification and ranking tables (PIRTs). PIRTs are ranked with respect to their impact on the critical safety parameters. For example, the vessel pressure is determined by the reactor short-term response to an ATWS. The coupled core neutronic and thermal-hydraulic characteristics and the response of mitigation systems govern the vessel pressure, clad and suppression pool temperature transients.

All processes and phenomena that occur during an ATWS do not equally influence plant behavior. The most cost efficient, yet sufficient, analysis reduces all candidate phenomena to a manageable set by identifying and ranking the phenomena with respect to their influence on the critical safety parameters. The phases of the events and the important components are investigated. The processes and phenomena associated with each component are examined. Cause and effect are differentiated. After the processes and phenomena are identified, they are ranked with respect to their effect on the critical safety parameters for the event.

The phenomena identification and ranking tables (PIRTs) represent a consensus of GEH expert opinions. PIRTs are developed with only the importance of the phenomena in mind and are independent of whether or not the model is capable of handling the phenomena and whether or not the model shows a strong sensitivity to the phenomena. For example, two phenomena may be of high importance yet tend to cancel each other in many AOO transient events so that there is little sensitivity to either phenomenon. Both phenomena would be ranked as high importance because the balance between these competing phenomena is important.

Table 3-1 was developed to identify the phenomena that govern ESBWR ATWS responses. In ranking the phenomena, it is helpful to divide the limiting scenarios into phases. The following five phases are defined in an ESBWR ATWS:

- (1) Short-term pressurization, neutron flux increase, and fuel heat up. This phase is similar to the forced circulation plants. Void and Doppler reactivity feedback limit the power increase. Safety valve opening limits the vessel pressure. The important phenomena and uncertainties are the same as References 1, 8 and 13.
- (2) Feedwater runback, water level reduction. This phase is similar to the forced circulation plants. Water level reduction reduces the reactor power. The important phenomena and uncertainties are the same as References 1 and 13.
- (3) Boron injection, mixing and negative reactivity insertion. This phase includes phenomena that were previously included in the Reference 13 PIRT, and applies TRACG boron transport models described in Reference 14.
- (4) Post Shutdown Suppression Pool Heat up. The phenomena involved in this phase are limited to those that affect decay heat and cooling of the suppression pool. The ranking of other

phenomena, which do not occur in this phase are left blank. This phase is of limited importance in ESBWR, because the Isolation Condenser is able to terminate steam flow to the pool once the core is subcritical.

- (5) Depressurization of the reactor. Although the ESBWR EOPs have not been developed at this time, they may direct the operator to depressurize the reactor during an ATWS, and this is considered in ESBWR ATWS analysis. If the suppression pool is calculated to reach the heat capacity temperature limit, the energy added to the pool by manual SRV opening is included in the analysis. The important phenomena and uncertainties are the same as References 1 and 13.

For each event type, the phenomena are listed and ranked for each major component in the reactor system. The ranking of the phenomena is done on a scale of high importance to low importance or not applicable, as defined by the following categories:

- *High importance (H):* These phenomena have a significant impact on the primary safety parameters and are included in the overall uncertainty evaluation. An example of such a parameter would be the *void coefficient* during the short-term pressurization phase (C1AX in Table 3-1). The void coefficient determines the amount of reactivity change due to void collapse during this phase.
- *Medium importance (M):* These phenomena have insignificant impact on the primary safety parameters and may be excluded in the overall uncertainty evaluation. An example of such a parameter would be the *direct moderator heating* during the pressurization, level reduction and boron injection phases (C3DX in Table 3-1). Direct moderator heating deposits some of the core energy in the in-channel and bypass moderator in the initial steady state and during the transient. Its modeling has some effect on the results, but the critical safety parameter is not highly sensitive to modeling uncertainty in this phenomenon
- *Low importance (L) or not applicable (N/A):* These phenomena have no impact on the primary safety parameters and are not considered in the overall uncertainty evaluation. An example of such phenomena would be *Steam Dome Condensation On Walls* during the pressurization phase of an ATWS (K2 in Table 3-1). The maximum energy that could be absorbed in the steam dome metal is a small fraction of the core power, and it could not impact the critical parameters in any significant way.

The PIRT serves a number of purposes. First, the phenomena are identified and compared to the modeling capability of the code to assess whether the code has the necessary models to simulate the phenomena. Second, the identified phenomena are cross-referenced to the qualification basis to determine what qualification data are available to assess and qualify the code models and to determine whether additional qualification is needed for some phenomena. As part of this assessment, the range of the PIRT phenomena covered in the tests is compared with the corresponding range for the intended application to establish that the code has been qualified for the highly ranked phenomena over the appropriate range.

Finally, uncertainties in the modeling of the highly ranked PIRT phenomena are carefully evaluated, and then combined through a statistical process, to arrive at the total model uncertainty. In this third stage, it is shown that some highly ranked phenomena do not contribute significantly to the overall uncertainty even when conservative values for the individual phenomena uncertainties are used. It is at this stage that the analysis determines how individual uncertainties influence the total uncertainty

so that the effort is focused on establishing the uncertainties for those phenomena that have the greatest impact on the critical safety parameters. These uncertainties are more fully developed later in this report and their impact on the critical safety parameters are quantified for each of the transient scenarios.

Phenomena involved in each phase are included in the PIRT. The phenomenon identification and ranking process for ESBWR involved reviewing the PIRTs in References 1, 8 and 13. The definitions of the PIRT parameters are provided in Reference 13, Supplement 1. For ESBWR ATWS evaluation, the following specific definitions are employed:

ATW1 Boron mixing/entrainment between the jets downstream of the injection nozzle.

ATW2 Boron settling in the guide tubes or lower plenum.

ATW3 Boron transport and distribution through the vessel, particularly in the core bypass region.















]]

## 4. APPLICABILITY OF TRACG TO ATWS ANALYSES

The objective of this section is to demonstrate the applicability of TRACG for the analysis of anticipated transient without scram events in ESBWR. To accomplish this purpose, the capability of the TRACG models to treat the highly ranked phenomena and the qualification assessment of the TRACG code for ATWS applications is examined in the next two subsections.

### 4.1 MODEL CAPABILITY

The capability to calculate an event for a nuclear power plant depends on four elements:

- Conservation equations, which provide the code capability to address global processes.
- Correlations and models, which provide code capability to model and scale particular processes.
- Numerics, which provide code capability to perform efficient and reliable calculations.
- Structure and nodalization, which address code capability to model plant geometry and perform efficient and accurate plant calculations.

Consequently, these four elements must be considered when evaluating the applicability of the code to the event of interest for the nuclear power plant calculation. The key phenomena for each event are identified in generating the PIRTs for the intended application, as indicated in Section 3. The capability of the code to simulate these key phenomena is specifically addressed, documented, and supported by qualification in References 11 and 15.

Important BWR phenomena are identified and TRACG models are developed to address these phenomena as indicated in Table 4.1-1.

































## 5. MODEL UNCERTAINTIES AND BIASES

The model biases and uncertainties for all items from the PIRT table (Table 3-1) identified as having a significant impact on the limiting ATWS scenario are evaluated. In Section 5.1, overall model biases and uncertainties for the ATWS application are assessed for each high ranked phenomenon.

The Effect of Nodalization and Effect of Scale are described in Section 5.2 and 5.3.

The uncertainty screening results for the Main Steam Isolation Valve Closure ATWS (MSIVC) event are described in Section 8.3.1.1.

### 5.1 MODEL PARAMETERS AND UNCERTAINTIES

This section discusses the uncertainties associated with each item that has been ranked High for some phase of the ATWS scenario. Past practice has been to evaluate all High and Medium ranked parameters. 31 parameters are ranked High in Table 3.1-1 and 32 are ranked Medium for a total of 63 parameters. Previous experience has shown that the Medium parameters rarely have any impact on the results and serve to dilute the identification of the truly significant parameters. It is expected that only a half dozen or so of the High ranked parameters demonstrate any significant sensitivity. Hence this study is restricted to the High ranked parameters. An estimate of bias and uncertainty for each parameter is obtained by using a combination of comparisons of calculated results to results from: (1) separate-effects test facility data (2) integral test facility test data (3) component qualification test data and (4) BWR plant data. Where data are not available, cross-code comparisons or engineering judgment are used to obtain approximations for the biases and uncertainties. For some phenomena that have little impact on the calculated results, it is appropriate to simply use a nominal value or to conservatively estimate the bias and uncertainty. Table 5.1-2 provides the dispositions of the high ranked ATWS model parameters from Table 4-2. The ID and description are listed for each item.

#### ATW1 Boron Mixing in the Bypass

The Standby Liquid Control System (SLCS) injection is through a header located near the top of the ESBWR downcomer. From the header, spaced equally around the downcomer, are four feeder pipes each of which has four nozzles at different elevations. Each nozzle extends through the shroud wall so that the nozzles discharge directly into the peripheral region of the bypass. The discharge elevations of the nozzles from the four feeder pipes are the same. The lowest injection point is 0.25m above the bottom of the active fuel and the three sets of higher nozzles are spaced at 0.4m intervals. The uppermost nozzle in each of the four banks is approximately at mid-core height (1.45m). Each nozzle has two discharge ports, so the injected liquid forms two jets, pointing at angles estimated to be 60 degrees on either side of a line through the nozzle centerline to the core center and in a horizontal plane at the elevation of the nozzle (Appendix 1, Figure A1.1-1).

APPENDIX 1 contains analysis for:

- a) movement of injected boron through the bypass region,
- b) the initial jet regime,

- c) plumes with negative buoyancy,
- d) spreading of downward plumes,
- e) settling of boron into guide tubes,
- f) settling of boron into the lower plenum from the channel inlet nosepieces,
- g) changes in bypass temperature during the ATWS transient, and
- h) implications for TRACG analysis.

### **B1 Bypass Flashing**

Bypass flashing is controlled by liquid-side interfacial heat transfer in the TRACG model. The bubbly flow regime is the dominant flow regime for this behavior. TRACG uses the Lee-Ryley correlation in conjunction with a bubble diameter based on a critical Weber number for liquid-side heat transfer in the bubbly flow regime [Reference 14]. The Lee-Ryley correlation applies to heat transfer to spherical particles under forced circulation conditions. It predicts the water droplet evaporation data from which it was originally developed with an error less than 10%. There are no experimental data for direct evaluation of the accuracy of the TRACG models for calculation of liquid-side interfacial heat transfer. Following the procedure previously adopted for the AOO application [Reference 12], the uncertainty in the PIRT multiplier on the interfacial heat transfer at the bubble surface is specified as a log-normal probability distribution with a mode of 1 and a gain of 2. This distribution has a standard deviation of 0.25 and imposes an effective cutoff on the multiplier at the extreme values of 0.5 and 2.

### **ATW3 Boron Transport to Core**

See ATW1 discussion.

### **ATW5 Boron Reactivity**

Boron reactivity is modeled in TRACG04 with the assumption that the removal of neutrons in the thermal energy group by B10 can be superposed in an unborated neutron flux spectrum on the other neutron removal mechanisms that are present. The B10 total neutron cross-section is modeled by a  $1/v$  relationship, which provides an excellent approximation to the B10 thermal neutron absorption. In comparison, the B11 neutron absorption cross-section is negligible over the neutron energy range of interest. The expression for the boron absorption cross-section accounts for the effects of fuel temperature and self-shielding by the boron. In order to support the model development, boron cross-sections are evaluated with the GEH lattice physics model (TGBLA06) [[

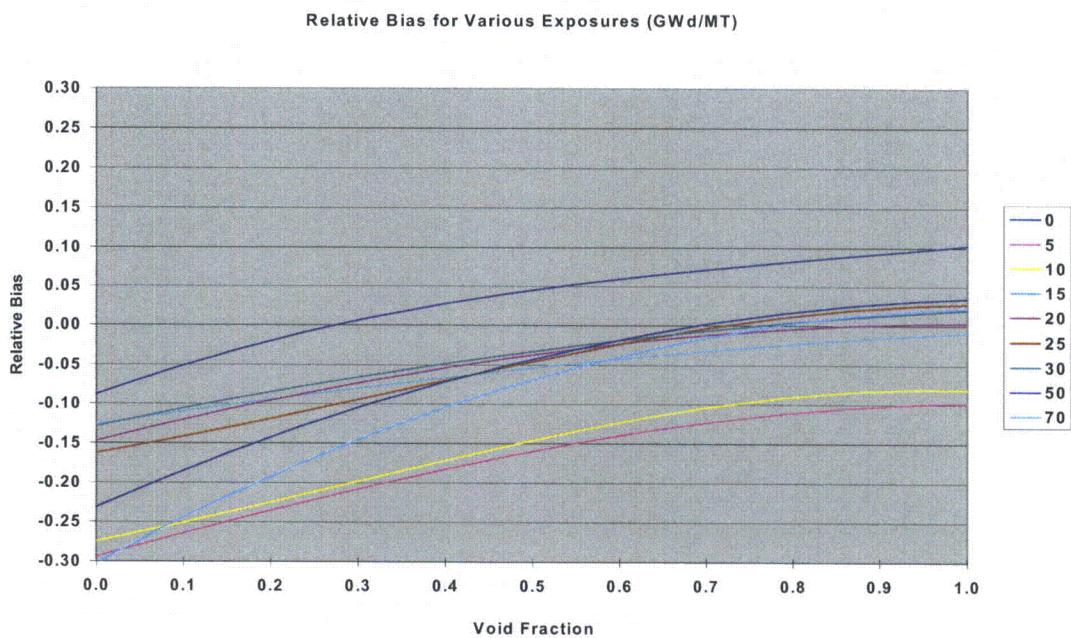
]] The results show that the B10 cross-sections are not sensitive to the void history and that the TRACG modeling error has a weak dependence on the exposure, boron concentration and fuel temperature. Based on these comparisons, the uncertainty in the boron cross-section is estimated to be of the order of [[ ]]. The lattice calculations do not capture the effect of change in neutron spectrum with voids, but the

consistency in the model predictions indicate that the  $1/v$  model captures the effect of the neutron spectrum.

**C1AX Void Coefficient**

[[

]]



[[ ]]

**Figure 5.1-1. TGBLA06 Void Coefficient Relative Bias and Relative Standard Deviation for Various Exposures (GWd/MT)**

### **C1BX Doppler Coefficient**

TRACG uses a 3-D neutron kinetics model based on the PANACEA [Reference 21] neutronic parameters. Fuel temperature affects resonance absorption in uranium and plutonium. This is accounted for by the Doppler coefficient modifying the reactivity for each node. The  $1\sigma$  uncertainty in the Doppler coefficient is [[        ]] [Reference 5].

### **C1DX 3-D Kinetics and Power Shape**

TRACG has a 3-D neutron kinetics model, based on the PANACEA formulation [Reference 21]. The TRACG kinetics model has been qualified against stability data for various BWRs, viz. LaSalle 2, Leibstadt. Steady-state power distribution comparisons have been made with data from several plants [Reference 11] and PANACEA predictions. The uncertainty of the kinetics model is determined by the uncertainty in scram reactivity, void and Doppler coefficient. For ATWS evaluations, the scram reactivity is not relevant.

### **C2AX Interfacial Shear**

Although this PIRT phenomenon is entitled "Interfacial Shear", it more generally concerns representation of the uncertainties of TRACG model parameters that affect the prediction of void fraction in the core and bypass. The core and bypass are distinguished from the regions of the vessel by their comparatively small hydraulic diameters. Two sets of TRACG comparisons with test data are used to define the bias and uncertainty of parameters influencing core and bypass void fraction for ATWS calculations. As described in the AOO application report [Reference 12], data from the FRIGG test facility [Reference 11], which form the basis for the GEH design void correlation, are the most relevant data for pressures within or near the normal operating range. [[

]]

For LOCA and ATWS applications, the database for specifying the void uncertainty is augmented by comparisons of TRACG predictions with a series of low-pressure void fraction tests performed by Toshiba [References 22 and 23]. These tests were conducted with a 16-rod bundle at pressures of 0.50 and 1.00 MPa. A total of 15 tests were run over a range of bundle powers at two mass fluxes. A statistical summary of the deviations between the TRACG predictions and the Toshiba void fraction measurements is shown in Figure 5.1-2. TRACG predicts the Toshiba data with a negligible bias and a standard deviation of [[        ]]. Figure 5.1-2 indicates that it is reasonable to assume that the void fraction deviations are normally distributed.

[[

]]

[[ ]]

**Figure 5.1-2. Void Fraction Deviations for Toshiba Tests**

[[ ]]

**Figure 5.1-3. Sensitivity of TRACG Prediction of Toshiba Void Fraction to PIRT Multiplier on  $(C_o-1)$**

[[ ]]

**Figure 5.1-4. Sensitivity of TRACG Prediction of Toshiba Void Fraction to PIRT Multiplier on Entrainment Coefficient,  $\eta$**

[[

]]

**Figure 5.1-5. Lognormal Probability Distribution for PIRT22 and PIRT52**

**C2BX Subcooled Void Fraction**

The void fraction in the subcooled flow regime is quite insensitive to the magnitude of the heat transfer coefficients at the interface between the bubbles and the subcooled liquid, as long as a reasonable value is used. The void fraction is more sensitive to the liquid enthalpy at which net vapor generation occurs ( $h_{ld}$ ), and to the distribution of the surface heat flux going into vapor generation versus liquid superheat at the wall ( $q''_l$ ). The Saha-Zuber criterion is used for  $h_{ld}$  and the Rouhani-Bowring model is used to calculate the fraction of the wall heat flux to the liquid,  $q''_l$  [Reference 14]. Of these, the void fraction is most affected by  $h_{ld}$ . Reference 24 shows that the scatter in the prediction of the subcooling at the net vapor generation point,  $h_f - h_{ld}$ , can be bounded by  $\pm$  [[ ]]. Comparisons to 8x8 bundle void fraction data show that the larger scatter in the void fraction for low qualities in the subcooled boiling region ([[ ]]) for the fully developed nucleate boiling region) is covered when a [[ ]] perturbation is applied to the subcooling for the onset of net vapor generation. The mean error is also slightly larger for subcooled boiling ([[ ]]). The statistical analysis of the comparison to the subcooled void fraction data is shown in Figure 5.1-6.

A [[ ]] variation in the subcooling for onset of net vapor generation corresponds to an average of [[ ]] and a maximum of [[ ]] variation in the void fraction for the subcooled boiling region. Therefore a  $1\sigma$  uncertainty of [[ ]] is assigned for this model. The impact on the calculated void fraction at the FRIGG test conditions of a PIRT multiplier (PIRT23) value of [[ ]] is seen in Figure 5.1-7.

[[ ]]

**Figure 5.1-6. FRIGG OF64 Void Fraction Data – Subcooled Boiling**

[[ ]]

**Figure 5.1-7. Void Fraction Sensitivity to PIRT23**

### **C3AX Pellet Heat Distribution**

The pellet power distribution is calculated by lattice physics codes and provided as an input to TRACG. Uncertainties in this parameter are reflected in the pellet temperature distribution, which is the parameter for which data are available. [[

]] Sensitivity studies show that the distribution calculated by lattice physics codes provides conservative results compared to a flat power distribution.

### **C3BX Pellet Heat Transfer Parameters**

The TRACG fuel rod model is based on the General Electric stress and thermal analysis of fuel rods (GESTR) model [Reference 25]. The uncertainty in measured fuel centerline to coolant temperature differences is [[ ]] and includes uncertainty in gap size and conductance, pellet conductivity and power distribution. The uncertainties in pellet power distribution, conductivity and gap conductance are lumped into a single uncertainty in the fuel conductivity, in qualifying the overall model against fuel temperature data. The dominant resistance is the pellet conductivity; an [[

]] variation in the pellet conductivity corresponds to the [[ ]] observed uncertainty in the centerline to coolant difference, while the gap conductance needs to be varied by a factor of [[

]] to produce the same variation in the temperature difference as shown in Figure 5.1-8 and Figure 5.1-9. In these figures, PIRT27 is a multiplier on the fuel thermal conductivity and PIRT28 is the multiplier on the gap conductance. When the gap conductance is increased, the resistance over the gap becomes insignificant compared to the thermal resistance of the pellet, and it is not possible to vary the temperature difference to the  $2\sigma$  level needed to produce a 95% probability estimate. Furthermore, normal distribution in the gap conductance would not produce a normal distribution in the center to fluid temperature difference due to the highly non-linear relationship between the gap conductance and the fuel center to fluid temperature difference.

[[

]]

[[

]]

**Figure 5.1-8. Sensitivity of Fuel Center to Fluid Temperature Difference for 8x8 Fuel**

[[

]]

**Figure 5.1-9. Sensitivity of Fuel Center to Fluid Temperature Difference for 9x9 Fuel**

**C3CX Gap Conductance**

[[

]]

**C3 Variable Gap Conductance**

The uncertainty in C3 is covered under C3BX.

**C4 Flashing in Core**

The uncertainty in flashing in the core region is taken into account through the uncertainty in liquid-side interfacial heat transfer. The magnitude of the interfacial heat transfer at the bubble surface is varied through a lognormal probability distribution as described above under B1.

**C8 Multiple Channel Effect**

The flow distribution between parallel flow paths such as the fuel channels in the core is controlled by the hydraulic characteristics of the channels. The flow in each individual channel is controlled by the pressure drop components such as static head (given by the void fraction), friction and accelerational pressure drop. Therefore, the uncertainty in the flow in the individual channels and the parallel channel effects are covered by the uncertainty in the interfacial shear and the friction factors. The uncertainty in the interfacial shear is defined in Item C2AX and the uncertainty in friction factors is defined in Item C24.

In addition to the uncertainty in void fraction and friction, the channel pressure drop is dependent on the channel power level and axial distribution. The modeling of the core is derived from the code qualification studies in Reference 11. [[

]]

**C10 Void Distribution, Axial and Between Channels**

The uncertainty in the void fraction distribution is included through an uncertainty in the interfacial shear. The uncertainty in interfacial shear is defined in Item C2AX.

**C11 Bundle – Bypass Leakage Flow**

The channel leakage flow is based on full-scale measurements for conditions covering the range of expected reactor conditions [Reference 26]. [[

]].

### **C12 Natural Circulation Flow**

Natural circulation is controlled by a balance between buoyancy and friction. Therefore, the uncertainty in this phenomenon is covered by the uncertainty in interfacial shear (which determines the void fractions) and the uncertainty in the friction factors and form losses. The uncertainty in interfacial shear is defined in Items C2AX, E2 and F1, and the uncertainty in frictional losses is defined in Items A11, C24 and I3.

### **C13 Dryout (Steady State and Transient Effects)**

Dryout is calculated to occur when the critical power/quality is exceeded; rewet occurs if critical power/quality is no longer exceeded and the wall temperature is below the minimum film boiling temperature  $T_{\min}$  (C20). Critical power/quality is calculated with the GE critical quality boiling length correlation (GEXL) or the modified Zuber or Biasi critical heat flux (CHF) correlations, depending on the flow conditions. The manner in which these correlations are employed depends on the direction of the liquid and vapor flows. For cocurrent upflow, the GEXL correlation is used for critical power. For countercurrent flow and cocurrent downflow, CHF is calculated with either the modified Zuber or Biasi correlation, depending on mass flux. In practical terms, the Biasi correlation is used in very limited circumstances involving high flow conditions.

The GEXL correlation is derived from full-scale ATLAS data. The correlation typically has a small bias and a standard deviation between 3 and 4% depending on fuel type. [[

]] The uncertainty is applied with a normal distribution.

An uncertainty in the modified Zuber correlation is derived by comparisons with the CHF data of Walkush [Reference 28]. Walkush obtained CHF data for flow through a vertical annulus with a heated inner ring. The measurements included tests with countercurrent flow and cocurrent upflow and downflow. The CHF data is correlated vs. exit void fraction for void fractions ranging from 10 to 70%. The distribution of the fractional deviations between the modified Zuber correlation and the Walkush measurements is shown in Figure 5.1-10. The deviations are well represented by a normal distribution with a conservative bias of [[

]]

[[

]]

**Figure 5.1-10. Fractional Error in Modified Zuber Critical Heat Flux Correlation**

Reference 14 presents information from a number of sources on comparisons between the Biasi CHF correlation and experimental data. The root mean square (RMS) error in the correlation with respect to the database from which it was originally derived is reported to be 7.3% [Reference 29]. Comparison of the Biasi correlation with 1928 data points from a Harwell round-tube data bank [Reference 30] gave a bias of -8% and a standard deviation of 17%. Comparison of the correlation with experimental points from a number of other data banks [Reference 31] shows that 73% and 99% of the data is within 30% of the correlation for constant dryout quality and constant inlet subcooling, respectively. On the basis of this collection of data comparisons, a [[  
 ]] is specified for the Biasi correlation.

**C15 Film Boiling (Dispersed Flow)**

Heat transfer for film boiling under dispersed flow conditions is calculated in TRACG with the Sun-Gonzalez-Tien heat transfer coefficient. The uncertainty in the Sun-Gonzalez-Tien heat transfer coefficient is assumed to be the same as the uncertainty in the Dittus-Boelter heat transfer coefficient for steam cooling conditions (C17). A second parameter influencing heat transfer under dispersed flow conditions is vapor side interfacial heat transfer. As in the case of liquid-side interfacial heat transfer (A1), TRACG uses the Lee-Ryley correlation in conjunction with a droplet diameter based on a critical Weber number to calculate vapor-side interfacial heat transfer in the dispersed flow regime [Reference 14]. [[

]]

**C17 Steam Cooling (H)**

TRACG calculates heat transfer to superheated steam with the Dittus-Boelter heat transfer coefficient [Reference 14]. An extensive investigation of heat transfer to superheated steam in a rod bundle is presented in Reference 33. Reference 33 describes a series of steady-state tests over a pressure range from 13.1 to 40.7 bar and a mass flux range from 33.9 to 169.6 kg/m<sup>2</sup>-s. The tests are conducted on an interior-peaked rod bundle with an outlet-peaked axial heat flux profile. Measured rod temperatures are compared with predictions based on several heat transfer coefficients including Dittus-Boelter. Two approaches are used to calculate the local steam temperature for the predictions - a bundle average approach and an extended rod-centered subchannel approach. The bundle average approach results in a non-conservative bias of about [[ ]] in the predicted wall temperatures. The extended rod-centered subchannel approach results in a conservative bias of slightly over [[ ]]. The RMS error in the predictions was [[ ]] for the bundle average approach and [[ ]] for the extended rod-centered subchannel approach. Combining the RMS error with the mean bias gives a standard deviation of about [[ ]] for both approaches. These results are summarized in the "Wall Temperature" columns of Table 5.1-11.

**Table 5.1-1. Error Measures for Wall Temperature [Reference 33] and Dittus-Boelter Heat Transfer Coefficient (Estimated)**

Error Measure	Bundle Average		Extended Subchannel	
	Wall Temperature [Reference 33]	Dittus-Boelter HTC (Est.)	Wall Temperature [Reference 33]	Dittus-Boelter HTC (Est.)
Mean bias (%)	[[			

]]

The error on which the statistical evaluation in Reference 33 is based was defined as

$$Error(T) = \frac{T_{w,m} - T_{w,p}}{T_{w,m}}$$

where

$T_{w,m}$  = measured wall temperature

$T_{w,p}$  = predicted wall temperature.

For purposes of TRACG analysis, our interest is in the corresponding error in the heat transfer coefficient, defined as

$$Error(h) = \frac{h_p - h_m}{h_p}$$

It is easily shown that

$$Error(h) = \frac{Error(T)}{1 - \frac{T_s}{T_{w,m}}} \quad \text{where } T_s = \text{steam temperature.}$$

It is obvious from this expression that the fractional error in the predicted heat transfer coefficient can be several times as large as that in the predicted wall temperature.

The data described in Reference 33 include 1935 measurement points. Of these, 60 points from four runs are shown graphically in the report along with the steam temperature calculated by both the

bundle average and extended rod-centered subchannel approaches. On the basis of these 60 points, it is determined that

[[

]]

The average values of the multipliers, determined on the basis of the 60 points for which the data are available, provide the estimates of the mean bias and standard deviation for the Dittus-Boelter heat transfer coefficient as shown in the "Dittus-Boelter HTC" columns of Table 5.1-1

[[

]]

[[ ]]

**Figure 5.1-11. Fractional Error in Wall Temperature Calculated with the Dittus-Boelter Heat Transfer Coefficient**

**C19X  $T_{\min}$  (Minimum Stable Film Boiling Temperature)**

TRACG calculates the minimum film boiling temperature as the maximum of the homogeneous nucleation temperature and the Iloeje correlation [Reference 14]. For the Iloeje correlation, the estimated error in  $T_{\min} - T_{\text{sat}}$  for conditions near those of the database is 10%. For conditions significantly outside the mass flux and quality range of the data, 20% is the recommended uncertainty [Reference 14]. [[

]]

**C24 Core Pressure Drop**

The core pressure drop is composed of static head given by the void fraction, accelerational pressure drop and friction. The uncertainty in the core pressure drop is therefore covered by the uncertainty in the interfacial shear and friction. The uncertainty in interfacial shear is defined in Item C2AX.

TRACG uses the GEH design correlation for the wall friction, [[ ]], is based on extensive

comparisons to rod bundle pressure drop data [Reference 14] from BWR bundles. For single-phase flow in smooth pipes TRACG predicts the pressure drop with an accuracy of [[

]] For two-phase flow, the majority of the comparisons with the correlation have been made for rod bundle data. Data for GE14 10x10 fuel shows a [[

]] Based on this data, it is judged that [[

]] is adequate for all other applications. The components of the flow losses in the fuel bundle and the uncertainty associated with each component are discussed in the following paragraphs.

The side entry orifice (SEO) and lower tie plate frictional pressure drop is based on full-scale measurements for conditions covering typical reactor operating conditions. The inlet orifice is a sharp-edged orifice with a well-defined flow coefficient. The inlet region upstream of the lower tie plate has turning losses and a flow expansion at the inlet. The lower tie plate accounts for approximately one third of the total pressure drop. Reference 14 shows that the typical scatter in the loss coefficient for the lower tie plate is of the order of [[

]] Data from GEH's single-phase pressure drop test facility show that the uncertainty for the combined pressure drop for the side entry orifice and the lower tie plate pressure drop is approximately [[

]], when the entire uncertainty is assigned to the lower tie plate [Reference 12].

[[

]].

The spacer frictional pressure drop is based on full-scale measurements for conditions covering the range of expected reactor conditions. For 9x9 and 10x10 fuel spacers the uncertainty in the pressure drop for the spacers is determined from full-scale ATLAS data and varies from [[

]], depending on bundle type [Reference 12]. The average uncertainty for all fuel designs is of the order of [[

]] [Reference 12].

The upper tie plate frictional pressure drop is based on full-scale measurements for conditions covering the range of expected reactor conditions. For 9x9 and 10x10 fuel upper tie plates, the uncertainty in the pressure drop is [[

]] [Reference 12].

Qualification of TRACG against full-scale bundle pressure drop data from the ATLAS facility for an 8x8 bundle with ferrule spacers shows that TRACG predicts the bundle pressure drop with a bias of [[

]] and a standard deviation of [[

]]. These comparisons for total pressure drop are consistent with the above uncertainties for the side entry orifice, lower tie plate, spacers and upper tie plate.

Based on the preceding discussion, the following approach is adopted.

[[

]].

**E2 Downcomer Void Profile / Two-Phase Level**

The downcomer void fraction is determined by the interfacial drag coefficient,  $C_i$ . An appropriate uncertainty range for  $C_i$  for large hydraulic diameter regions is discussed below under F1. The downcomer two-phase level is an initial condition depending on the plant operating state. The uncertainty in this parameter is discussed in Section 6.

**E7 Feedwater Sparger Uncovery/ Condensation**

Condensation in the downcomer is controlled by liquid-side interfacial heat transfer, which is addressed in the same manner as described under B1.

**F1 Chimney Void Distribution/Two-Phase Level**

The chimney void distribution is controlled by the interfacial drag coefficient,  $C_i$ . An appropriate uncertainty range for  $C_i$  is obtained on the basis of TRACG predictions of void fraction data from separate-effects tests by [[

]]. These data are characterized by their applicability to the prediction of void fraction in regions with relatively large hydraulic diameter. Accordingly, they are used as the basis for defining the uncertainty in interfacial drag in all regions of the reactor except the core and bypass. A statistical summary of the comparisons of TRACG predictions with measurements from these four data sets, combined as a single set of deviations, is shown in Figure 5.1-12. [[

]].

[[

]]. The results are shown in Figure 5.1-13

[[

]].

[[

]]

**Figure 5.1-12. Void Fraction Deviations for Tests Applicable to Regions with Large Hydraulic Diameter**

[[

]]

**Figure 5.1-13. Sensitivity of TRACG Prediction of Average Void Fraction in EBWR Test Facility to PIRT Multiplier on Interfacial Drag Coefficient**

[[

]]

**Figure 5.1-14. Probability Distribution for Multiplier on Interfacial Drag Coefficient**

[[

]].

### **I1 Separator Carryunder**

Separator carryunder affects the core inlet subcooling. Carryunder is calculated by the TRACG separator model. Typical values of carryunder at normal operation are of the order of [[ ]]. An uncertainty of [[ ]] (absolute) bounds the differences between TRACG and separator data and are used as an estimate of the  $1\sigma$  uncertainty in the model.

### **I2 Separator L/A**

The separator inertia (L/A) has a small effect in rapid pressurization events. Reduced inertia increases the severity of the calculated transient. The spiraling liquid film along the separator barrel primarily determines the separator inertia. A 25% variation is representative of the  $1\sigma$  uncertainty in the separator inertia [Reference 12].

### **I3 Separator Pressure Drop**

The loss correlations for the separator pressure drop in TRACG are best fit to two and three stage separator pressure drop data [Reference 11]. 95% of the data falls within [[ ]] of the correlation, which has been implemented into TRACG. 95% corresponds to the  $2\sigma$  level and therefore [[ ]] is a good approximation for the  $1\sigma$  uncertainty in separator pressure drop.

### **L1 Critical Flow through SRV**

The uncertainty in the critical flow model is assessed for TRACG [Reference 11], and a zero bias and a  $1\sigma$  uncertainty of [[ ]] is determined to be appropriate. However, for ATWS application the nameplate capacity of the SRVs is specified and used as a limiting value. This value is not varied in the sensitivity studies.

### **L2X Acoustic Effects in Steamline**

Sudden closure of the turbine stop valves or control valves results in the propagation of a pressure pulse at sonic speed from the valve to the steam dome. (This effect is less severe for the slower closing of the MSIVs). The timing and arrival of the pressure pulse has a significant effect on the severity of the transient. The uncertainty in the sonic propagation speed comes primarily from the carryover of liquid droplets into the steamlines. TRACG uses a bounding assumption of perfect separation of droplets from the steam in the dryer, and therefore evaluates the steam line response

with dry steam. This conservatively maximizes the velocity of sound in the steam line and produces a bounding power peak for the pressurization event.

**Q2 Isolation Condenser (IC) Tube Side Condensation Capacity, H; Q5 IC Secondary Side Heat Transfer, H**

In the TRACG analysis, the heat removal output from each IC train under normal operating pressure is assured to be equal to or less than 33.75 (Mega-Watt thermal) MWth, which is the minimum design heat removal capacity for each IC unit (Table 5.4-1 in Reference 39). Periodic technical specification surveillance requirements (Chapter 16 in Reference 39) provide assurance that each IC train is capable of removing the required heat load. Also, the ESBWR ITAAC, Table 2.4.1-3 of Reference 38, requires that the acceptance criterion for the IC system heat removal capacity for each IC train is greater than or equal to 33.75 MWth for the reactor at or above normal operating pressure.





## 5.2 EFFECTS OF NODALIZATION

The nodalization strategy for the various reactor components was developed from the qualification of TRACG against test data for these components. The same consistent nodalization strategy was then applied for full-scale plant calculations. The adequacy of the nodalization has been demonstrated and supported by sensitivity studies. Standard nodalization for modeling of BWR reactor vessels and other components have been presented in the TRACG Qualification Report [Reference 11].

The nodalization for ATWS is the same as that used for ESBWR stability [Reference 19]. [[

]].

### 5.2.1 Vessel Nodalization for ESBWR ATWS Analysis

Figure 8.1-1 shows the axial and radial nodalization of the ESBWR vessel. The axial levels and radial rings are the same as used previously for stability analysis for the ESBWR. [[

]]

### 5.2.2 Channel Grouping for ATWS Applications

Individual fuel bundles in the core may be modeled in TRACG as individual channels or may be grouped together into a single TRACG channel component. Because of current code limitations within TRACG on the number of components allowed, it is not possible to model every fuel bundle as a single TRACG channel. Consequently, it is necessary to group or combine individual fuel bundles into thermal hydraulic groups. [[

]]

The channels are grouped based on (a) hydraulic considerations to separate hydrodynamic characteristics and (b) neutron kinetics considerations to separate dynamic power sensitivity characteristics.

The channel grouping accounts for additional TRACG capability in the areas of limiting channel response, peripheral channel grouping, and vessel modeling detail. [[

]]

Figure 8.1-3 shows the typical grouping of channel components for ATWS analysis. [[

]]

### 5.3 EFFECTS OF SCALE

Effects of scale are specifically addressed as part of the model development as well as the qualification. In the TRACG model description report [Reference 14], the ranges of applicability of the basic models and correlations are stated and shown to cover the scale and operating range of BWRs [Table 6.0-1 of Reference 14]. This is a *necessary* condition for the validity of TRACG calculations for the full-scale BWR.

The qualification of TRACG [Reference 11] covers separate-effects tests, full and reduced scale component performance tests, scaled integral system effects tests, and full-scale BWR plant tests. Accurate predictions of data at various scales (up to a sufficiently large scale) constitute a *sufficient* condition for the validity of TRACG calculations for full-scale plants. In general, the qualification results show that both data from scaled test facilities as well as full-scale plant data are well predicted, and that there is no apparent effect of scale in the TRACG calculations.

The conclusion that there is no effect of scale in the TRACG calculations is substantiated in this section.

#### 5.3.1 Full Scale Test Coverage

Table 3.2 shows the coverage of the Medium and High ranked PIRTs for ATWS by test data. A number of ESBWR components have been tested at full scale. [[

]]

### **5.3.2 Operating Plant Data**

Tests performed at BWR plants validate a number of phenomena that are highly ranked for ATWS.

[[

]]

In summary, TRACG is validated over a range of test data and no additional uncertainty is needed to account for scale-up effects.

### **5.4 SENSITIVITY ANALYSIS**

Sensitivity studies are performed, varying each highly ranked model parameter from  $-1\sigma$  to  $+1\sigma$ . These results are shown in Section 8. These studies serve to identify the parameters that have the largest impact on the calculated safety parameters (vessel pressure, PCT, containment pressure and suppression pool temperature).

## 6. APPLICATION UNCERTAINTIES AND BIASES

### 6.1 INPUT

Specific inputs for each transient event are specified via internal procedures, which are the primary means used by GEH to control application of engineering computer programs. The specific code input is developed in connection with the Application Licensing Topical Report (LTR), the NRC SER and the development of the application specific procedure. This section is limited to a general discussion of how input is treated with respect to quantifying the impact on the calculated results. As such, it serves as a basis for the development of the application specific procedures.

Code inputs are divided into four broad categories: (1) geometry inputs; (2) model selection inputs; (3) initial condition inputs; and (4) plant parameters. For each type of input, it is necessary to specify the value of the input. A discussion of categories (1) and (2) is contained in Section 6.1 of Reference 1. Since initial conditions and plant parameters are handled slightly differently for ATWS analyses than for AOOs, Section 6.2 and Section 6.3 provide the basis for ATWS initial conditions and plant parameters.

### 6.2 INITIAL CONDITIONS

As described in Section 6.2 of Reference 1 *initial conditions* are those conditions that define a steady-state operating condition. Initial conditions may vary due to the allowable operating range or due to uncertainty in the measurement at a given operating condition. The key plant initial conditions and associated uncertainties are given in Table 8.2-1.

Due to the extremely low probability of the occurrence of an ATWS, the NRC Staff has accepted nominal initial conditions for ATWS analysis. However, as previously mentioned, defining a nominal initial condition is not always straightforward. Consequently, the transients are initiated from the limiting point(s) in the allowed operating domain. Specifically, the impact of a particular initial condition on the results is characterized in the following manner:

- The results are sensitive to the initial condition and a basis for the limiting initial condition cannot be established. Future plant analyses consider the full allowable range of the initial condition.
- The results are sensitive to the initial condition and a basis for the limiting initial condition can be established. Future plant analyses consider the parameter to be at its limiting initial condition.
- The results are not sensitive to the initial condition and a nominal initial condition is assumed for the parameter.

Consistent with past ATWS licensing analyses, initial conditions are not adjusted to account for instrumentation or simulation uncertainties. As demonstrated in Section 8 (see Table 8.2-2), the PCT is sensitive to uncertainties in power, feedwater enthalpy, pressure setpoint and core exposure. The peak power is sensitive only to the core exposure. Other parameters are not significantly affected.

### 6.3 PLANT PARAMETERS

A *plant parameter* is defined as a plant-specific quantity such as a protection system setpoint, valve capacity or stroke time, or a scram characteristic. *Plant parameters* influence the characteristics of the transient response and have essentially no impact on steady-state operation, whereas *initial conditions* are what define a steady-state operating condition.

Due to the extremely low probability of the occurrence of an ATWS, the NRC Staff has accepted nominal plant parameters for ATWS analysis. AOO transient analyses require [Reference 12] application of conservative *analytic limits* for plant parameters. The value of the analytical limit (AL) can be typically related to the plant technical specification as discussed in Section 6.3 of Reference 1. Application of an analytic limit for ATWS overpressure is simpler to apply and less difficult to defend than nominal plant parameters. Analytical limits are applied for the ESBWR ATWS analyses unless it is determined that the sensitivity to a plant parameter is not significant. Table 8.2-4 presents the plant parameters that were examined as part of this study.

GEH procedures for Customer Technical Requirements (CTRs) require that both GEH and the Licensee agree to design input. All critical ATWS plant parameters are reviewed in this manner.

## 7. COMBINATION OF UNCERTAINTIES

### 7.1 APPROACHES FOR COMBINING UNCERTAINTIES

In order to determine the total uncertainty in predictions with a computer code, it is necessary to combine the uncertainties due to model uncertainties (CSAU Step 9), scaling uncertainties (CSAU step 10), and plant condition or state uncertainties (CSAU Step 11). Various methods are used to combine the effects of uncertainties in safety analysis. Section 7.3 of Reference 12 summarizes different methods for combining uncertainties. The approaches described are within the framework of the CSAU methodology, since the CSAU methodology does not prescribe the approach to use. Table 7-1 gives a summary description of different methods of combining uncertainties. Table 7-2 summarizes the pros and cons of each approach.

**Table 7.1-1 Methods for Combining Uncertainty**

Method	Description
Propagation of Errors	Uncertainties in the calculated safety parameters to individual phenomena are evaluated from single perturbations and the overall uncertainty is determined as the square root of the sum of the squares of the individual uncertainties.
Response Surface Technique	Response surface for the safety parameter is generated from parameter perturbations.  Statistical upper bound is determined from the Monte Carlo method using a response surface.
Order Statistics Method - Single Bounding Value (GRS Method)	Monte Carlo method using random perturbations of all important parameters. Sample size defined to yield desired statistical confidence.  Statistical upper bound is determined from most limiting perturbation (for first order statistics).
[[	]]

**Table 7.1-2 Comparisons of Methods for Combining Uncertainties**

<b>Method for Combining Uncertainties</b>	<b>Advantages</b>	<b>Disadvantages</b>
Propagation of Errors	Relatively small number computer runs, when the number of input variables is small. The number of cases is linearly related to the number of input parameter uncertainties considered.	Approximate because it involves linearization.  Necessary either to demonstrate independence of effects of individual uncertainties on responses, or else must include covariances explicitly.
Response Surface	Very precise statistical characterization of results with a large number of Monte Carlo Trials using response surface.  Different distributions can be specified for each input uncertainty.  Independence of the effect of individual input parameters on response is not necessary.	Number of computer runs depends on the response surface model and increases exponentially with the number of input parameter uncertainties considered.  Interactions between input parameters have to be established and considered in the development of the response surface.
Order Statistics (GRS)	The number of random trials is independent of the number of input parameters considered.  The method requires no assumption about the probability density function (PDF) of the output parameter.  It is not necessary to perform separate calculations to determine the sensitivity of the response to individual input parameters.  It is not necessary to make assumptions about the effect on the output of interactions of input parameters.	Since the tolerance limits are based on order statistics, they vary from one set of TRACG trials to another, and these differences may be substantial, especially for small sets of TRACG trials, and particularly if the tolerance bound is the sample extreme.

Method for Combining Uncertainties	Advantages	Disadvantages
[[		]]

**Recommended Approach for Combining Uncertainties**

[[

]]

**7.2 STATISTICAL ANALYSIS FOR QUALIFICATION EVENTS**

Section 7.6 of Reference 12 provides a statistical analysis of selected AOO events. Since there is no ATWS transient event to compare to, these events provide the best possible evaluation of TRACG's accuracy. They provide a general confirmation that the code uncertainty determined by varying PIRT parameters is consistent with the event measurements.

## 8. DEMONSTRATION ANALYSIS

The TRACG performance is demonstrated on the MSIVC, LCV, and LFWH scenarios specified in Section 2.7. This demonstration includes:

- (1) A TRACG baseline analysis for the three category 1 scenarios using an equilibrium core designed for the ESBWR,
- (2) A demonstration of the sensitivity of the transient to initial conditions and plant parameters for the limiting scenario of MSIVC, and
- (3) A demonstration of the sensitivity of the transient to the individual model uncertainties using the limiting scenario of MSIVC.

The analyses provided in this section form the bases for future application of TRACG for the ESBWR. The baseline analysis (Section 8.1) is a demonstration of the process. The initial conditions (Section 8.2.1) and plant parameters (Section 8.2.2) analyses are performed to determine the sensitivity to the critical parameters. Section 8.2.3 contains details of analyses performed to demonstrate core stability during an ATWS event. Section 8.3 presents the analyses performed to quantify the sensitivity of the critical parameters to individual model uncertainties.

### 8.1 BASELINE ANALYSIS

The ESBWR plant has 1132 bundles and a rated thermal power of 4500 MWth. The vessel modeling is illustrated in Figures 8.1-1a and 8.1-1b. The plant has an equilibrium core of GE14E 10x10 fuel. Figures 8.1-2a and 8.2-2b also show the average bundle power in the core sectors utilized in the model for azimuthal nodalization. The bundles in Ring 3 are grouped into two groups, with the bundles with inlet orificing corresponding to the peripheral region having a much lower average power level. Figures 8.1-3a and 8.1-3b illustrate the TRACG core map showing the thermal hydraulic channel groups. The number of channels in each thermal hydraulic group and the peaking factors for each group are shown in Tables 8.1-1a and 8.1-1b. Channel groups are created based on core position, chimney position, orifice geometry, and peaking factor. [[

]]

The model used for the baseline analysis has a simple model of the S/RV discharge line and the suppression pool (see Figure 8.1-4). The pool cooling system is modeled using the TRACG control system.

The SLCS system in the ESBWR consists of two accumulators, each pressurized to 17.2 MPa, which adiabatically expand upon opening the valves to inject the hot shutdown volume of 10.8 m<sup>3</sup> (5.4 m<sup>3</sup> from each accumulator) at an approximate vessel pressure of 8.6 MPa.

The SLCS is modeled using the TRACG control system and a flow velocity profile versus time for the accumulators. The average velocity at the flow nozzles that inject the solution into the bypass region is 30.5 m/s during the first half of the injection.

NEDO-33083 Supplement 2-A, Rev. 2

Based on the velocity versus time profile, the total volume of  $10.8 \text{ m}^3$  is injected at high pressure into the bypass in about 9 minutes. A delay time of 2s for the SLCS valve opening, 1s for distributed control and information system logic delay and a further delay of 4s for the solution to reach the nozzle after initiation are assumed. This is in addition to the 180s delay for SLCS initiation amounting to a total delay of 191 seconds after the start of the transient.



[[

]]

**Figure 8.1-1b. TRACG ESBWR Vessel R-Z Modeling**

[[

]]

[[

]]

[[

]]

**Figure 8.1-3a. TRACG Channel Grouping for ESBWR Core**

[[

]]

**Figure 8.1-3b. TRACG Channel Grouping for ESBWR Core**

[[

]]

**Figure 8.1-4. SR/V Discharge Line and Suppression Pool Nodalization**





The baseline model also has conservatisms included in it to bound model phenomena or certain plant component specifications. [[

]]

**8.1.1 MSIV Closure ATWS (MSIVC) Baseline Analysis**

The main steam isolation valve (MSIV) stroke time for these analyses is set at the minimum value of 3s. ESBWR includes an automated feedwater runback on ATWS signal, to reduce core power. This is modeled through the feedwater level control system. To simulate the FW runback, and Emergency Procedure Guideline actions, the vessel level setpoint is dropped to 1.524m (5') above top of active fuel (TAF) over a period of 15s and maintained at this minimum level through the event. Analyses are performed to ensure that refilling the vessel did not lead to recriticality. The suppression pool cooling model is activated at the set point of 322 K. A hot rod model is included for the four hot channels. In addition, a bundle power peaking is applied to one of the hot channels to operate at a Critical Power Ratio (CPR) of 1.3. Table 8.1-2 presents the initial conditions, Table 8.1-3 presents the equipment performance characteristics as modeled in the baseline analysis, and Table 8.1-4 presents a summary of main events in the transient scenario. This transient scenario corresponds to Figures 8.1-1b, 8.1-2b, 8.1-3b, 8.2-1b and Table 8.1-1b.

**Table 8.1-2. ATWS Initial Operating Conditions and Initial CPR for Nominal Case**

<b>Parameters</b>	<b>Value</b>
Dome Pressure, MPa (psia)	7.17 (1040)
Power, MW	4500
Steam/Feed Flow, kg/sec (Mlbm/hr)	2433 (19.31)
Feedwater Temperature, °C (°F)	215.6 (420)
Initial Suppression Pool Temperature, °C (°F)	43.3 (110)
Initial CPR for nominal case	1.3

**Table 8.1-3. ATWS Equipment Performance Characteristics**

Parameters	Value
Nominal MSIV Closure Time, sec	≥ 3.0
SLC system transportation DCIS logic delay time, sec	≤ 11
Safety/Relief Valve (S/RV) System Capacity, % of Rated Steam Flow / No. of Valves	≥ 102 / 18
High reactor pressure vessel (RPV) Dome pressure setpoint, MPaG (psig)	7.76 (1125)
S/RV Setpoint Range, MPaG (psig)	8.62 to 8.76 (1250-1270)
S/RV Opening Time, sec	< 0.5
Pressure drop below setpoint for SRV closure, % nameplate	≤ 96
Low water level (Level 2) trip setpoint (from vessel bottom reference zero), m (in)	16.05 (631.9)
CRD (High pressure make-up function) Low water level initiation setpoint, m (in)	16.05 (631.9)
CRD (High pressure make-up function) flow rate, m <sup>3</sup> /s (gpm)	0.07 (1035)
ATWS Dome Pressure Sensor Time Constant, sec	≤ 0.5
ATWS Logic Time Delay, sec	≤ 1
Pool Cooling Capacity, KW/°C (Btu/hr)	430.6 (816200)
Non-Regenerative Heat Exchanger Shell Side Water Temperature for Pool cooling, °C (°F)	38.3 (101)
Low water level for closure of MSIVs, cm (in)	1065 (631.9)
Low steamline pressure for closure of MSIVs, MPaG (psig)	5.41 (785)
Temperature For Automatic Pool Cooling, °C (°F)	48.9 (120)
IC Capacity (4 IC units), MWth	135
Feedwater runback time, sec	15

The steam line isolation causes a rapid increase in reactor vessel pressure (see Figure 8.1-8), which results in core void reduction (see Figure 8.1-12). Consequently, power increases (see Figures 8.1-5 and 8.1-12) with positive void reactivity insertion (see Figure 8.1-10). For ATWS simulation purposes, the expected MSIV position, high flux, and high pressure scrams do not occur. The power excursion is initially mitigated by void production from the increased core heat flux, as well as negative Doppler reactivity from increasing fuel temperature. High-pressure signals and average

power range monitor not downscale initiates feedwater runback to minimum flow (see Figures 8.1-5 and 8.1-6). Feedwater runback results in dropping the water level (see Figure 8.1-7), stopping the recirculation of liquid through the steam separators, reducing channel flow (see Figure 8.1-9), increasing core void fraction and reducing power level. The isolation condensers (see Figure 8.1-6) also activate at this point. At about the same time, the Safety/Relief Valves (S/RVs) open (see Figure 8.1-6), reducing the rate of pressure increase. As core flow continues to decrease, core voiding increases, causing the power to decrease in parallel. The pressure peaks and finally, as the steam production decreases to the point at which the S/RV capacity is sufficient to relieve all of the steam generation, and the pressure begins to fall (see Figure 8.1-8). The peak-clad temperature also occurs shortly after the pressure peaks. The pressure drops to about 8.6 MPa and remains at approximately this value until the SLCS initiation. The pressure begins to drop shortly after the boron begins to shut down the reactor.

**Table 8.1-4. Sequence of Events for MSIVC**

<b>Time (s)</b>	<b>Event</b>
0	MSIV Closure starts
0.5	IC initiation
3.8	ATWS trip set at high pressure
3.8	Feedwater runback initiated
5	SRVs open
19	Feedwater runback complete
21	Suppression pool cooling starts
42	Level drops below L2 set point
52	HP CRD flow starts
195	SLCS injection starts
326	Peak Pool Temperature
350	Hot shutdown achieved
715	High pressure design volume of borated solution injected into bypass

At approximately 195s the SLCS flow is activated (see Figure 8.1-10) and the borated solution starts to flow into the bypass. With the external circulation loop cut off by the low water level (see Figure 8.1-7), flow to the fuel channels from the vessel lower plenum matches what is required to makeup for steam generation in the core. The total channel mass flow is higher than this, due to liquid entering from the core bypass through the Lower Tie Plate (LTP) holes. The LTP flow direction is reversed from normal operation. Liquid exiting the top of channels recirculates down the bypass, and re-enters the LTP holes. Because the flow in the bypass is downward under these conditions, the diluted plume of boron moves with the bulk bypass flow. Boron enters the LTP

holes and flow up the channel. [[

]] As boron is transported to the center of the core, the power level drops due to the large negative reactivity insertion (see Figure 8.1-10) and reaches decay heat levels after 119s from the time of injection (power is within half a percent of the decay heat). The timing for the S/RV discharge into the suppression pool is shown in Figure 8.1-6 and the pool temperature peak is shown in Table 8.1-5. This is well below the HCTL limit for the pool at the corresponding dome pressure (see Figure 8.1-11).

Table 8.1-5 summarizes the key results from the baseline analysis of the MSIVC event. The PCT is much lower due to the initial CPR of 1.3 compared with a lower value in the original ATWS LTR.

**Table 8.1-5. Key Results from MSIVC**

<b>Parameter</b>	<b>Value</b>	<b>Time (s)</b>
Maximum Neutron Flux, %	257	3
Maximum Vessel Bottom Pressure, MPaG (psig)	9.34 (1354)	22
Maximum Bulk Suppression Pool Temperature, °C (°F)	71.2 (160.2)	326
Associated Containment Pressure, kPaG (psig)	200 (29.32)	326
Peak Cladding Temperature, °C (°F)	592.9 (1099)	23





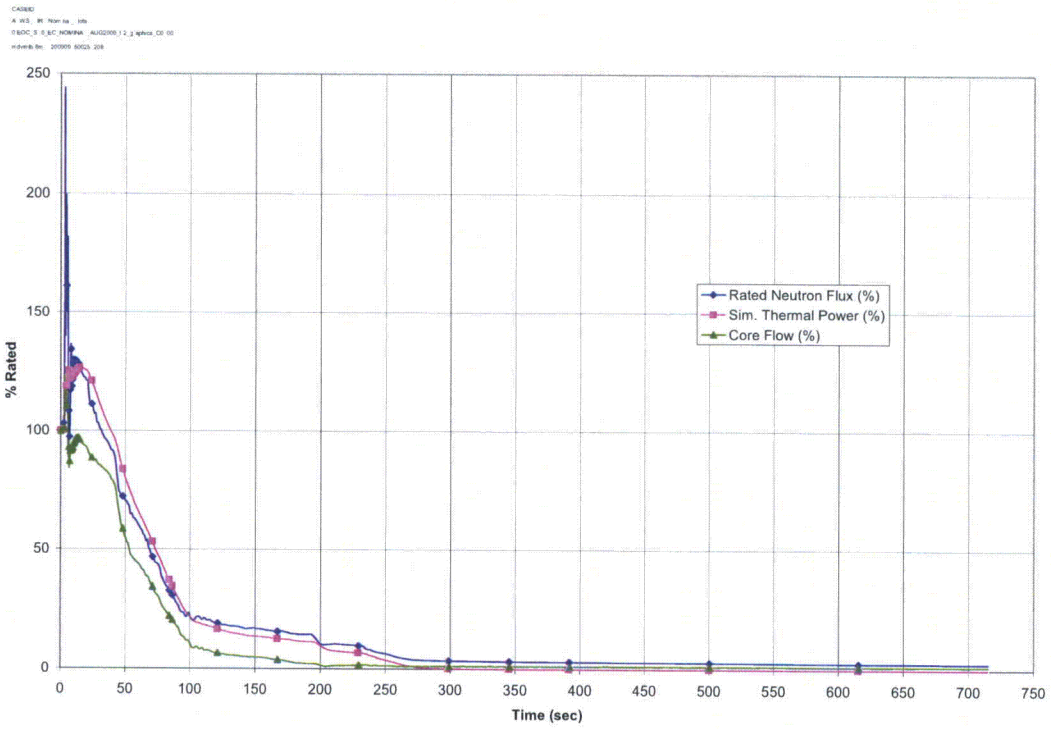


Figure 8.1-9. MSIVC Neutron Flux and Core Flow

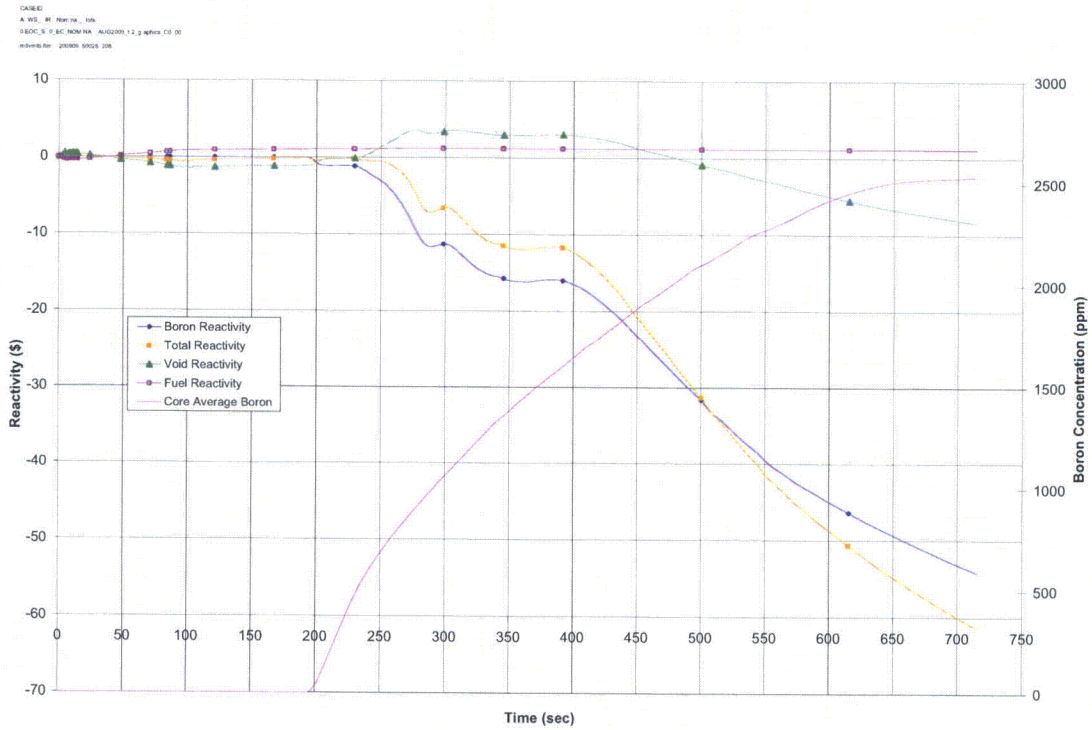


Figure 8.1-10. MSIVC Reactivity Feedback and Boron Concentration

NEDO-33083 Supplement 2-A, Rev. 2

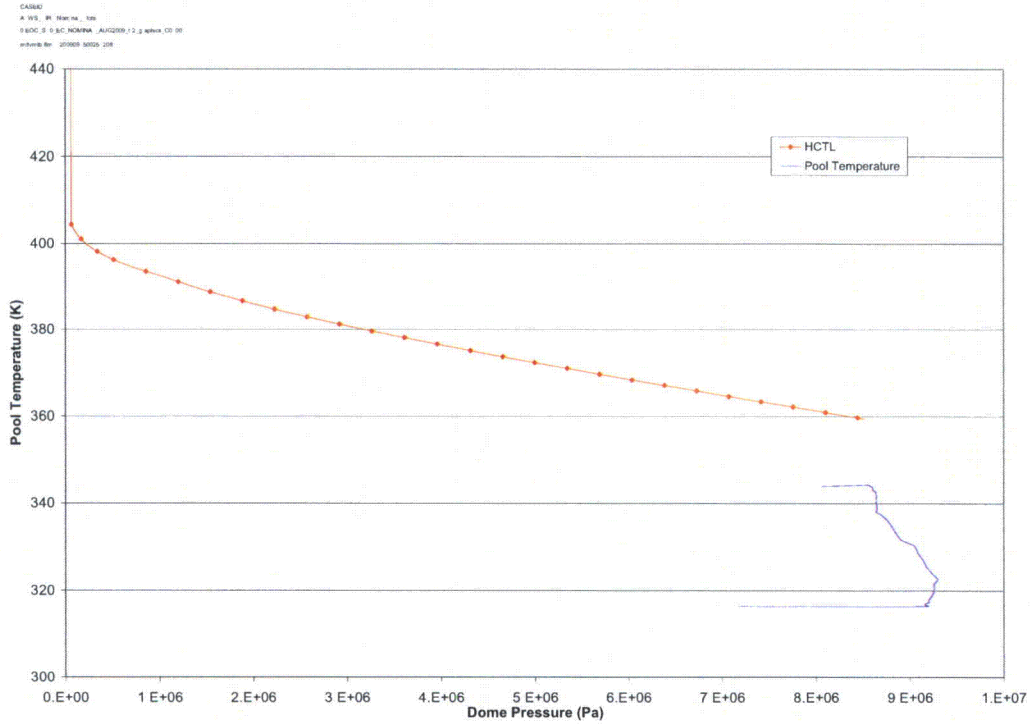


Figure 8.1-11. MSIVC HCTL and Pool Temperature Response

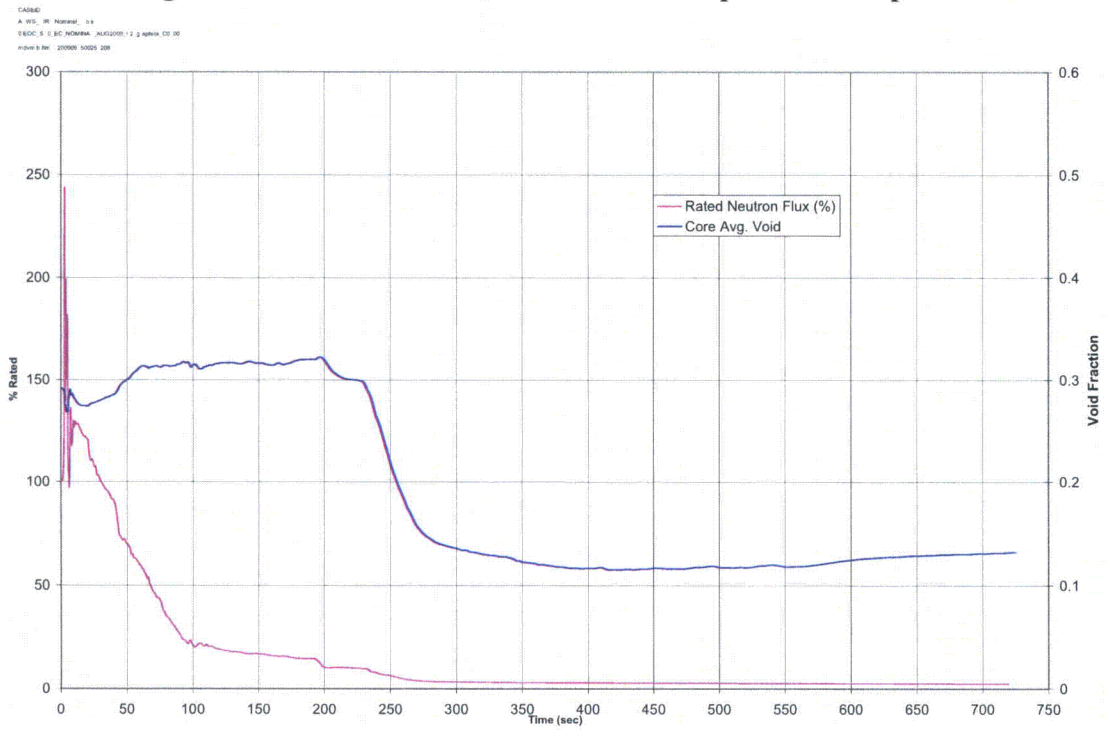


Figure 8.1-12. MSIVC Neutron Flux and Core Average Void

**8.1.2 Loss of Condenser Vacuum ATWS (LCV) Baseline Analysis**

This transient starts with a turbine trip because of the low condenser vacuum; therefore, the beginning is the same as the turbine trip event. However, the MSIVs and turbine bypass valves also close after the condenser vacuum has further dropped to their closure setpoints. Hence, this event is similar to the MSIV closure event for all the key parameters. Table 8.1-6 shows the sequence of events for this transient. This transient scenario corresponds to Figures 8.1-1a, 8.1-2a, 8.1-3a, 8.2-1a and Table 8.1-1a.

**Table 8.1-6 Sequence of Events for LCV**

<b>Time (s)</b>	<b>Event</b>
0	Loss of Condenser Vacuum
0	Turbine Trip initiated and bypass opening
6	Bypass valves start to close, MSIVs close shortly thereafter.
7	IC initiation
10	ATWS trip set at high pressure
11	SRVs open
11	Feedwater runback initiated
26	Feedwater runback complete
27	Suppression pool cooling starts
49	Level drops below L2 set point
59	HP CRD flow starts
200	SLCS injection starts
352	Peak Pool Temperature
445	Hot Shutdown achieved
720	High pressure design volume of borated solution injected into bypass

The key results from this analysis are presented in Table 8.1-7 and Figures 8.1-13 through 8.1-20. The results for the LCV case are very similar to those in the MSIVC case. The PCT is much lower due to the use of initial CPR of 1.3 compared with a lower value in the original ATWS LTR.

**Table 8.1-7. Key Results from LCV**

<b>Parameter</b>	<b>Value</b>	<b>Time(s)</b>
Maximum Neutron Flux, %	211	9
Maximum Vessel Bottom Pressure, MPaG (psig)	9.20 (1335)	12
Maximum Bulk Suppression Pool Temperature, °C (°F)	71.11 (160)	350
Associated Containment Pressure, kPaG (psig)	200 (29.28)	350
Peak Cladding Temperature, °C (°F)	521.91 (971)	23

Z:\Mugica\ATWS\Updated\_Files\LCV-NOM INAL-P100\LCV-NOM INAL-P100.CDR  
 Proc ID 431802  
 1/3/2008 8 2 45

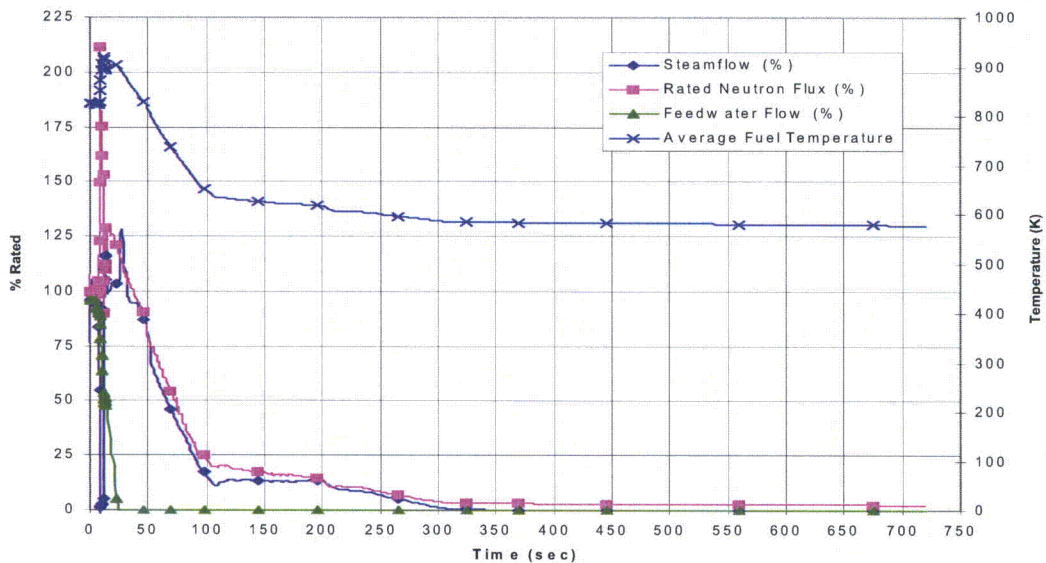


Figure 8.1-13. LCV Neutron Flux , Feedwater Flow, and Steam Flow

Z:\Mugica\ATWS\Updated\_Files\LCV-NOM INAL-P100\LCV-NOM INAL-P100.CDR  
 Proc ID 431802  
 1/3/2008 8 2 45

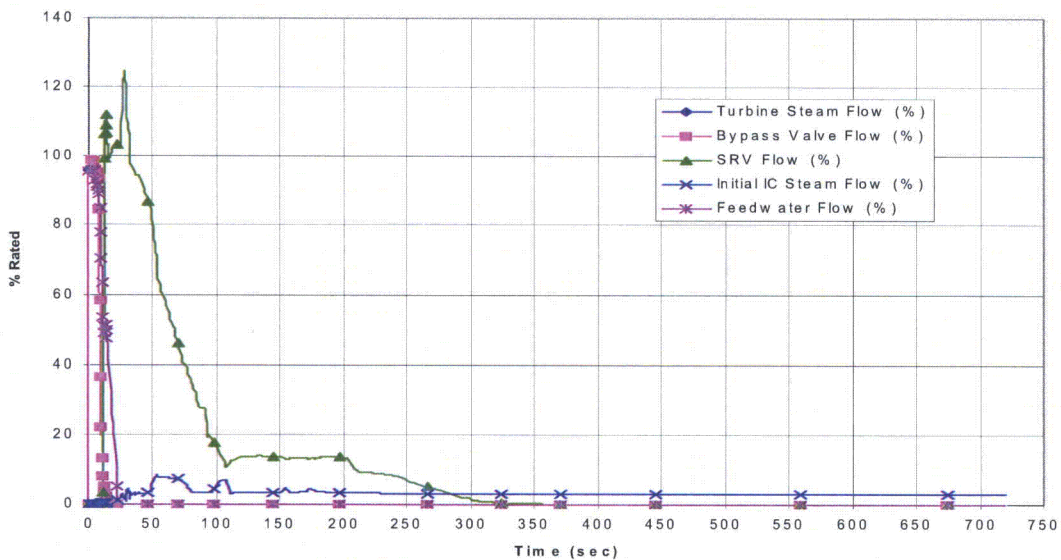


Figure 8.1-14. LCV Steam and Feedwater Flow, and SRV Flow

NEDO-33083 Supplement 2-A, Rev. 2

Z:\M ugical\ATW S\Updated\_Files\LCV-NOM INAL-P100\LCV-NOM INAL-P100.CDR  
 Proc ID 431802  
 1/3/2008 8 2 45

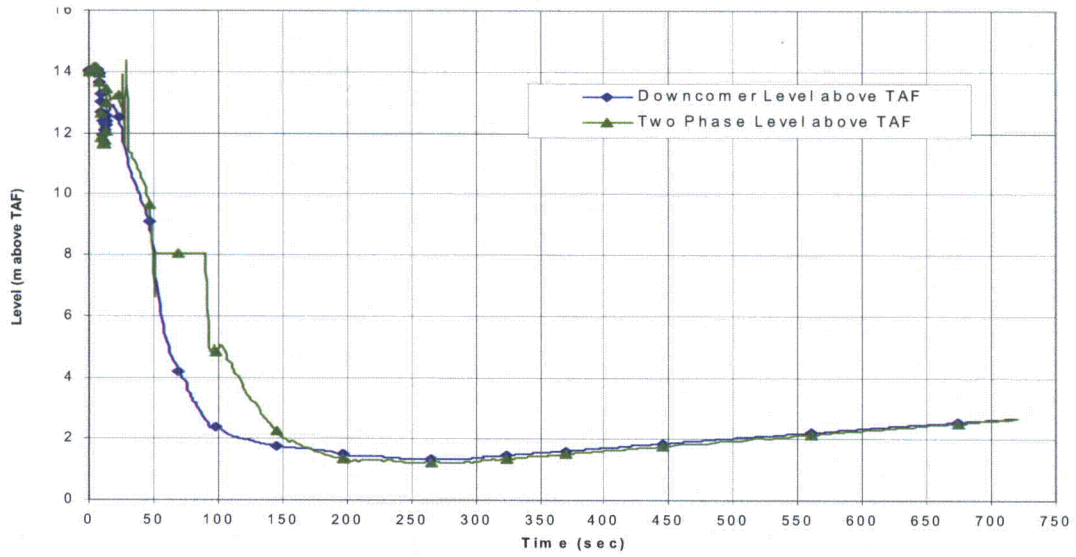


Figure 8.1-15. LCV Water Levels

Z:\M ugical\ATW S\Updated\_Files\LCV-NOM INAL-P100\LCV-NOM INAL-P100.CDR  
 Proc ID 431802  
 1/3/2008 8 2 45

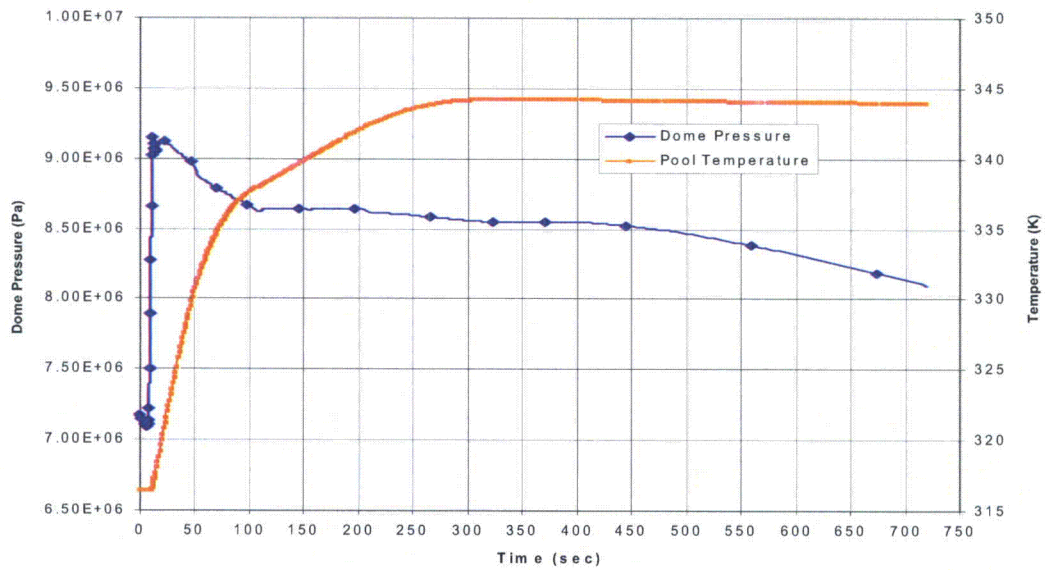
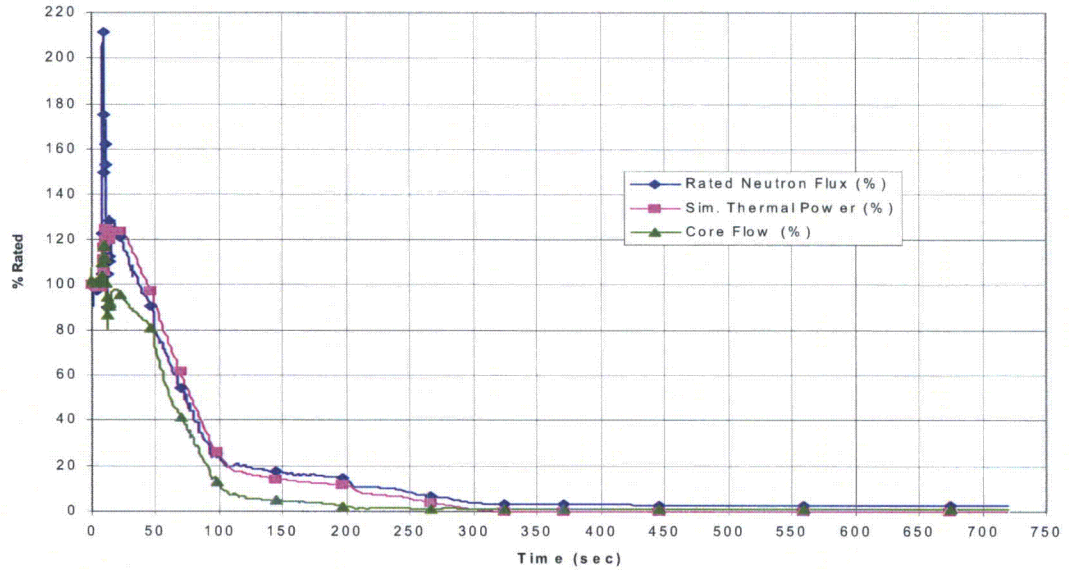


Figure 8.1-16. LCV Dome Pressure and Pool Temperature

# NEDO-33083 Supplement 2-A, Rev. 2

Z:\M ugical\ATW S\Updated\_Files\LCV-NOM INAL-P100\LCV-NOM INAL-P100.CDR  
 Proc ID 431802  
 1/3/2008 8 2 45



**Figure 8.1-17. LCV Neutron Flux and Core Flow**

Z:\M ugical\ATW S\Updated\_Files\LCV-NOM INAL-P100\LCV-NOM INAL-P100.CDR  
 Proc ID 431802  
 1/3/2008 8 2 45

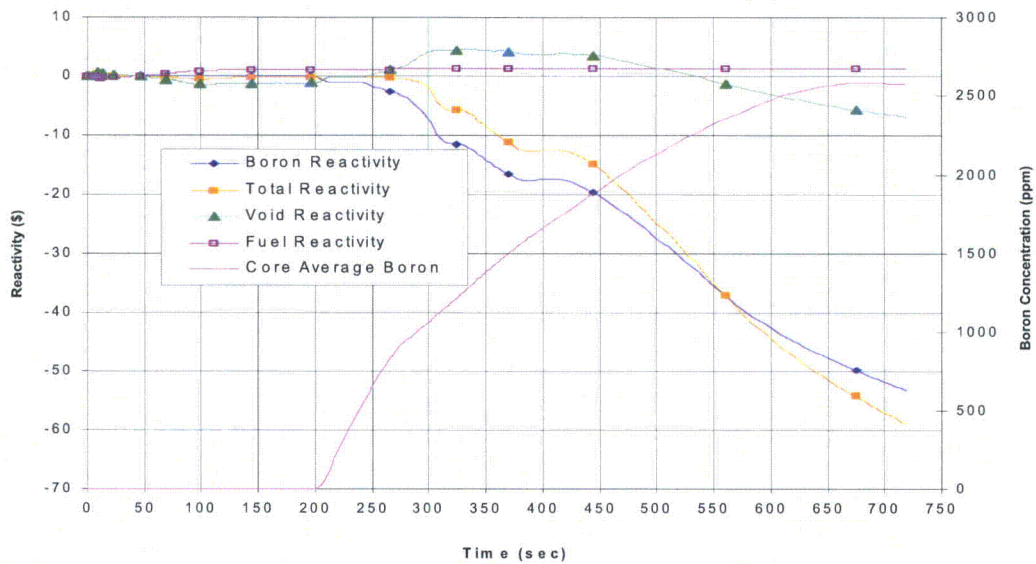


**Figure 8.1-18. LCV Reactivity Feedback and Boron Concentration**

# NEDO-33083 Supplement 2-A, Rev. 2

Z:\M ugical\ATW S\Updated\_Files\LCV-NOM INAL-P100\LCV-NOM INAL-P100.CDR  
Proc ID 431802  
1/3/2008 8 2 45

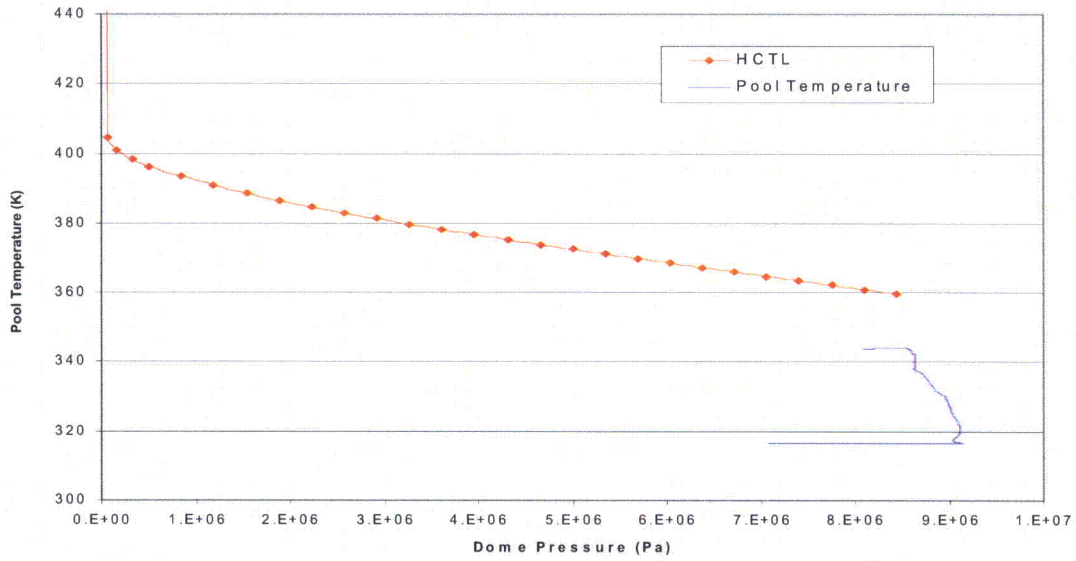


Figure 8.1-19. LCV HCTL and Pool Temperature Response

Z:\M ugical\ATW S\Updated\_Files\LCV-NOM INAL-P100\LCV-NOM INAL-P100.CDR  
Proc ID 431802  
1/3/2008 8 2 45

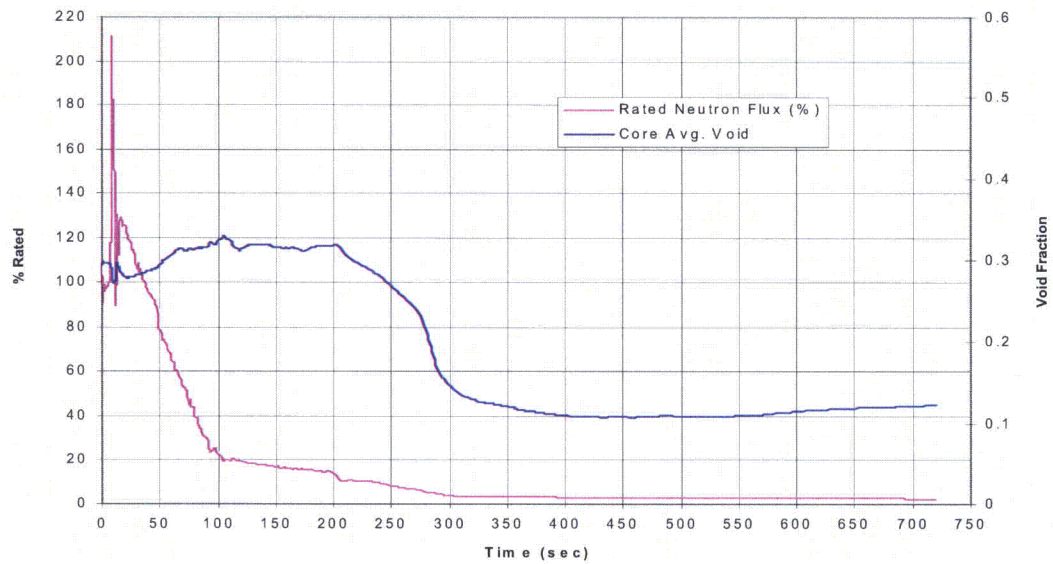


Figure 8.1-20. LCV Neutron Flux and Core Average Void

**8.1.3 Loss of Feedwater Heating ATWS (LFWH) Baseline Analysis**

This transient does not immediately trip any automatic ATWS logic. A 10-minute delay is assumed at the beginning of this event before the ARI is initiated. FMCRD run-in, and SLC timer are activated with the ARI initiation. At this time, the reactor has settled in a new steady state at a higher power level. However, the feedwater runback initiated by ARI signal and startup range neutron monitor ATWS permissive signal causes the water level to drop below Level 2. Low water level results in a closure of all MSIVs, and subsequent reactor pressure increase. SRV opening mitigates the pressure increase. Upon failure of rod insertion, boron injection via the SLC system brings the reactor to hot shutdown at approximately 15 minutes after the event starts. The transient behavior for the case is shown in Figures 8.1-21 through 8.1-27. Table 8.1-8 presents a sequence of main events that occur during this transient. The peak values of the key parameters are shown in Table 8.1-9. This transient scenario corresponds to Figures 8.1-1a, 8.1-2a, 8.1-3a, 8.2-1a and Table 8.1-1a.

**Table 8.1-8. Sequence of Events for Loss of Feedwater Heating**

Time (s)	Event
0	Loss of Feedwater heating
600	Feedwater runback initiated by operator
637	L2 setpoint reached
637	ATWS trip set at L2
648	HP CRD flow starts
667	MSIV closure starts
671	IC initiates
692	SRVs open
791	SLCS flow starts
1312	High pressure design volume of borated solution injected into bypass

**Table 8.1-9. Key Results from Loss of Feedwater Heating**

<b>Parameter</b>	<b>Value</b>	<b>Time (s)</b>
Sensed Maximum Neutron Flux, %	119	472
Maximum Vessel Bottom Pressure, MPaG (psig)	8.72 (1264.2)	693
Maximum Bulk Suppression Pool Temperature, °C (°F)	48.8 (119.9)	903
Associated Containment Pressure, kPaG (psig)	163.3 (23.69)	903
Peak Cladding Temperature, °C (°F)	313.2 (595.8)	622

Z:\Bart\FinAR\_LP\WHLFWH\_P100\_DCD\_REV.GRF  
 Plot ID: 389177  
 9/2007 9:23:15 PM

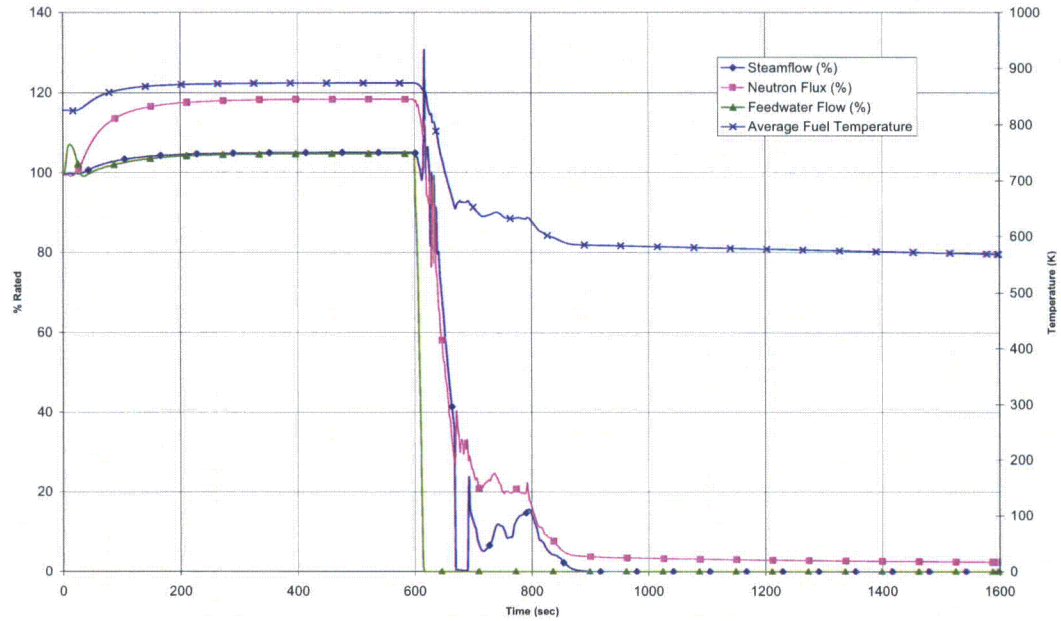


Figure 8.1-21. Loss of Feedwater Heating Neutron Flux, Feedwater Flow, and Steam Flow

Z:\Bart\FinAR\_LP\WHLFWH\_P100\_DCD\_REV.GRF  
 Plot ID: 389177  
 9/2007 9:23:15 PM

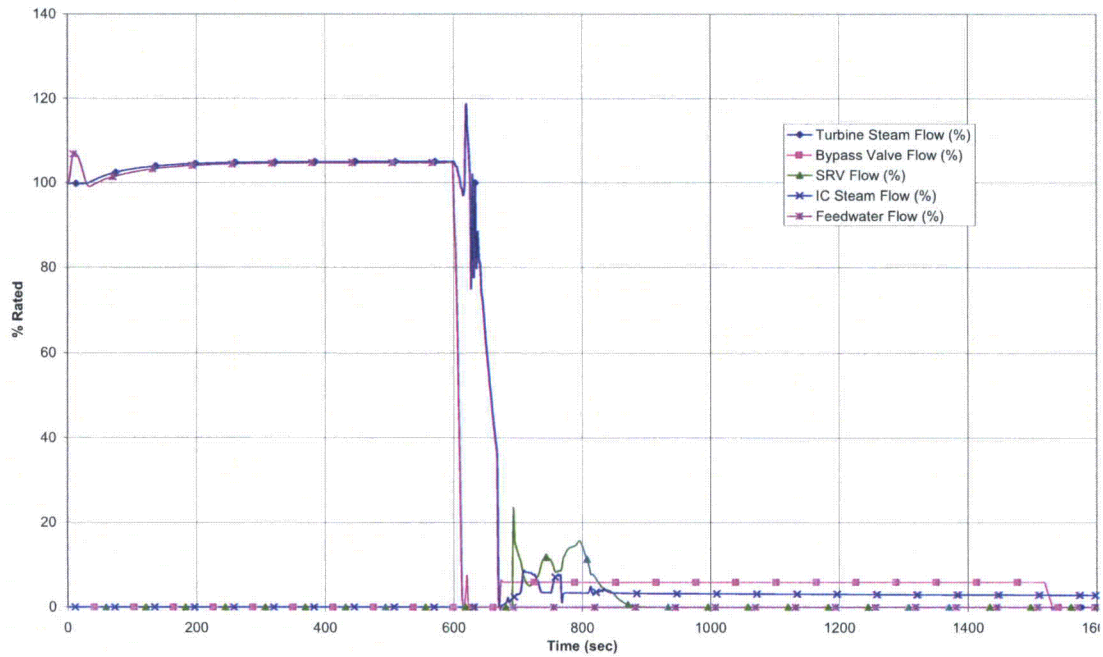


Figure 8.1-22. Loss of Feedwater Heating Steam and Feedwater Flow, and SRV Flow

NEDO-33083 Supplement 2-A, Rev. 2

Z:\Barratt\FinalR4\LF\FW\LF\FWH\_P100\_DCD\_REV4.GRF  
 Proc ID 388177  
 9/4/2007 9:23:15 PM

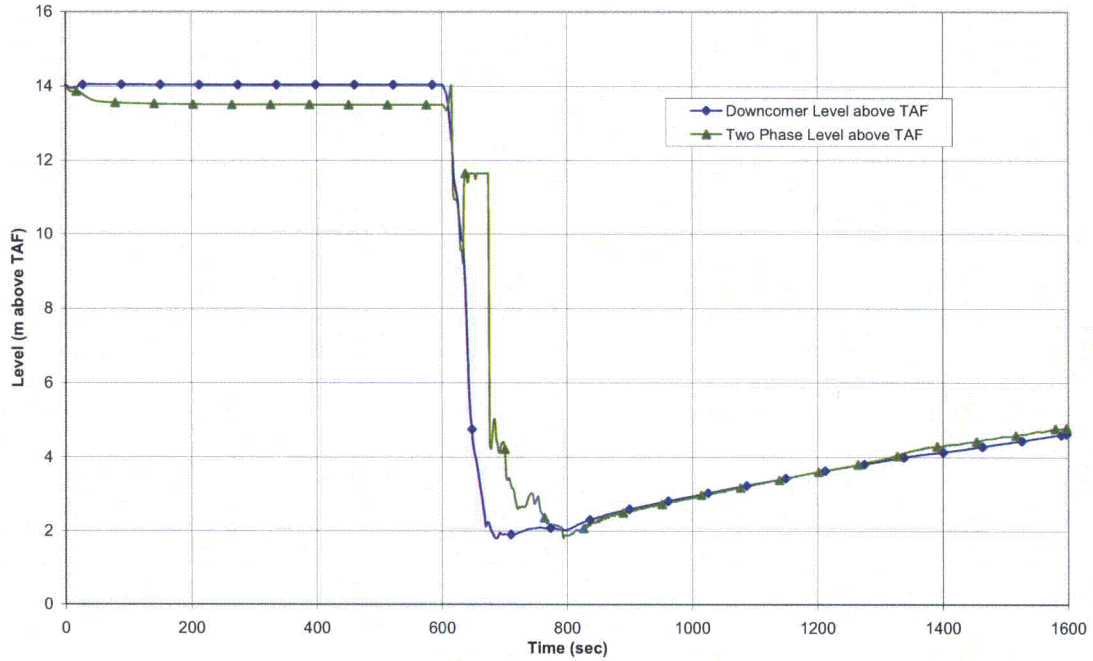


Figure 8.1-23. Loss of Feedwater Heating Water Levels

Z:\Barratt\FinalR4\LF\FW\LF\FWH\_P100\_DCD\_REV4.GRF  
 Proc ID 388177  
 9/4/2007 9:23:15 PM

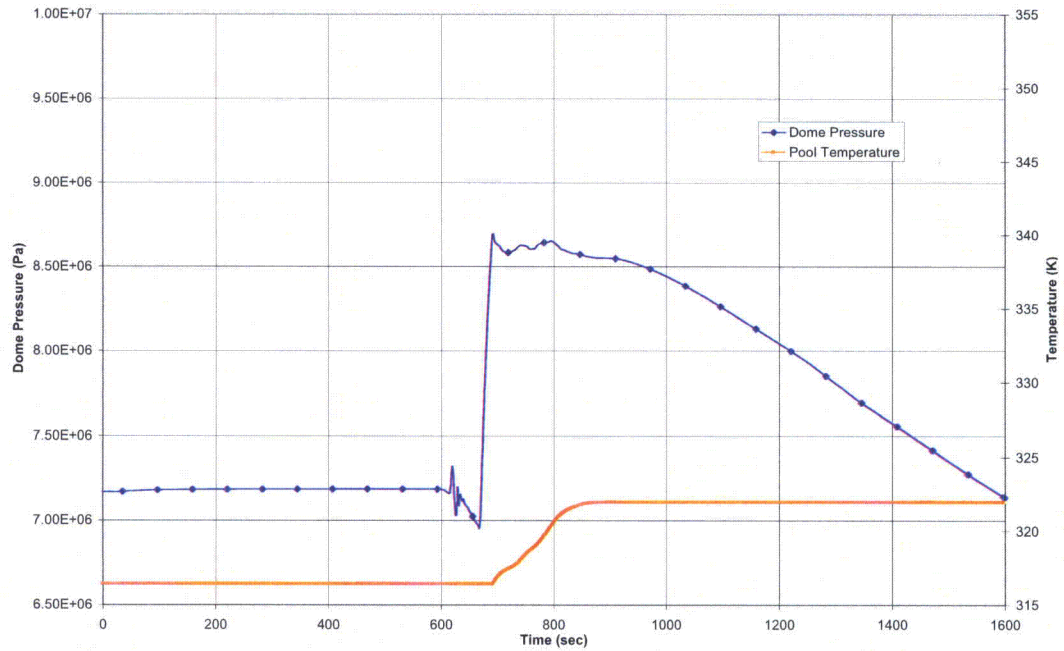
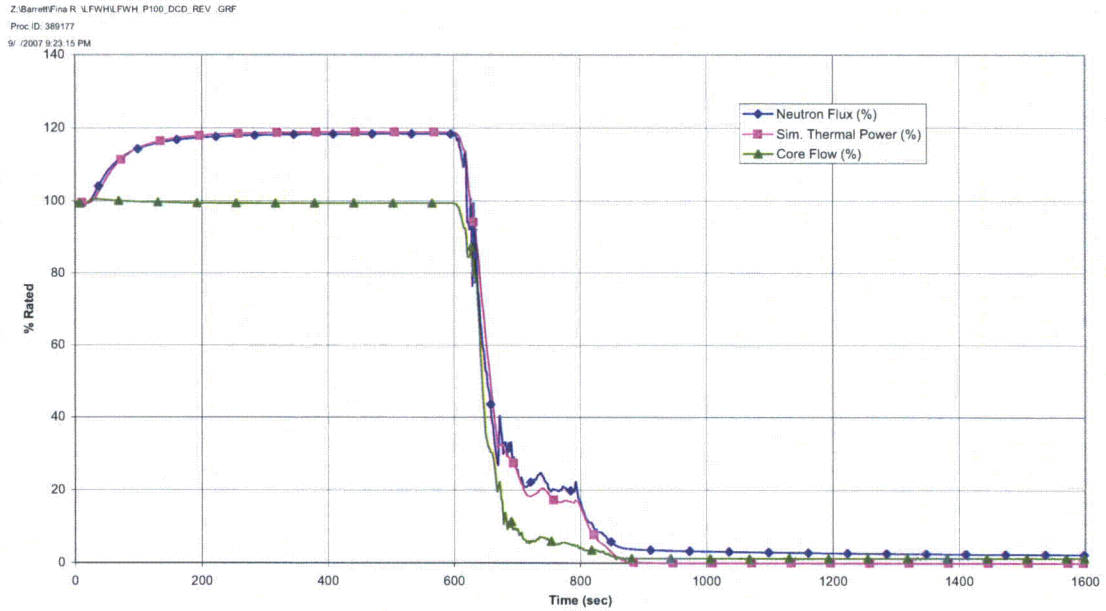
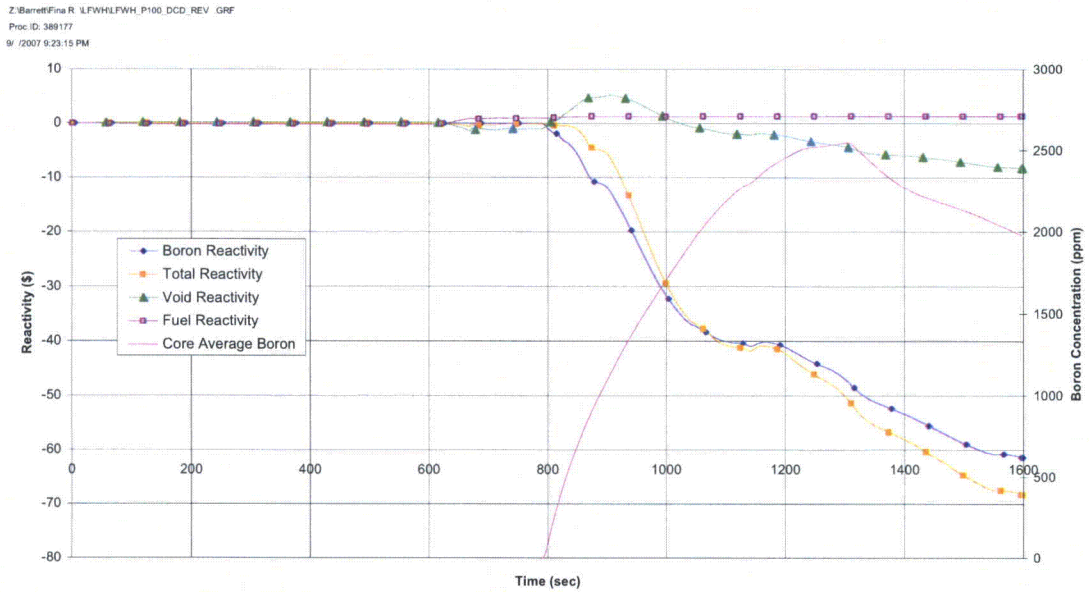


Figure 8.1-24. Loss of Feedwater Heating Dome Pressure and Pool Temperature



**Figure 8.1-25. Loss of Feedwater Heating Neutron Flux and Core Flow**



**Figure 8.1-26. Loss of Feedwater Heating Reactivity Feedback and Boron Concentration**

NEDO-33083 Supplement 2-A, Rev. 2

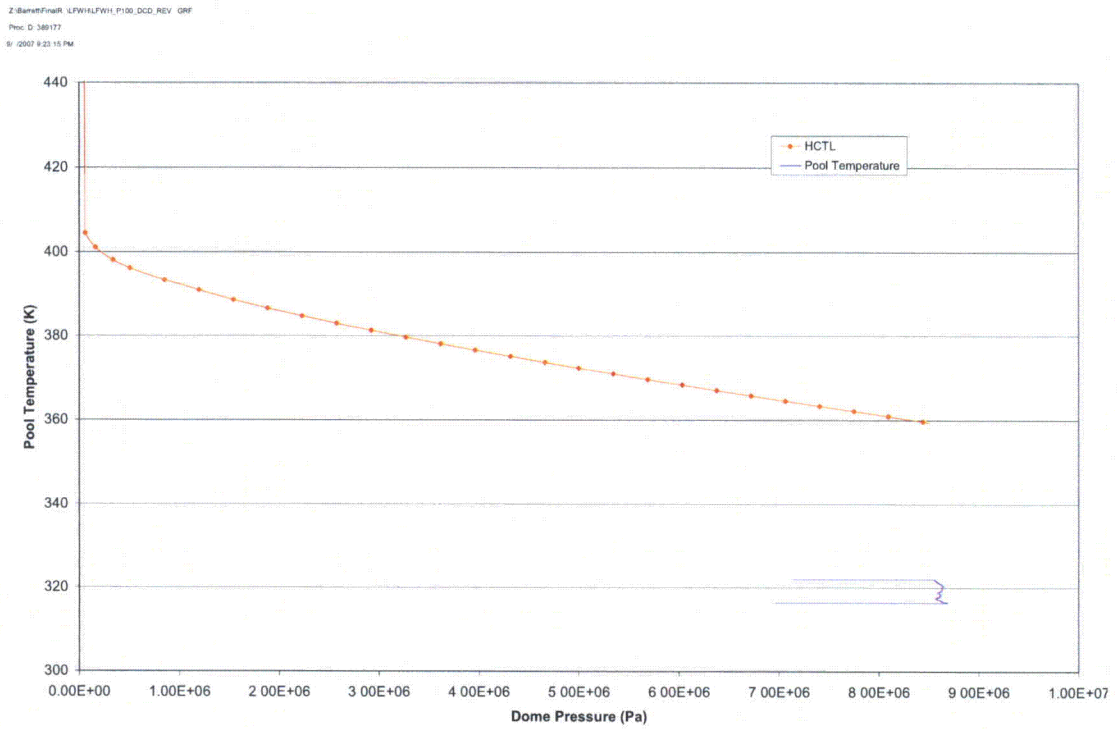


Figure 8.1-27. Loss of Feedwater Heating HCTL and Pool Temperature Response

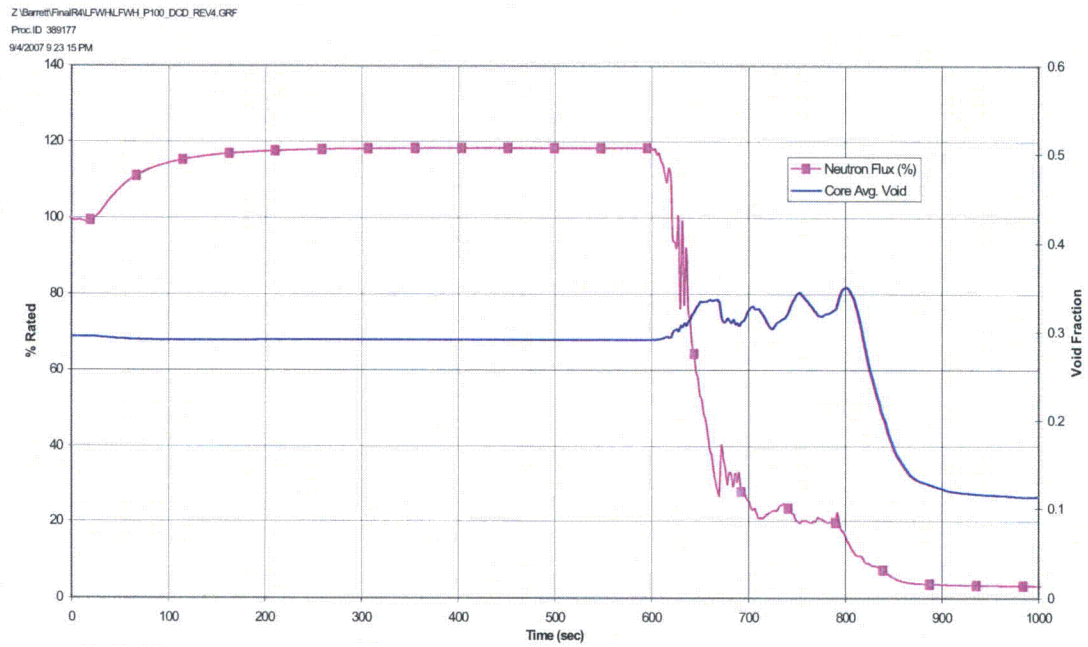


Figure 8.1-28. Loss of Feedwater Heating Neutron Flux and Core Average Void

#### **8.1.4 MSIV Closure Depressurization ATWS Baseline Analysis**

In order to study a postulated operator initiated depressurization behavior during ATWS, TRACG depressurization analysis results for the most limiting ATWS event, Main Steam Isolation Valve Closure (MSIVC) event, is provided in this subsection. The MSIVC event is reanalyzed with one significant exception. The Safety Relief Valves (SRVs) are held open so that the vessel dome pressure vs. suppression pool temperature response has a similar slope to the HCTL curve coincident with the initiation of the standby liquid control system (SLCS) injection at about 189 seconds into the transient. Holding the SRVs open simulated an operator activated depressurization event. This transient scenario corresponds to Figures 8.1-1a, 8.1-2a, 8.1-3a, 8.2-1a and Table 8.1-1a.

Following the initiation of depressurization the reactor vessel pressure decreases. Additionally, the suppression pool temperature increases due to the blowdown steam flow from the vessel. The relative rates of vessel pressure decrease vs. suppression pool temperature increase are expected to be consistent with the HCTL curve. The HCTL curve is shown in Figure 8.1-34. In operating plants this curve is the design limitation of a plant's ability to depressurize. If the suppression pool temperature is in excess of the HCTL value for any given dome pressure the RPV cannot be safely depressurized.

Operator initiated depressurization is not expected during ATWS scenarios for the ESBWR. This is because the calculated suppression pool temperatures are well below the HCTL curve for all limiting ATWS events.

The depressurization case results in reactor shutdown at the beginning of depressurization and the HCTL curve adequately protects the containment from heat up during depressurization. This case does not need an uncertainly evaluation.

**Table 8.1-10. Sequence of Events for MSIVC Depressurization**

<b>Time (s)</b>	<b>Event</b>
0	MSIV Closure starts
2	IC initiation
3.5	ATWS trip set at high pressure
5	Feedwater runback initiated
5	SRVs open
21	Suppression pool cooling starts
47	Feedwater runback complete
54	Level drops below L2 set point
65	HP CRD flow starts
189	Initiation of depressurization
195	SLCS injection starts
368	Hot shutdown achieved
720	Peak pool temperature
715	High pressure design volume of borated solution injected into bypass

The key results from this analysis are presented in Table 8.1-11. and Figures 8.1-29a through 8.1-35.

**Table 8.1-11. Key Results from MSIVC Depressurization**

<b>Parameter</b>	<b>Value</b>	<b>Time (s)</b>
Maximum Neutron Flux, %	229.5	3
Maximum Vessel Bottom Pressure, MPaG (psig)	9.22 (1337)	6
Maximum Bulk Suppression Pool Temperature, °C (°F)	93.85 (200.93)	720
Associated Containment Pressure, kPaG (psig)	268 (38.91)	720
Peak Cladding Temperature, °C (°F)	787.8 (1449.95)	32

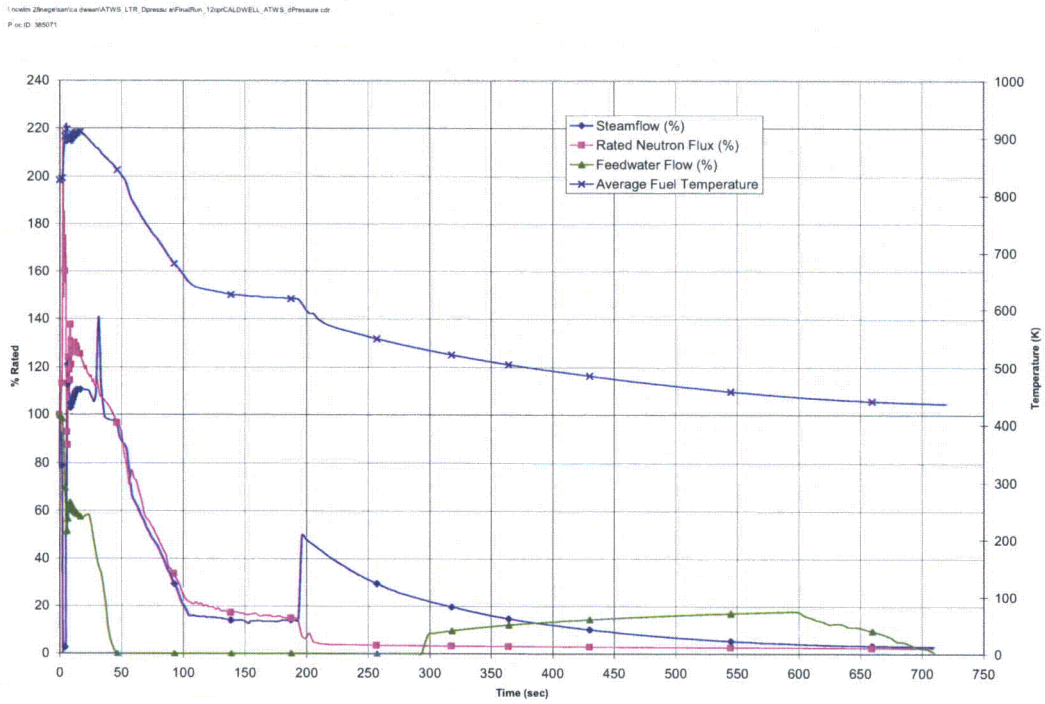


Figure 8.1-29a. MSIVC Depressurization Neutron Flux, Feedwater Flow, and Steam Flow

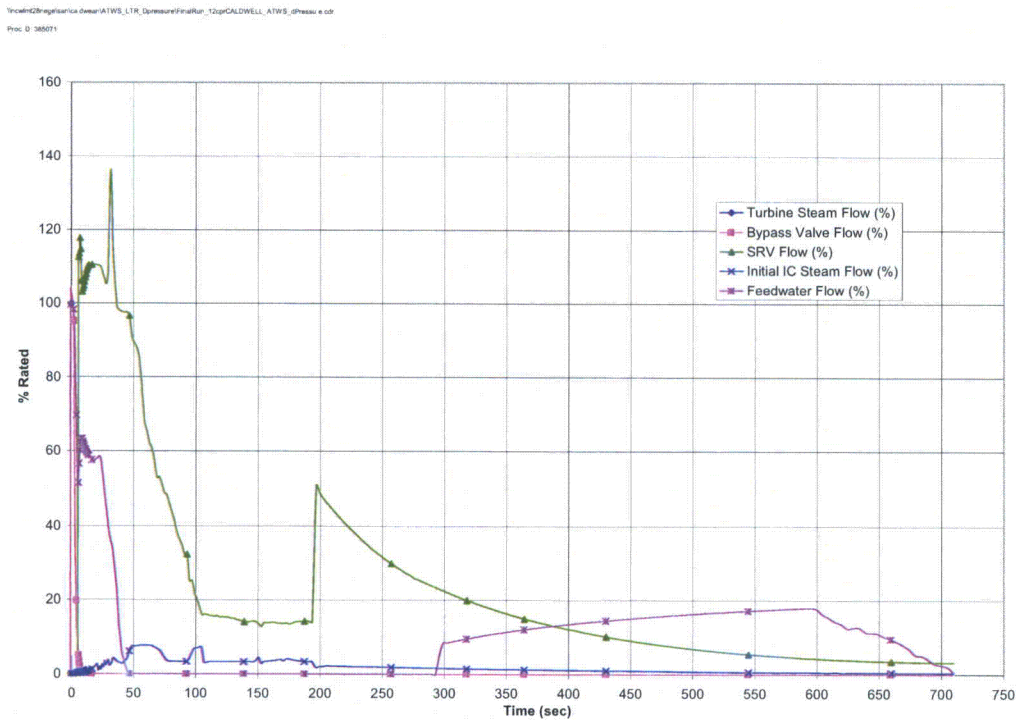


Figure 8.1-29b. MSIVC Depressurization Steam and Feedwater Flow, and SRV Flow

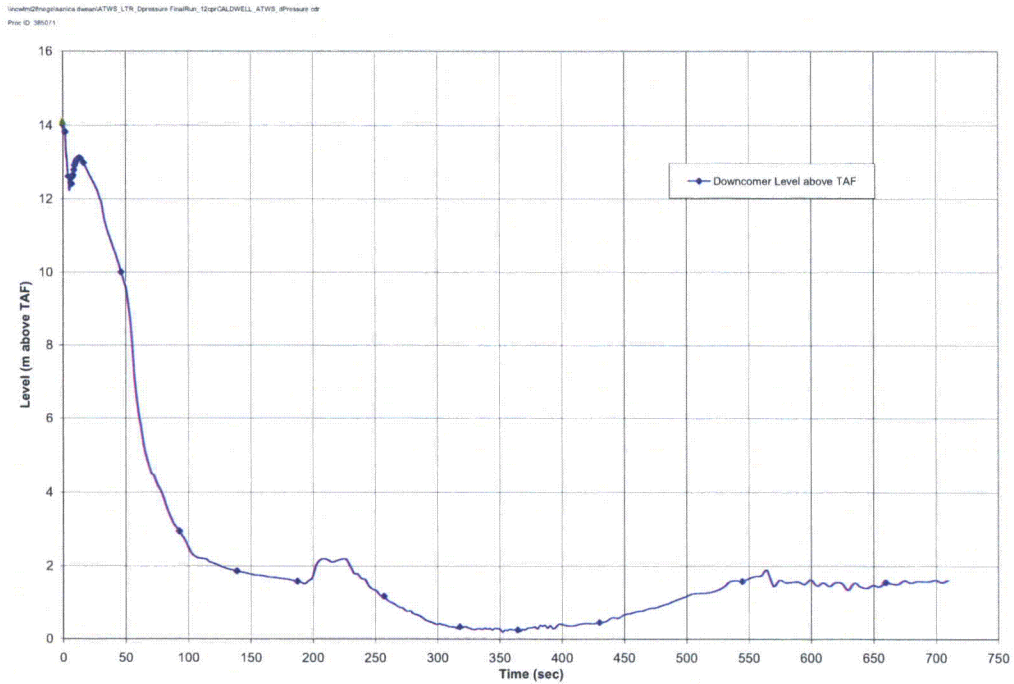


Figure 8.1-30. MSIVC Depressurization Water Levels

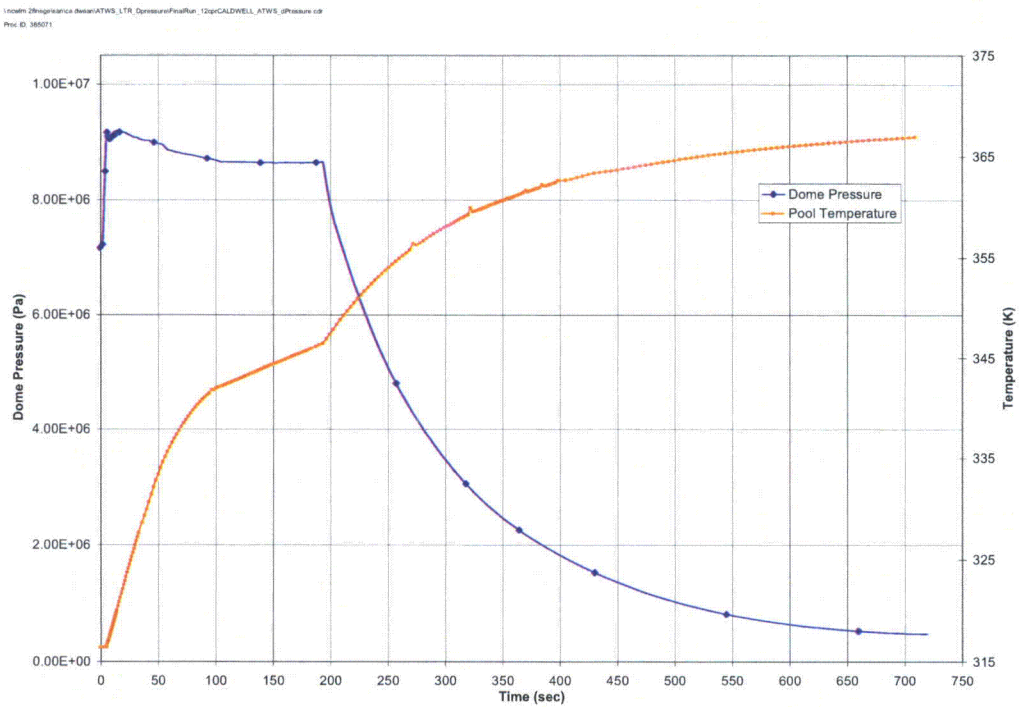


Figure 8.1-31. MSIVC Depressurization Dome Pressure and Pool Temperature

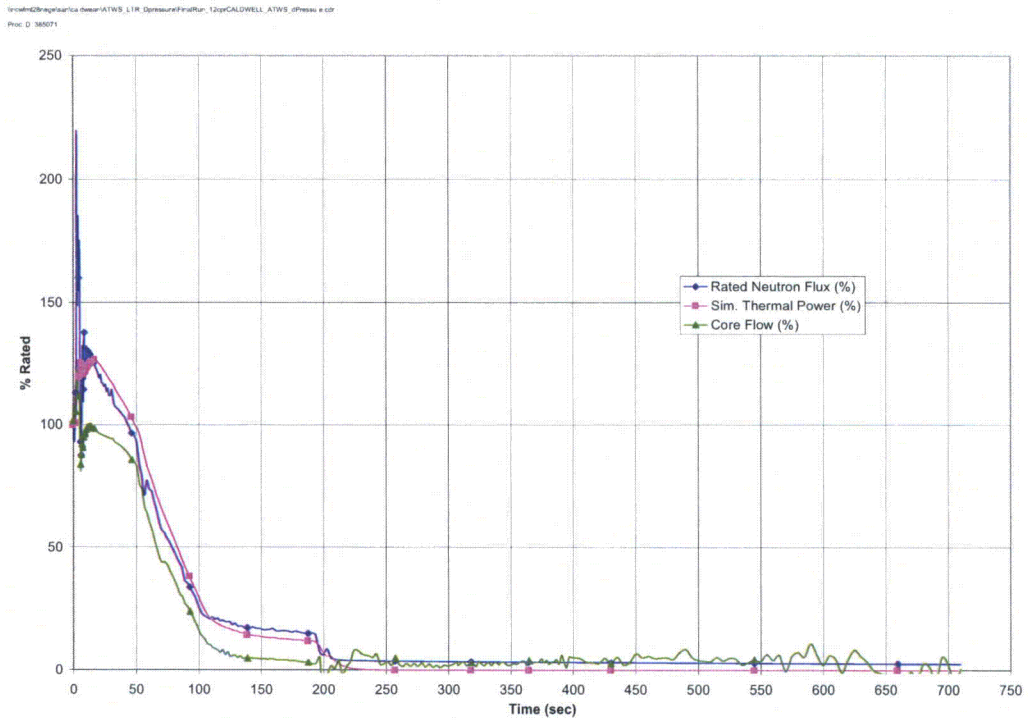


Figure 8.1-32. MSIVC Depressurization Neutron Flux and Core Flow

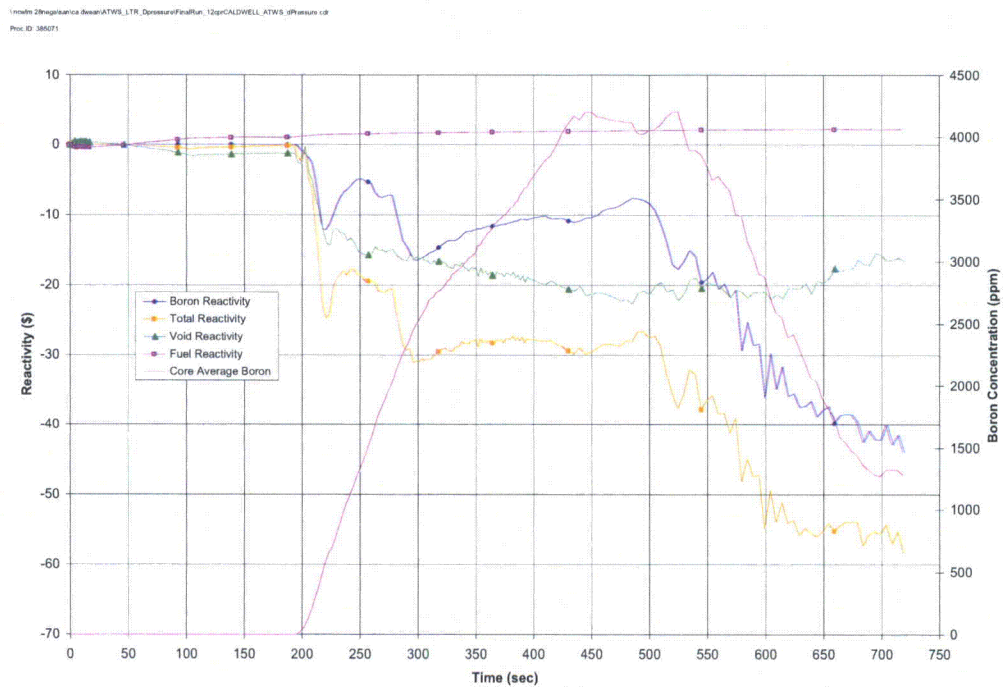


Figure 8.1-33. MSIVC Depressurization Reactivity Feedback and Boron Concentration

NEDO-33083 Supplement 2-A, Rev. 2

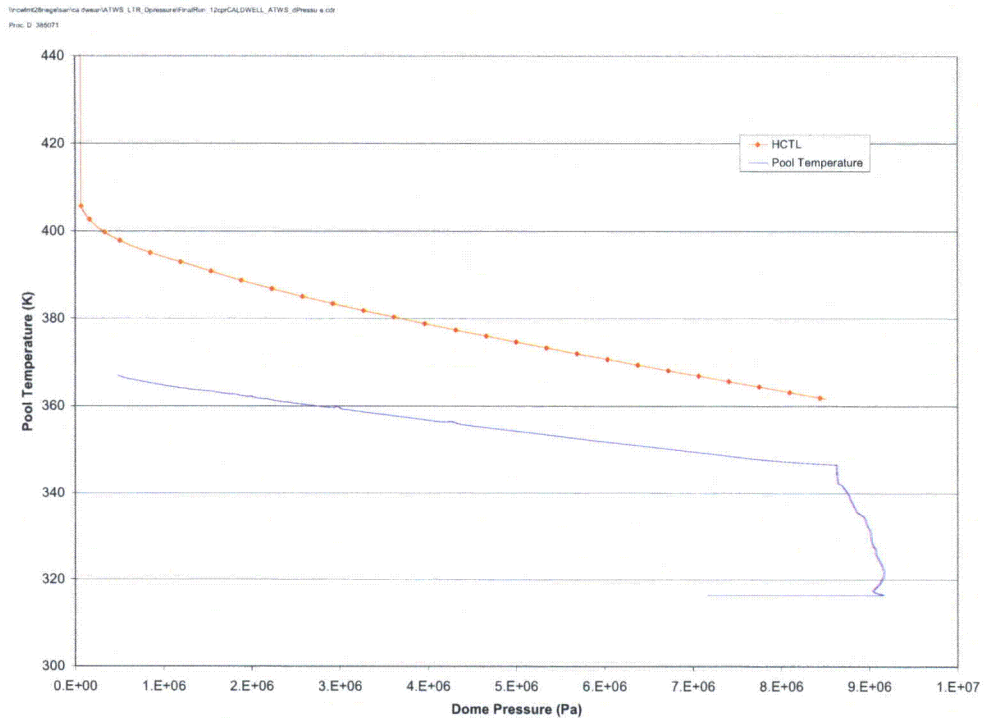


Figure 8.1-34. MSIVC Depressurization HCTL and Pool Temperature Response

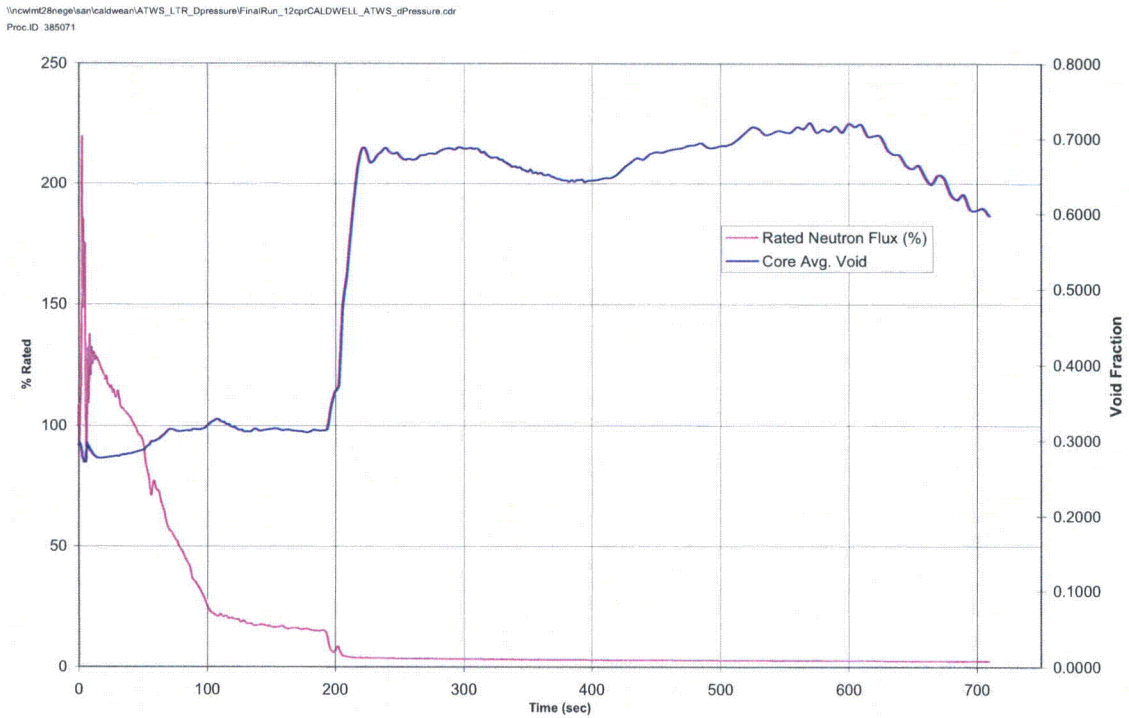


Figure 8.1-35. MSIVC Depressurization Neutron Flux and Core Average Void

**8.2 INITIAL CONDITION AND PLANT PARAMETER REVIEW**

**8.2.1 Initial Conditions**

This section considers the sensitivity of the limiting MSIVC ATWS case to initial conditions in the plant. Table 8.2-1 summarizes the initial condition sensitivity analyses performed as part of this study. The critical parameters studied are peak pressure, peak clad temperature, peak suppression pool temperature, and peak power.

**Table 8.2-1. Initial Conditions Sensitivity Analysis**



]]

**8.2.1.1 Initial Conditions Sensitivity Results**

A summary of the sensitivity analysis for the MSIVC transient is provided in Table 8.2-2. The sensitivity analyses were performed at the EOC state point and the changes in various parameters as a result of initial condition uncertainties are discussed in this subsection. If depressurization does occur the results are not more severe with respect to margin to HCTL curve. (See subsection 8.1.4).

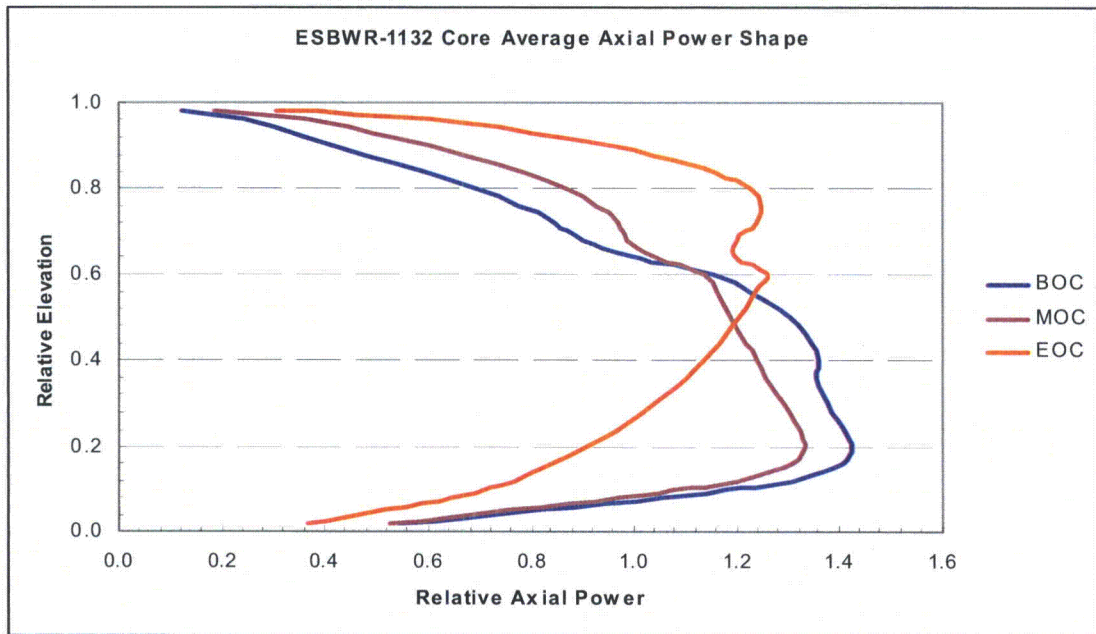


Figure 8.2-1a. Relative Axial Power Distribution for Three Exposure State Points

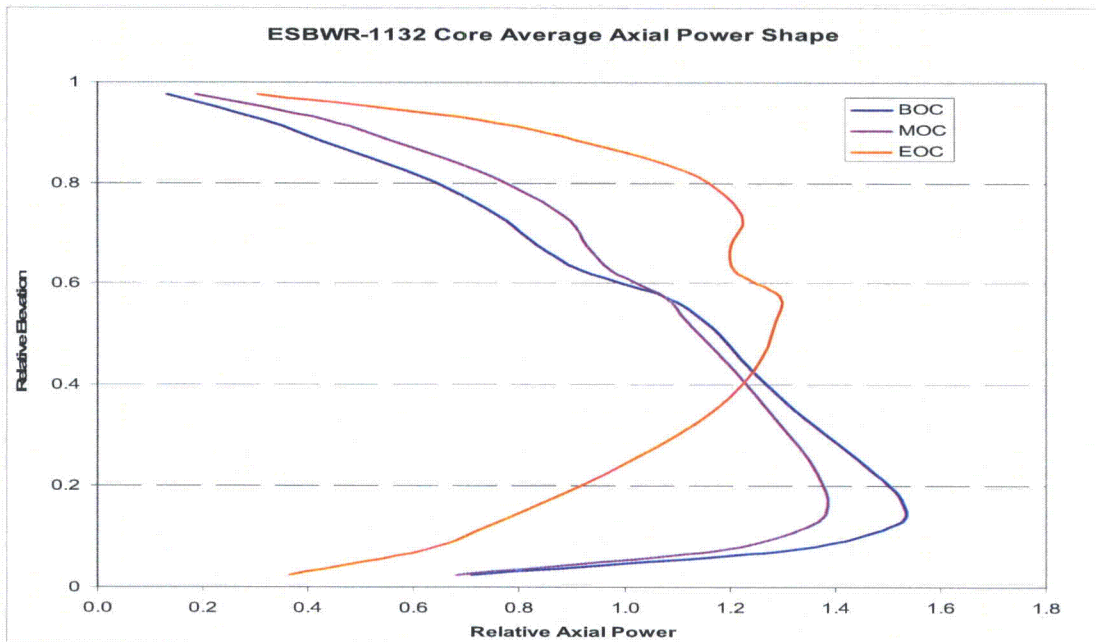


Figure 8.2-1b. Relative Axial Power Distribution for Three Exposure State Points

**Table 8.2-2. MSIVC Allowable Operating Range Results: Change from Base Case**

[[



]]

- (1) These sensitivity analyses correspond to Figures 8.1-1b, 8.1-2b, 8.1-3b, 8.2-1b and Table 8.1-1b.
- (2) These sensitivity analyses correspond to Figures 8.1-1a, 8.1-2a, 8.1-3a, 8.2-1a and Table 8.1-1a.

The characterization of these results is presented in Table 8.2-3.

**Table 8.2-3. MSIVC Initial Conditions Characterizations**


]]

**8.2.2 Plant Parameters**

As described in Section 8.1, plant parameters like S/RV capacity, MSIV stroke time, and IC capacity have been conservatively modeled in the baseline analyses. This section details the studies undertaken to determine the impact of other plant parameters that have a direct impact on one or more of the critical safety related parameters during an ATWS event. The sensitivity analyses were performed at the EOC state point and the changes in various parameters as a result of plant parameter uncertainties are discussed in this subsection.

Table 8.2-4 presents the set of plant parameters studied with a description of how each parameter was different from the baseline analysis.

**Table 8.2-4. MSIVC Plant Parameters**

<b>Plant Parameter</b>	<b>Base Case</b>	<b>Sensitivity Case</b>	<b>Purpose/Remarks</b>
Lower EOP ATWS Water Level	TAF + 1.524m	TAF	Impact on pool temperature
Higher EOP ATWS Water Level	TAF + 1.524m	TAF + 3.048m	Impact on pool temperature
Boron Enrichment	94% in B-10	19.8% in B-10	Impact on pool temperature
FAPCS	On	Off	Impact on pool temperature
SLCS flow velocity at nozzle	Time dependent flow based on accumulator depressurization	Constant flow of 30.5m/s	Impact on shutdown time and potential impact on pool temperature
SLCS flow velocity at nozzle at 90%	Time dependent flow based on accumulator depressurization	Time dependent flow reduced to 90% of base case	Impact on shutdown time and potential impact on pool temperature
SRV Capacity*	Tech Spec	Nominal	Impact on Pressure, pool temperature
IC	75% IC Capacity	Full IC capacity	Impact on pool temperature
Suppression Pool HCTL	S/RVs are not held open at approximate SLCS initiation	S/RVs held open at approximate SLCS initiation, (simulates pool reaching HCTL at the start of boron injection).	Determine whether reactor would be critical after a depressurization if the HCTL curve were reached.

\* See Section 8.3 for more information

**8.2.2.1 Plant Parameter Sensitivity Results**

Table 8.2-5 presents results from the plant parameter sensitivity studies. These sensitivity studies correspond to Figures 8.1-1a, 8.1-2a, 8.1-3a, 8.2-1a and Table 8.1-1a.

**Table 8.2-5. MSIVC Plant Parameter Sensitivity Study, Change from Base Case**

[[


]]

The peak power was not sensitive to any of the plant parameters. Increasing the SRV capacity from the nameplate value to the nominal value (approximately 8%), decreased the PCT by approximately [[            ]]. The peak pool temperature was not sensitive to any of the plant parameters. Changes to the other plant parameters had very little effect on the key quantities.

The depressurization case is covered in Section 8.1.4. In this case the increase in pool temperature is caused by dumping energy from the RPV into the pool and the reactor remains subcritical at the low pressure. Adequate margin is maintained between the pool temperature and the HCTL curve, as seen in Fig. 8.1-34.

Additional cases, with and without depressurization, where the vessel was refilled to the normal water level over a period of one half hour after the termination of SLCS flow, did not lead to recriticality of the system.

[[

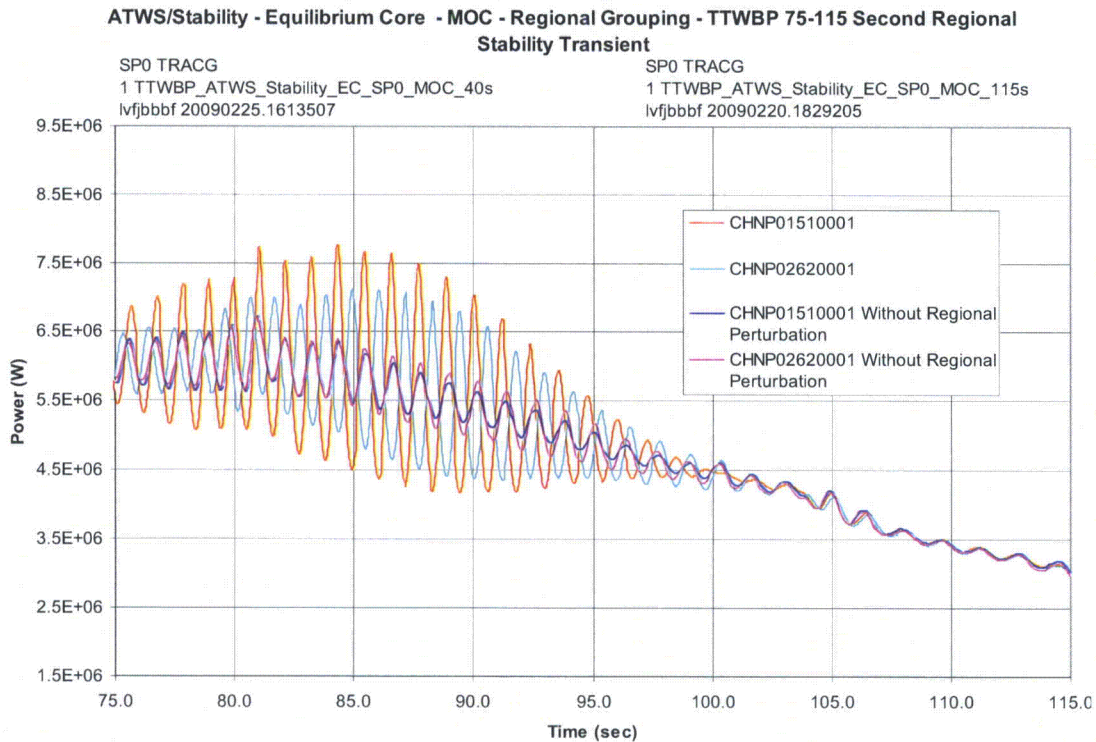
]] A case with natural boron as opposed to the 94% enriched boron used in the plant indicated that the shut down takes about [[ ]] minutes longer, for a total of [[ ]] minutes from the initiation of the SLCS. The pool temperature did not show any sensitivity to the reduction in flow velocity at the SLCS nozzles by 10%.

### 8.2.3 ATWS Stability Study

Studies are performed to examine coupled neutronic-thermal hydraulic instability in the core during ATWS initiating from bounding operating conditions.

Regional perturbations are introduced to the channel inlet liquid flow in the out-of-phase mode, at different times during the transient when power-flow ratios are steady and high. The transient response to these perturbations is evaluated. Furthermore, the void reactivity coefficient is increased by 30% in the stability analysis to gain margin.

The limiting case, where a regional perturbation is introduced at 75 seconds into Turbine Trip with Full Bypass ATWS at Peak Hot Excess (PHE) during middle of cycle (MOC) exposure, is illustrated in Figure 8.2-2 for channels susceptible to high amplitude oscillations. It is seen that the oscillations in power are quickly damped out, as is the case for all channels, indicating that ESBWR operation remains stable during this event.



151 and 262 symmetrically located fuel channels.

**Figure 8.2-2. Core Stability During Turbine Trip with Full Bypass ATWS Event**

#### **8.2.4 Summary of Initial Conditions, Plant Parameters and Stability**

The following can be concluded based on the initial condition, plant parameter, and stability analyses results:

- Peak power and peak PCT are limiting for the EOC condition. Other critical parameters are not sensitive to the initial conditions. Clad oxidation is insignificant in all cases.
- Core stability is maintained during ATWS.
- The pool heat up is impacted primarily by the core power and the SR/V steam flow before the water level is reduced by FW runback to the EOP specified level, and secondarily the core power and steam flow after level reduction. The response after SLCS injection does not have a strong effect on pool temperature.
- The analyses indicate that none of the critical parameters exceeds safety limits and the plant achieves shutdown conditions safely.

#### **8.2.5 Sensitivity to Azimuthal Sector Size for Boron Injection (RAI 21.6-8)**

Appendix 2 contains response to RAI 21.6-8. Sensitivity to boron injection in the small vs. the large azimuthal sectors, and also sensitivity to radial/azimuthal blockage in the TRACG Nodalization vs. no blockage cases are established.

#### **8.2.6 Sensitivity to Finer Nodalization of the Peripheral Bypass Region (RAI 21.6-41)**

Appendix 2 contains response to RAI 21.6-41 where the core region is modeled with four TRACG radial rings with the peripheral bypass region was radially subdivided into two radial rings.

### **8.3 UNCERTAINTY ANALYSIS FOR LICENSING EVENTS**

The uncertainty analysis is performed for the highly ranked phenomena and initial conditions as discussed in Section 3 of this report. The effects of the uncertainty associated with these phenomena on peak vessel pressure, PCT, peak pool temperature and the peak power for the MSIVC case are examined in this section.

Using the estimated deviations from the base case obtained from the uncertainty analyses, an overall uncertainty for these key parameters is obtained and added to the respective values obtained in the nominal case.

#### **8.3.1 Uncertainty Screening**

Analyses have been performed at both the  $+1 \sigma$  and  $-1 \sigma$  level for each of the model uncertainties and initial conditions (some of these results have been discussed in Section 8.2). Figures 8.3-1 through 8.3-4 present these results. These sensitivity analyses correspond to Figures 8.1-1a, 8.1-2a, 8.1-3a, 8.2-1a and Table 8.1-1a.

[[

]]

**Figure 8.3-1. MSIVC –Peak Power Sensitivity**

[[

]]

**Figure 8.3-2. MSIVC –Peak Vessel Bottom Pressure Sensitivity**

[[

]]

**Figure 8.3-3. MSIVC –Peak Cladding Temperature Sensitivity**

[[

]]

**Figure 8.3-4. MSIVC –Peak Pool Temperature Sensitivity**

The peak power is sensitive to a decrease in upper plenum interfacial drag coefficient to the extent that it is less than a [[ ]] differential, with the parameter remaining insensitive to all other phenomena. The vessel bottom pressure is less than [[ ]] of the peak value in the base case for all phenomena. The PCT is the most sensitive parameter and is impacted by the steam dome pressure set point, feedwater enthalpy, SEO loss coefficient, Zuber/Biasi GEXL critical quality, total power, rewet quality margin and the interfacial shear in the core; there is large margin to the acceptance criterion for the PCT. The peak pool temperature is insensitive to the application of uncertainties to the various phenomena.

### 8.3.2 Overall Uncertainty

The overall uncertainty applicable to each of the parameters is obtained by taking the square root of the sum of squares of the difference between the base case and the PIRT phenomena that changed these parameters in a positive sense. The uncertainty for each parameter is then compared to the difference between the values for these parameters for a bounding case when compared to a nominal case. Any excess uncertainty over this difference is added as a bias to the bounding case.

Following the uncertainty analyses, a further set of conservatisms in the form of initial condition uncertainties were added to the original bounding case *viz.* 102% power, 0.125 MPa lower dome pressure setpoint, an approximate 5% increase in feedwater enthalpy, and a delay in feedwater runback coastdown, as these conditions are limiting when considering an initial CPR of 1.2 or less for the limiting channel.

Table 8.3-1 outlines the main differences in nominal and bounding cases.

**Table 8.3-1. Main Features of the Nominal, and Bounding Cases**

[[


]]

A summary of the results for the nominal and bounding cases is presented below in Table 8.3-2.

**Table 8.3-2. Nominal and Bounding Cases: Summary**

[[


]]

The overall uncertainty associated with each parameter was obtained as described above. Table 8.3-3 presents differences between the nominal and the bounding cases as well as any bias to be applied.

Finally, Table 8.3-4 presents bounding numbers and their comparison to the design limits. The Peak containment pressure is calculated based on the peak suppression pool temperature.

**8.3.3 Summary of Plant Parameter Sensitivity Study**

- The results of the plant parameter and initial conditions sensitivities are shown in Section 8.2.2. The key plant parameter is S/RV flow rate - the minimum S/RV flow being the most conservative. Approximately 11.5 kPa (1.66 psi) of margin to the limiting result exists when applying more nominal S/RV capacities as compared to the ASME certified capacities (assuming the certified capacity is 92% of the expected capacity).
- The key plant parameter for the suppression pool temperature is the feedwater runback (FWRB) time. Approximately 1.7 K (3.1°F) margin exists when applying more nominal FWRB time, assuming the expected FWRB delay is 10 second shorter.
- The key plant parameter for the PCT is the initial CPR. Approximately 335 K (603° F) of margin exists when applying more nominal initial CPR of 1.3.

**Table 8.3-3. Summary of Uncertainty Analyses**

[[


]]

**Table 8.3-4. Final Results**

[[


]]

All the key parameters in the bounding case are within design limits.

## 9. CONCLUSIONS

- TRACG is capable of simulating ESBWR ATWS events. It models the important phenomena, and the models of the important phenomena are qualified.
- An application methodology is defined for ESBWR ATWS analysis. The procedure for performing the calculation considers specific modeling applied in the code qualification for ESBWR.
- The nominal TRACG calculation, combined with bounding initial conditions and plant parameters, produces an overall conservative estimate of ATWS peak vessel pressure and peak fuel clad temperature.
- These analyses demonstrate that significant conservatism is included by applying bounding initial conditions and plant parameters. Further, the effect of model uncertainties is small compared to this conservatism. This conclusion can be applied to other plant types and fuel types based on these results and analysis experience.

## 10. REFERENCES

- 1 B. S. Shiralkar and Y. K. Cheung, TRACG Application for ESBWR, NEDC-33083-PA, March 2005.
- 2 United States Nuclear Regulatory Commission Standard Review Plan – NUREG 0800, 15.8, Rev 1, July 1981.
- 3 Assessment of BWR Mitigation of ATWS, NEDE-24222 (Volume 2), December 1979.
- 4 Qualification of the One-Dimensional Core Transient Model for Boiling Water Reactors, NEDO-24154-A and NEDE-24154-P-A, Volumes I, II and III. August 1986.
- 5 Qualification of the One-Dimensional Core Transient Model for Boiling Water Reactors, NEDO-24154-P-A (Supplement 1 – Volume 4), Revision 1. February 2000.
- 6 B. Boyack, et al., Quantifying Reactor Safety Margins: Application of Code Scaling, Applicability, and Uncertainty Evaluation Methodology to a Large-Break, Loss-of-Coolant Accident, NUREG/CR-5249. December 1989.
- 7 General Electric Standard Application for Reactor Fuel (GESTAR II), NEDE-24011-P-A-14. June 2000.
- 8 F. Bolger, et al., TRACG Application for Anticipated Transient Without Scram Pressure Analyses, NEDE-32906P Supplement 1 -A. November 2003.
- 9 TASC-03A, A Computer Program for Transient Analysis of a Single Channel, NEDC-32084P-A, Revision 2. July 2002.

- 10 Anticipated Transients Without Scram for Light Water Reactors, NUREG-0460, Volumes 1, 2, 3, December 1978.
- 11 J. G. M. Andersen, et al., TRACG Qualification, NEDE-32177P. January 2000.
- 12 J. G. M. Andersen, et al., TRACG Application for Anticipated Operational Occurrences Transient Analyses, NEDE-32906P. January 2000.
- 13 B. S. Shiralkar and R. E. Gamble, ESBWR Test and Analysis Program Description, NEDC-33079P, August 2002.
- 14 J. G. M. Andersen, et al., TRACG Model Description, NEDE-32176P.
- 15 J. R. Fitch, et al., TRACG Qualification for SBWR (Licensing Topical Report), NEDC-32725P, September 1997.
- 16 B. S. Shiralkar and R.E. Gamble, ESBWR Test and Analysis Program Description, NEDC-33079P, Supplement 1, Revision 0, August 2002.
- 17 J. R. Fitch, et al, NEDC-33080P, TRACG Qualification for ESBWR, Class III (GE Proprietary Information), dated August 2002.
- 18 S. A. Eide, et al., Reliability Study: General Electric Reactor Protection System, 1984–1995, NUREG/CR-5500, Vol. 3, INEL/EXT-97-00740, February 1999.
- 19 B. S. Shiralkar, L. A. Klebanov, and Y. K. Cheung, NEDE-33083P Supplement 1, TRACG Application for ESBWR Stability Analysis, December 2004.
- 20 K. T. Schaefer, NEDO-33175, Revision 1, Classification of ESBWR Abnormal Events and Determination of Their Safety Analysis Acceptance Criteria, February 2005.
- 21 NEDO-30130-A, Steady State Nuclear Methods, April 1985.
- 22 S. Morooka, T. Ishizuka, M. Iizuka and K. Yoshimura, Experimental Study on Void Fraction in a Simulated BWR Assembly (Evaluation of Cross-Sectional Averaged Void Fraction), Nuclear Engineering and Design 114, pp. 91-98 (1989).
- 23 T. Mitsutake, S. Morooka, K. Suzuki, S. Tsonoyama and K. Yoshimura, Void Fraction Estimation within Rod Bundles Based on Three-Fluid Model and Comparison with X-Ray CT Void Data, Nuclear Engineering and Design 120, pp. 203-212, (1990).
- 24 P. Saha and N. Zuber, Point of Net Vapor Generation and Vapor Void Fraction in Subcooled Boiling, Proceedings of the 5th International Heat Transfer Conference, Tokyo 1974.
- 25 NEDO-23785-1-A, Rev. 1, The GESTR-LOCA and SAFER Modes for the Evaluation of the Loss-of-Coolant Accident, Vol. 1: GESTR-LOCA – A Model for the Prediction of Fuel Rod Thermal Performance.

- 26 Supplemental Information for Plant Modifications to Eliminate Significant In-Core Vibrations", NEDE-21156, Jan 1976.
- 27 B. S. Shiralkar and R. E. Gamble, "ESBWR Test and Analysis Program Description", NEDC-33079P, (section 3.3), August 2002.
- 28 J. P. Walkush, "High Pressure counterflow CHF", EPRI Report 292-2, January 1975
- 29 V. P. Carey, Liquid-Vapor-Phase-Change Phenomena, Hemisphere Publishing, 1992.
- 30 R. E. Dimenna, et al., RELAP5/MOD2 Models and Correlations, NUREG/CR-5194 (EGG-2531), August 1988.
- 31 D. C. Groeneveld, S. C. Cheng and T. Doan, 1986 AECL-UO Critical Heat Flux Lookup Table, Heat Transfer Engineering 7, (pp. 46-62), 1986.
- 32 B. S. Shiralkar, et al., The GESTR-LOCA and SAFER Models for the Evaluation of the Loss-of-Coolant Accident, Volume III: SAFER/GESTR Application Methodology, NEDE-23785-1-PA, Rev. 1, October 1984.
- 33 P. Saha, A Study of Heat Transfer to Superheated Steam in a 4x4 Rod Bundle, NEDE-13462, June 1976.
- 34 B. S. Shiralkar, et al., SBWR Test and Analysis Program Description, NEDC-32391P, Rev.C, August 1995.
- 35 Takashi Hara, et al., *TRACG Application to Licensing Analysis*, (ICONE-7311), 7<sup>th</sup> International Conference on Nuclear Engineering, Tokyo, April 19-23 1999.
- 36 R. D. Blevins, Applied Fluid Dynamics Handbook, Van Nostrand, 1984.
- 37 G. B. Wallis, One-Dimensional Two-Phase Flow, McGraw-Hill, 1969.
- 38 GE Hitachi Nuclear Energy, ESBWR Design Control Document, Tier 1.
- 39 GE Hitachi Nuclear Energy, ESBWR Design Control Document, Tier 2.

## Appendix 1

**Movement of Injected Borated Solution through the Bypass Region**

The borated solution emerges from the injection nozzles as high velocity jets. The discharge velocity from the nozzles is of the order of 34 m/s. The borated solution is at a much lower temperature than the ambient fluid in the bypass region. Consequently, the density of the injected solution is approximately 40% higher than the bypass water. Note that the density of the sodium pentaborate salt is not a major factor at the salt concentrations in the injected solution; the density difference is almost entirely due to the difference in the density of water at the lower temperature. The specific gravity of the injected solution is 1.065, relative to a water specific gravity of 1.0 at 18 °C.

The jets traverse the annular space that constitutes the peripheral bypass region and impinge on the peripheral channels. Because of the density difference, the jets may also move downwards, but the horizontal velocities, being much larger, are predominant. Figure A1-2 shows a schematic of the cross-section at an injection elevation. By the time the jet reaches the channel boundary, the jet has entrained a substantial amount of ambient fluid and slowed down to a velocity of about 2 m/s and warmed up to within about 13 °C of the bypass ambient fluid. The impinging jet has begun to spread sideways and towards the shroud wall (as indicated in the figure by the backward arrows) but the complex geometry due to the channel walls is likely to prevent it from spreading extensively.

(For this analysis a jet angle with respect to the nozzle of 60 degrees was assumed. If the angle is greater and the jet is closer to the shroud wall, it could attach itself to the wall. This jet reattachment behavior is called the Coanda effect and has been observed in jets near solid boundaries [Reference 36]. This would result in even more mixing and dilution of the SLCS jet, which would adhere to the shroud wall and carry around until it encountered the wall jet from the adjacent nozzle. However, no credit is taken for a potential Coanda effect in this analysis.)

As the jet impinges on the channel wall, the heavier solution tends to sink downwards in the gap between the channels and the shroud wall. The movement of this plume is affected by the fluid velocity in the bypass. A sufficiently large upward velocity could carry the plume upwards. However, the TRACG results show that the vertical velocity in the bypass prior to boron injection is close to zero and slightly negative. This results in negatively buoyant downward plumes. The plumes sinking from the top injection point interacts with those directly below and reaches the bottom of the bypass with a small density surplus relative to the ambient fluid. The path of these plumes is sketched in Figure A1-3. The plumes are not likely to spread significantly in their descent and are confined to fairly narrow regions, one in each quadrant corresponding to the four nozzle locations along the periphery of the core shroud.

Having reached the bottom of the bypass, the borated solution (considerably diluted by this point) spreads peripherally and radially inwards along the top of the core support plate. As it spreads, the borated solution moves over guide tube openings (left side of Figure A1-4). Some of the solution could sink into the guide tubes and be lost from the viewpoint of achieving shutdown of the nuclear fission reaction in the core. The bulk of the boron makes its way into the fuel channels through the

leakage holes in the lower tieplates of the fuel channels. The peripheral fuel bundles could have a downward velocity at the inlet. If so, the boron entering these channels move downwards into the lower plenum. This boron re-enters the core when the flow velocities at the top of the lower plenum are upwards. The boron that enters the central channels moves upwards into the fuel bundles, carried up by the upward velocities in these bundles. Boron in the bypass as well as that in the fuel channels results in negative reactivity and the desired shutdown of the fission reaction.

The flow regimes discussed above are pieced together in a more quantitative manner in the following paragraphs.

**Initial Jet Regime**

Figure A1-1 is a schematic showing the nozzle location in the shroud wall and the approximate location of the outer boundary of the fuel channels. The channel boundary is based on a channel pitch of 15.5 cm and a distance of 19 channels from the core center to the periphery on four sides. This may underestimate the channel boundary at some locations but applies on the 90 degree sector boundaries. With a jet angle estimated to be 60 degrees on either side of the nozzle centerline, the distance along the jet centerline from the shroud wall to the channel boundary is estimated to be about 0.5m, or over 80 diameters, using a 6 mm initial jet diameter. The characteristics of the circular turbulent submerged jet are summarized by the empirical equations given below [Reference 36]. These are time-averaged properties of the turbulent jet, based on experimentally measured coefficients. The equations apply to the ‘fully developed’ region of the jet, that is the axial distance from the discharge point must be greater than the length of the initial region,  $x_i$

Circular Turbulent Jet Characteristics [Reference 36, Table 9-3, p 236]

Length of initial region, $x_i$	$10 r_0$
Centerline Velocity, $u_m$	$12 (r_0/x) U_0$
Velocity Profile, $u/ u_m$	$\exp[-94 (r/x)^2]$
Width, $b$ (where $u/ u_m = 0.5$ )	$0.086 x$
Volume flow rate, $Q$	$0.16 (x/r_0) Q_0$
Centerline Temperature Deficit, $\Delta T_m$	$10 (r_0/x) \Delta T_0$
Temperature Deficit Width, $b_{\Delta T}$ (where $\Delta T/\Delta T_m=0.5$ )	$0.11 x$
Temperature Deficit Profile, $\Delta T/\Delta T_m$	$\exp[-57 (r/x)^2]$

where

- $x$  – distance along jet centerline
- $r$  – jet radius at  $x$
- $r_0$  – initial jet radius
- $u_m$  – jet centerline velocity at  $x$
- $\Delta T_m$  – jet centerline temperature deficit at  $x$
- $U_0$  – jet initial velocity
- $\Delta T_0$  – jet initial temperature difference relative to the ambient temperature  
 $= T_{\text{bypass}} - T_0$ , where  $T_0$  is the injection temperature (18 °C) and  $T_{\text{bypass}}$  is the bypass temperature (300 °C) at the time SLCS injection begins based on TRACG calculations (Figures A1-5 and A1-6).

These equations have been derived assuming fluid at an ambient temperature  $T_{\text{bypass}}$  is drawn into the mixing region, but the density difference corresponding to the different temperature is not accounted for in the mass and momentum balances. Hence, this solution must be considered approximate when there are large differences between the injected and ambient densities. Accordingly, we use only the expression for the entrained volume of ambient liquid, but calculate the temperatures and densities using mass and energy balances.

Applying the above equations,

At jet discharge,

$$\begin{aligned} r_0 &= 0.003 \text{ m} \\ A_0 &= \pi r_0^2 = 2.827 \times 10^{-5} \text{ m}^2 \\ U_0 &= 34.2 \text{ m/s} \\ Q_0 &= U_0 A_0 = 0.000967 \text{ m}^3/\text{s} \end{aligned}$$

At channel outer boundary ( $x = 0.5\text{m}$ )

$$\begin{aligned} u_m &= 2.46 \text{ m/s} \\ Q_{\text{ch}} &= 0.026 \text{ m}^3/\text{s} \end{aligned}$$

This suggests that the centerline velocity of the jet is reduced by a factor of over 12 and the fluid entrained decreases the temperature deficit at the jet centerline by a large factor. Because the jet fluid is also heavier than the surrounding fluid, the jet likely droops, resulting in longer distance between the discharge and the channel boundary. Reference 36 provides criteria for determining if a buoyant jet behaves like a jet or like a buoyant plume. For jet-like behavior, the distance along the jet should be less than:

$$X_j < \Pi_0^{3/4} / B^{1/2}$$

where

$$\begin{aligned} \Pi_0 &= \text{initial jet specific momentum} = A_0 U_0^2 \\ B_0 &= \text{specific buoyancy flux} = Q_0 g (\rho_0 - \rho_{\text{bypass}}) / \rho_{\text{bypass}} \\ A_0 &= \text{initial jet area} \\ \rho_0 &= \text{density of injected fluid} \\ \rho_{\text{bypass}} &= \text{density of bypass inventory} \end{aligned}$$

Using typical values for the injected liquid density of  $1058 \text{ kg/m}^3$  and bypass water density at  $300 \text{ }^\circ\text{C}$  of  $712 \text{ kg/m}^3$  and the jet properties from the above relations,  $X_j$  becomes about  $1.14\text{m}$ , so the jet should retain jet-like behavior to the channel boundary.

### **Plumes with Negative Buoyancy**

The jet impinging on the channel wall tries to spread in a plane normal to the incident jet, i.e. the plane of the channel wall. Horizontal spreading is restricted by the adjacent channels and the shroud wall, and upward spreading is limited by negative buoyancy effects. It is assumed that a well-mixed region results from the termination of each jet, which is the source for a vertical plume with negative buoyancy. The size of this region is of the order of a channel width. The properties of this well-mixed region are calculated by averaging the jet conditions at the channel boundary.

$$\begin{aligned} M_0 &= Q_0 \rho_0 \\ M_{\text{induced}} &= (Q_{\text{ch}} - Q_0) \rho_{\text{Bypass}} \end{aligned}$$

$$M_{\text{total}} = M_0 + M_{\text{induced}}$$

Designating enthalpy by  $h$ ,

$$h_{\text{ave}} \sim (M_0 * h_0 + M_{\text{induced}} * h_{\text{bypass}}) / M_{\text{total}}$$

$$T_{\text{ave}} = 287.3 \text{ } ^\circ\text{C}$$

$$\rho_{\text{ave}} = 737 \text{ kg/m}^3$$

$$\text{Average temperature deficit} = \Delta T_{\text{ave}} = 13 \text{ } ^\circ\text{C}$$

First, we check for the effects of the bypass vertical velocity.

A modified Froude number can be calculated based on the hydraulic diameter of the peripheral bypass (twice the effective gap = 0.453 m), the average vertical velocity in the peripheral bypass (calculated by TRACG just prior to boron injection), and the density difference between the plume and the bypass ambient liquid.

$$Fr = \frac{\rho V^2}{g \Delta \rho D_h}$$

Generally, the Froude number must be of the order of 1 to cause the plume to be carried upwards. Experimental evidence exists in the form of tests for counter current flow limiting (CCFL) with gas-liquid flows. Tests have been performed in large downcomers with upward flow of a light species (gas) and downward flow of liquid. Downward liquid penetration was shut off when the square root of the gas Froude number is of the order of 0.14 [Reference 14].

If we assume a similar critical Froude number for the situation of liquid/liquid countercurrent flow, the critical upward velocity given by:

$$V_{\text{crit}} = 0.14 * \sqrt{(\Delta \rho / \rho) g D_h} = 0.055 \text{ m/s}$$

The velocity in the bypass region calculated by TRACG is downwards. Therefore, the plumes descend in the gap between the outer channels and the core shroud.

### **Spreading of Downward Plumes**

Each set of nozzles produces a plume that starts descending in the peripheral bypass to the core plate. The plume behaves more like a submerged jet at smaller distances from the sources. A minimum distance can be calculated beyond which plume spreading can be assumed.

This distance is given by:

$$X_j = \Pi^{3/4} / B^{1/2}$$

where

$$B = \text{specific buoyancy flux} = Q_{\text{ch}} g (\rho_{\text{ave}} - \rho_{\text{bypass}}) / \rho_{\text{bypass}}$$

where  $Q_{\text{ch}}$  is the initial volumetric flow source for the plume, taken as the flow carried in by the turbulent submerged jet with an initial mixed density  $\rho_{\text{ave}}$ .

$$\Pi = \text{initial plume specific momentum} = Q_{\text{ch}} U_{\text{ch}}$$

$\Pi$  is estimated as follows:

By conservation of momentum,  $(\rho_{ave} U_{ch}^2 A_{ch}) \sim (\rho_0 U_0^2 A_0)$

$$\Pi = (U_{ch}^2 A_{ch}) = (\rho_0 U_0^2 A_0) / \rho_{ave}$$

$$X_j = \Pi^{3/4} / B^{1/2} = 1.08m$$

The calculations based on a plume are valid only for distances greater than 1.08m. For distances shorter than 1.08m, it is assumed that the plume has not spread or mixed further with the ambient fluid.

Circular Plume Characteristics [Reference 36, Table 9-7, p 250]

Centerline Velocity, $u_m$	$3.5 B^{1/3} x^{-1/3}$
Axial Velocity Profile, $u / u_m$	$\exp[-57 (r/x)^2]$
Width, $b$ (where $u / u_m = 0.5$ )	$0.11 x$
Volume flow rate, $Q$	$0.15 B^{1/3} x^{5/3}$
Centerline Temperature Deficit, $\Delta T_m$	$11 (Q_{ch} \Delta T_{ave}) B^{-1/3} x^{-5/3}$
Temperature Deficit Width, $b_{\Delta T}$ (where $\Delta T / \Delta T_m = 0.5$ )	$0.10 x$
Temperature Deficit Profile, $\Delta T / \Delta T_m$	$\exp[-69 (r/x)^2]$

If the plumes from the four different elevations are assumed not to interact with each other, the volumetric flow rates in the plumes when they reach the bottom of the bypass can be calculated from the above table.

Only the top plume source is more than 1.08m from the bottom of the bypass. The lower plumes are assumed not to spread. The plume flow and average temperatures when they reach the core plate are calculated as below:

The volumetric flow rate  $Q_p$  is evaluated from Row 4 of the above table for  $x > 1.08m$ . For  $x < 1.08m$ , it is assumed flow is not entrained from the bypass and the initial plume flow reaches the core plate.

- 1)  $x = 1.45m$ ,  $Q_{p1} = 0.058 \text{ m}^3/\text{s}$
- 2)  $x = 1.05m$ ,  $Q = 0.026 \text{ m}^3/\text{s}$
- 3)  $x = 0.65m$ ,  $Q = 0.026 \text{ m}^3/\text{s}$
- 4)  $x = 0.25m$ ,  $Q = 0.026 \text{ m}^3/\text{s}$

The total source from the four elevations is  $0.136 \text{ m}^3/\text{s}$ . The average temperature deficit is calculated as before through an energy balance:

$$M_{ch} = 4 * M_{jet} = 4 * 18.7$$

$$M_{induced} = (0.136 - 4 * 0.026) * \rho_{bypass}$$

$$T_p = (M_{ch} * T_{ave} + M_{induced} * T_{bypass}) / M_{total} = 290.2 \text{ C}$$

$$\Delta T_p = 10 \text{ C.}$$

The corresponding density difference relative to the ambient fluid ( $\Delta \rho / \rho$ ) is 0.027.

These sources of borated solution spread peripherally and radially at the bottom of the bypass.

### Settling of Boron into Guide Tubes

The possibility of boron settling into the guide tubes is evaluated by calculating the critical velocity at the top of the guide tubes that prevents settling. The critical velocity is based on a corresponding critical Froude number. Analogy with CCFL data at similar locations shows that the square root of the Froude number for shutoff of downflow is of the order of 0.5 to 0.6, though values as high as 1 are possible with sharp edged openings [Reference 37].

Using a limiting value of 1 yields a critical velocity of:

$$V_{crit} = 1.0 * \sqrt{(\Delta\rho / \rho)gD_h}$$

For a temperature deficit of 10 °C,  $\Delta\rho / \rho$  is 0.027. The hydraulic diameter for the guide tube opening is approximately 1 cm.

$$V_{crit} = 0.05 \text{ m/s}$$

Thus, velocities of the order of 5 cm/s at the top of the guide tubes should prevent any settling of boron into the guide tubes.

### Settling of Boron into the Lower Plenum from the Channel Inlet Nosepieces

Boron enters the bottom of the fuel channels with the leakage flow through leakage paths between the bypass and the fuel bundles. The largest leakage path consists of holes drilled in the lower tieplate (right hand side of Figure A1-4). If flow is draining through the lower nosepiece of the tieplate, the boron travels with this flow into the lower plenum. If the inlet velocity at the nosepiece is large and upward, the boron will tend to move up with the flow into the active fuel region. In a range of velocities between zero and a critical upward velocity, boron could settle downwards due to the density difference between the borated solution and the ambient liquid in the inlet region. TRACG would not calculate this settling behavior and would therefore be non-conservative in this range of velocities. The critical velocity is calculated as before through a critical Froude number.

$$V_{crit} = 1.0 * \sqrt{(\Delta\rho / \rho)gD_h}$$

The leakage flow enters the channel inlet region through small leakage paths, with the dominant path being two 7 mm holes in the wall of the inlet nosepiece. About 40% of the flow comes through leakage paths between the tieplate and the channel box, with clearances of the order of 1 mm. An area-averaged path size of 3 mm was calculated for the leakage flow. The inlet temperature of the jets is assumed to be the temperature of the boron plumes at the core plate. The temperature inside the nosepiece is assumed to be the same as the bypass temperature of 300 °C. Typical velocities for the leakage jets are of the order of 1 to 2 m/s. Jet like behavior persists for

$$X_j < \Pi_0^{3/4} / B^{1/2}$$

where

$$\Pi_0 = \text{initial jet specific momentum} = A_0 U_0^2$$

$$B_0 = \text{specific buoyancy flux} = Q_0 g (\rho_0 - \rho_{LTP}) / \rho_{LTP}$$

$$X_j < \Pi_0^{3/4} / B^{1/2} = 0.12 \text{ m}$$

Thus, the entering leakage travels as jets for approximately 4 cm to the center of the nosepiece. Using the formula for circular jets from Section 3 above,

$$Q = 0.16 (x/r_0) Q_0 = 4.26 Q_0$$

and the temperature deficit is reduced by this factor to  $(300-290.2)/4.26=2.3$  °C.

Thus, the temperature deficit of 10°C at the bottom of the bypass is reduced to approximately 2.3 °C by mixing within the nosepiece. For a temperature deficit of 2.3 °C,  $\Delta\rho/\rho$  is 0.0065. The hydraulic diameter for the lower tieplate opening is approximately 8 cm.

$$V_{crit} = 0.07 \text{ m/s}$$

Thus, velocities of the order of 7 cm/s at the inlet to the fuel bundle should prevent any settling of boron into the lower plenum. The MSIV closure ATWS transient was analyzed with TRACG and the period where bundle inlet velocities were in the range of 0- 7 cm/s was evaluated. The fraction of the boron that could settle into the lower plenum through the lower tieplate holes was calculated to be less than 10% of the injected boron up to the time of core shutdown. A sensitivity study in Section 8.2 (Table 8.2-5) shows that the effect of this settling is negligible.

In the peripheral bundles, the flow through the lower tieplates is downwards. Hence, the borated flow through the leakage paths is carried down into the lower plenum. The borated flow enters with a density differential of 0.027. It is further considerably diluted by the downward flow of saturated water through the bundle. Thus the flow discharging from the side entry orifices into the lower plenum are well mixed and essentially at saturation temperature. Further consideration of stratification within the lower plenum is not required.

#### **Change in Bypass Temperature during the ATWS Transient**

The SLCS jets discharging into the peripheral bypass entrain large amounts of ambient fluid from the peripheral bypass region. As the transient progresses, the average temperature of the bypass fluid feeding the jets changes. In order to account for the transient history, results of the TRACG analysis are examined. The flow in the bypass region is downward through this phase of the transient. Flow leaving the bypass through the leakage holes in the channels is replaced by downflow from the upper plenum. Figures A1-5 and A1-6 show the temperature history in the bypass region during an ATWS event. Here Level 5 is the SLCS injection level (all four elevations are within Level 5) and Level 7 is above the injection location. At the time of boron injection (~200 s), the bypass temperatures are uniform and close to 573 K (300°C). Shutdown by boron is achieved before 400 s. During this period, the temperature in the upper level, which is the upstream region away from the immediate vicinity of the jets, drops by less than 1°C. Level 5 shows a bigger drop (~15 C in the sectors where boron is injected) because TRACG calculates the mixed temperature with the colder borated solution. However, it is reasonable to assume that the liquid entrained by the jets from the bypass is closer in temperature to that in Level 7. Hence, no changes are needed in the current analysis to track the temperature history in the bypass ambient temperature.

#### **Implications for TRACG Analysis**

[[

]]

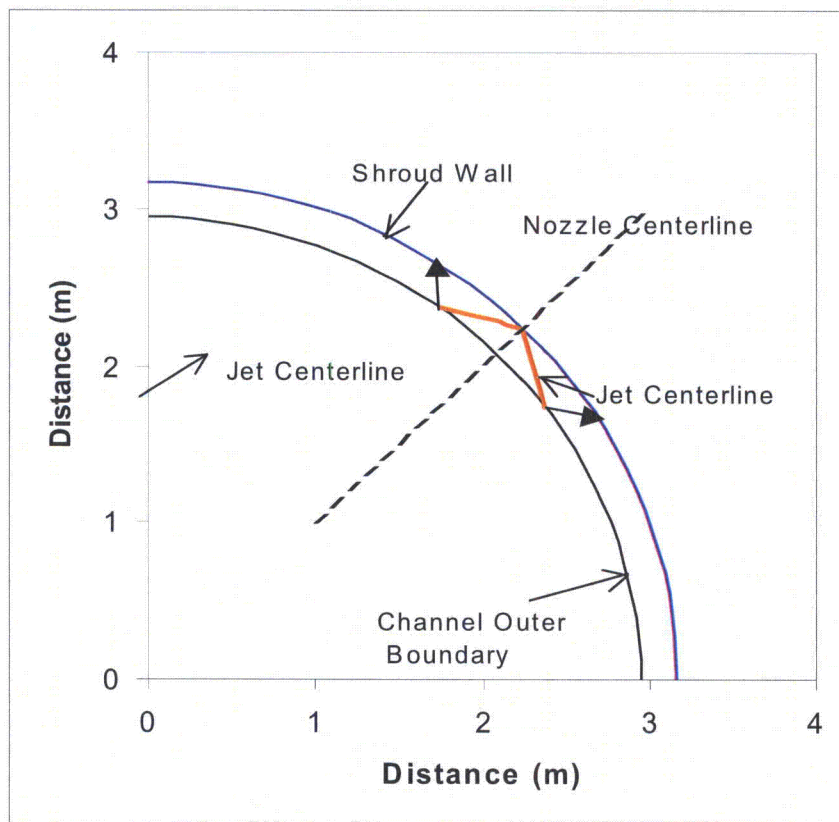


Figure A1-1. Overall geometry of Injected jets and peripheral Bypass

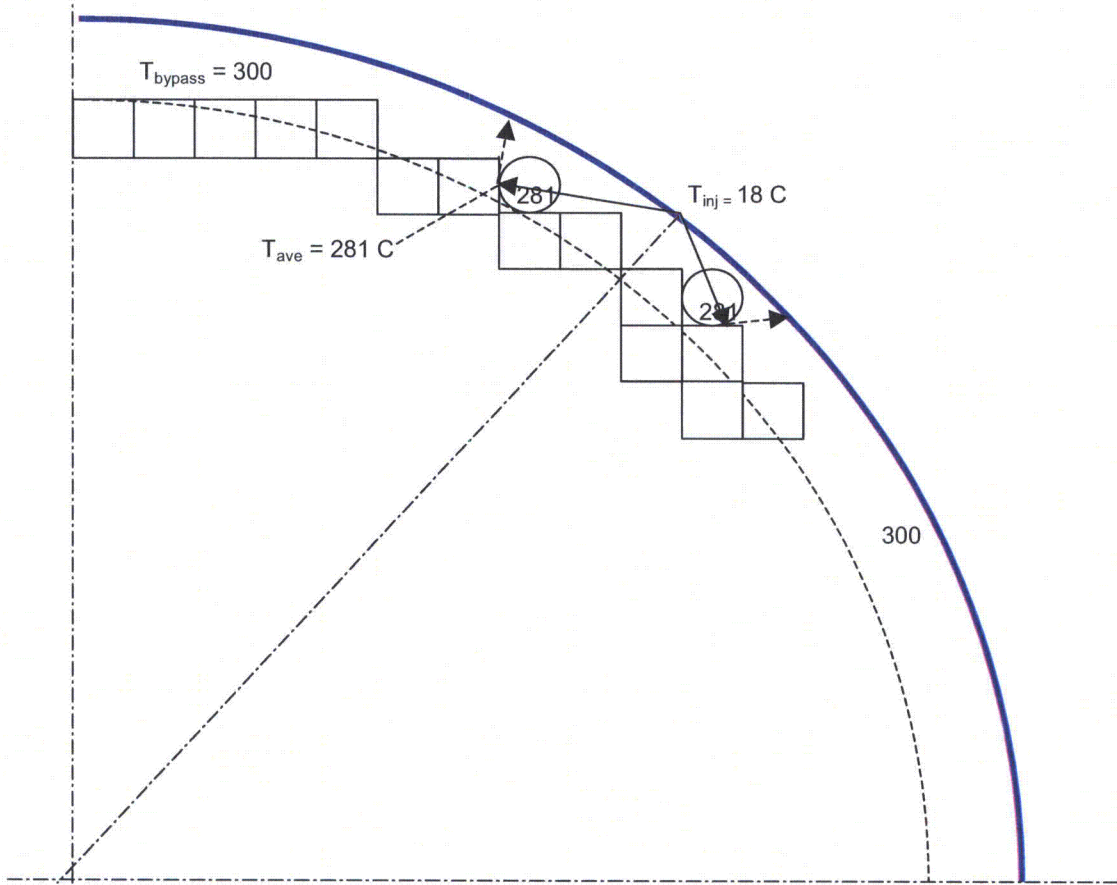
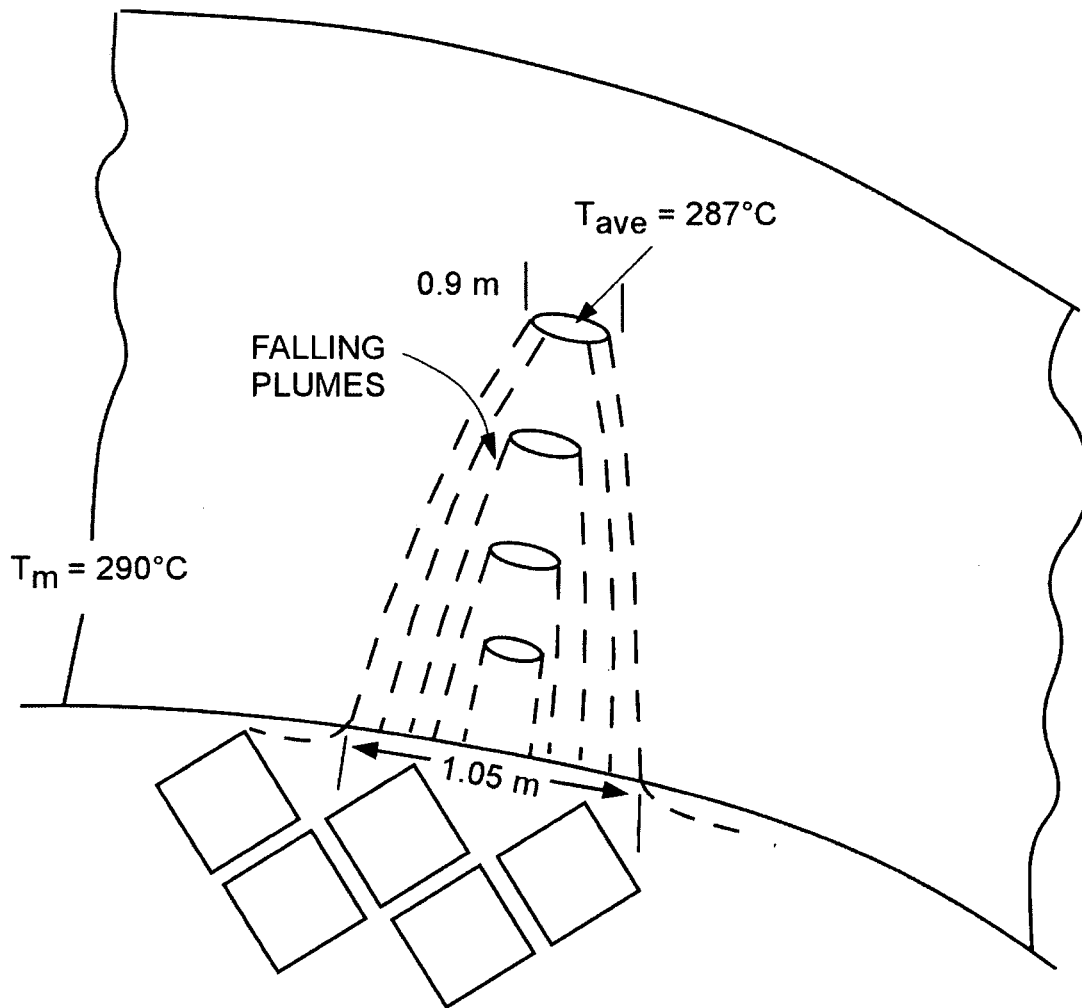


Figure A1-2. Channel Geometry and Jet Properties in Cross-section of Injection Locations



**Figure A1-3. Downward Plumes in Annular Space**

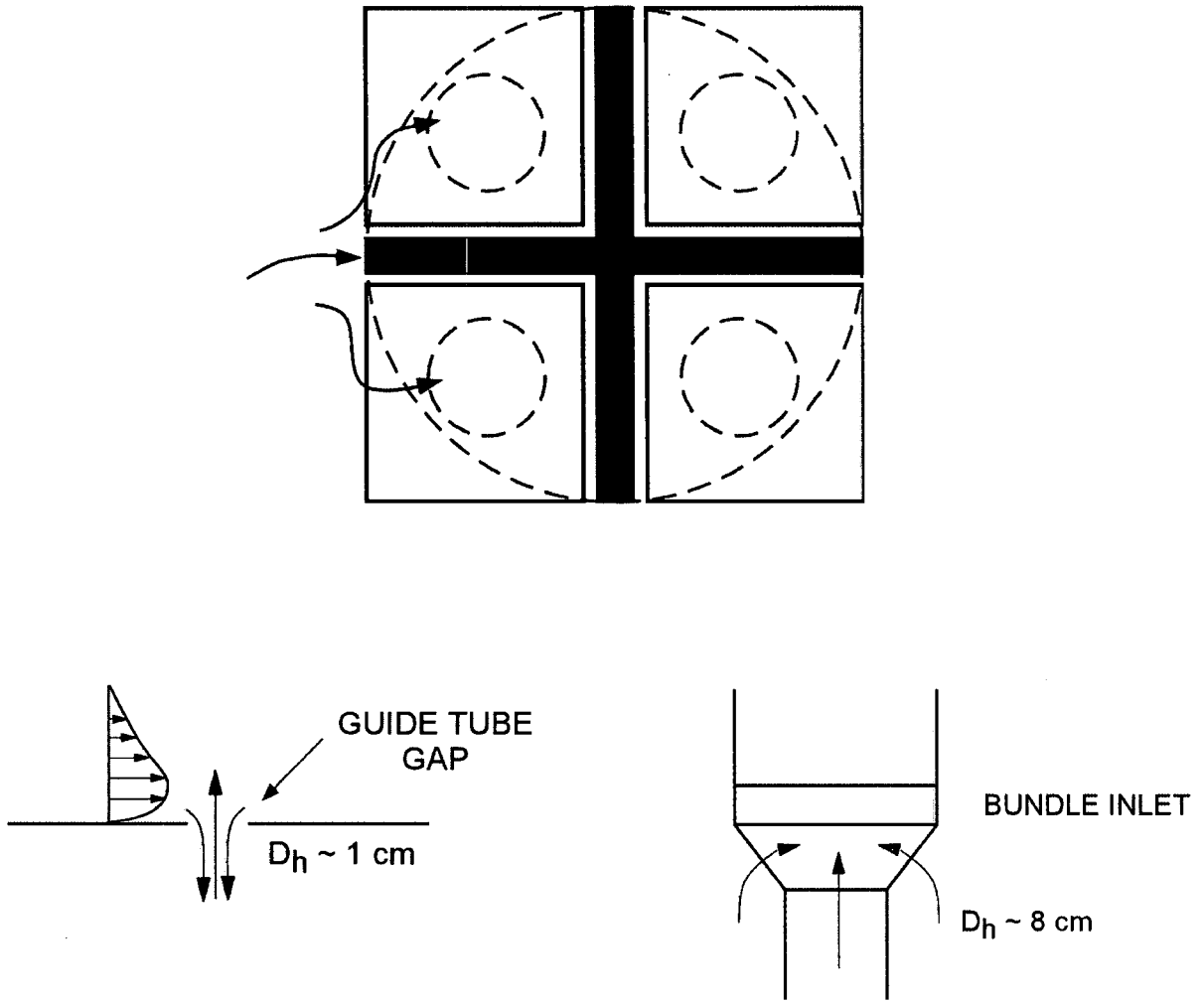


Figure A1-4: Boron settling in guide tubes and lower plenum

[[

]]

**Figure A1-5: Liquid temperatures calculated in the bypass region by TRACG at Level 7  
(above injection elevation)**

[[

]]

**Figure A1-6. Liquid temperatures calculated in the bypass region by TRACG at Level 5  
(Injection Elevation)**

## Appendix 2

Note: The numbering of references, tables, figures, and appendices within this appendix correspond to the RAI reference number, and the RAI is reproduced verbatim as submitted.

### **NRC RAI 21.6-8**

*You state on Page 5-8 (there is a similar statement on Page 5-2) "the boron will be confined to fairly narrow regions of the shroud circumference (~1m in width) as it descends to the bottom of the bypass. One way to bound this issue is to confine the azimuthal movement of liquid between sectors by isolating them above the lowest level in the bypass." Which azimuthal sectors is the SLCS injecting into? Explain how the azimuthal noding is conservative even though the smallest node it could inject into is much larger than 1m. [[*

*]]*

### **GE Response**

Page 5-8 of the ATWS LTR (Reference 21.6-8-1) states, "the boron will be confined to fairly narrow regions of the shroud circumference (~1 m in width) as it descends to the bottom of the bypass." In the LTR (Reference 21.6-8-1) SLCS is injected into [[ ]], as shown in red in Figure 21.6-8-1. The injection sectors are [[ ]] in width (interpreting "width" to mean "arc length of the outside wall of the sector").

The purpose of this RAI response is to demonstrate that the size of the injection sector does not have a significant effect on shutdown time, peak suppression pool temperature or peak dome pressure. The approach taken is to perform TRACG sensitivity calculations for the injection sector size, [[ ]] and the number of radial rings modeling the peripheral bypass, and compare the key ATWS parameters with the LTR case in Reference 21.6-8-1. [[

]]

These comparisons confirm the conservatism demonstrated in the TRACG ATWS analysis for the MSIVc event in the ATWS LTR (Reference 21.6-8-1).

**Figure 21.6-8-1 Injection Sectors in ESBWR Core**

[[ ]]

In order to evaluate the effect of sector size, [[ ]] and nodalization, three different sets of cases are compared. In the LTR case in Reference 21.6-8-1, the “net shutdown duration”, which is the time from the initiation of SLCS injection to the time when the core power reduced to [[ ]], was about [[ ]]. From core shutdown perspective, the longer this calculated duration in the analysis, the more conservative is the analysis.

Case 1. (Sensitivity to Injection Sector Size) Comparison of key ATWS output parameters such as shutdown time, peak pool temperature, and peak dome pressure is made between the base case calculation with large sector injection (similar to the ATWS calculation in Reference 21.6-8-1), and a case run with small sector injection.

Case 2. (Sensitivity to Radial and Azimuthal Blockage) Comparison is made between a large sector injection case and a small sector injection case, both with azimuthal and radial blockage removed.

Case 3. (Sensitivity to Finer Radial Nodalization of the Peripheral Bypass) A comparison between a [[ ]] core (an additional core ring compared to the base case in Reference 21.6-8-1) and the base case core. The additional ring of the core represents the peripheral bypass and includes only the peripheral bypass space of the core and the peripheral orifice bundles. Both large and small sector injection sensitivity cases have been performed with this combination. The additional core ring case with large sector injection is described in response to RAI 21.6-41.

**Summary of Results for the ATWS TRACG Sensitivity Analysis Cases**

Key results are summarized below by case. Details follow in the subsequent sections.

Results for Case 1: Sensitivity comparisons (Large Sector vs. Small Sector Injection, with Blockage) shown in Table 21.6-8-1 indicate that the shutdown time for the large sector injection case (LTR) is [[ ]] than for the small sector injection case. The peak pool temperature and peak dome pressure are [[ ]].

Results for Case 2: Sensitivity comparisons (Large and Small Sector Injection without Artificial Blockage) shown in Table 21.6-8-2 indicate [[ ]]

]]

Results for Case 3: Sensitivity comparisons in Table 21.6-8-3 [[ ]]

]]

### **Case 1 - Large Sector Versus Small Sector Injection with Artificial Blockage**

In order to evaluate the possible non-conservatism of injecting into the large vs. small azimuthal sectors, a TRACG sensitivity study has been performed injecting SLCS flow to the small sectors, which are [[ ]] in arc length compared to the [[ ]] arc length for the large sectors.

The shutdown time is [[ ]] in the case of the small sector injection, as shown in Table 21.6-8-1. [[ ]]

]]

Appendix 21.6-8-A includes a mass balance over the injection cells, [[ ]] Evaluation of Equations 1 and 2 in the Appendix shows that the flow velocity out of one small sector versus two large sectors differs only by the area of the sectors. A larger sector, with a larger bottom face area, yields a slower velocity out of the bottom of the node.

The difference between the large and small sector injection is only [[ ]] maximum suppression pool temperature. [[ ]]

This result of this sensitivity study [[ ]]

]]

**Table 21.6-8-1 Main ATWS Parameters for Large Versus Small Sector Injection (both with artificial blockage)**

Case 1	Shutdown Time (s)	Maximum Suppression Pool Temperature (°K)	Peak Dome Pressure (MPa)
[[			
			]]

**Case 2 – Large and Small Sector Injection without Artificial Blockage**

The second set of cases is large and small sector injection with the artificial blockage removed. The outputs of interest to this calculation are shown in Table 21.6-8-2.

[[

]]

**Table 21.6-8-2 Main ATWS Parameters for Large vs. Small Sector Injection (no blockage)**

Case 2	Shutdown Time (s)	Maximum Suppression Pool Temperature (°K)	Peak Dome Pressure (MPa)
[[			
			]]

**Case 3 - 4 Core Rings (Blocked and Unblocked Case)**

Table 21.6-8-3 shows sensitivity comparisons for the blocked vs. unblocked 4-Ring core case

[[

]]

**Table 21.6-8-3 Main ATWS Parameters for 4-Ring Case  
(Blocked vs. Unblocked)**

Case 3	Shutdown Time (s)	Maximum Suppression Pool Temperature (°K)	Peak Dome Pressure (MPa)
[[			
			]]

[[

]]

Figures 21.6-8-4 and 21.6-8-5 illustrate boron mass flow rate from bypass region into the channels through the leakage holes. [[

]]

[[

]]

[[

]]

[[ ]]

**Figure 21.6-8-2 Boron Mass Flow Rate Into Channels in Blocked 4 Ring Core Case**

[[ ]]

**Figure 21.6-8-3 Boron Mass Flow Rate into Channels in Unblocked 4 Ring Core Case**

**Conclusions**

[[

]]

**Reference**

- 21.6-8-1. NEDE 33083P Supplement 2, "Licensing Topical Report TRACG Application for ESBWR Anticipated Transient Without Scram Analysis," GE Energy Nuclear, January 2006.

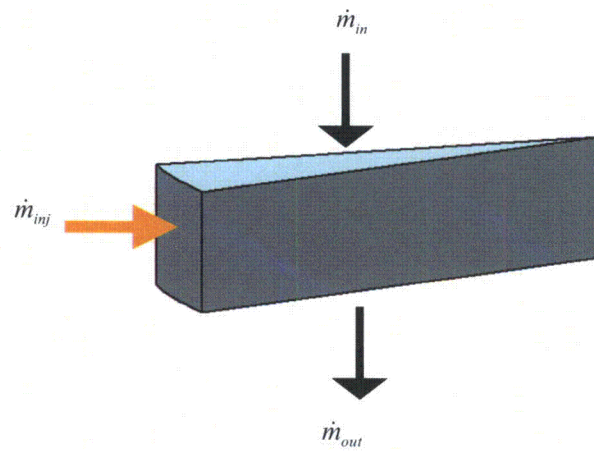
**Affected Documents**

No changes to the ESBWR Tier 2 DCD will be made in response to this RAI.

The ATWS LTR (NEDE 33083P Supplement 2) will be revised to include discussion of the sensitivity studies that are described in this RAI response. The revision is scheduled for issue September 20, 2007.

Appendix 21.6-8-A: Mass Flow in Large and Small Sector Blockage Cases

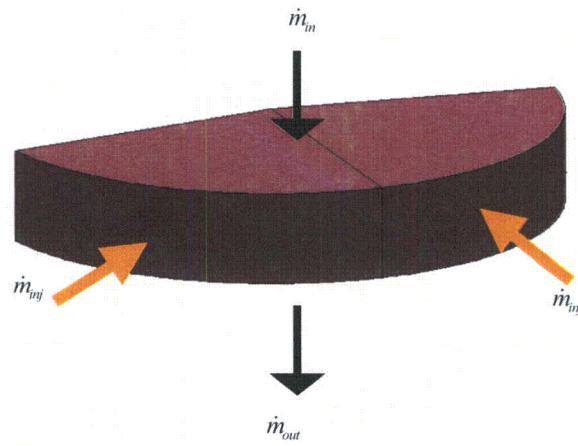
[[



$\dot{m}$   
 $\dot{m}$   
 $\dot{m}$   
 $\dot{m}$

$\dot{m}$     $\dot{m}$     $\dot{m}$   
 $\dot{m}$

$$V_{botLS} = \frac{\rho_w V_{in}}{\rho_{mix}} + \frac{\dot{m}_{inj}}{A_{SS} \rho_{mix}}$$



$\dot{m}$   
 $\dot{m}$   
 $\dot{m}$   
 $\dot{m}$

$\dot{m}$

$\dot{m}$     $\dot{m}$     $\dot{m}$   
 $\dot{m}$   
 $\dot{m}$

$$V_{outLS} = \frac{\rho_w V_{in}}{\rho_{mix}} + \frac{\dot{m}_{inj}}{2A_{LS}\rho_{mix}}$$

]]

**NRC RAI 21.6-41**

*When SLCS injects boron into the outer ring of the TRACG model, a uniform boron concentration is smeared throughout the entire fluid volume. Provide additional information justifying how this is conservative.*

**GE Response**

In the TRACG ATWS analysis, the injected boron is averaged over the entire injection cell. [[

]] The areas over which the boron reactivity is averaged in Reference 21.6-41-1 (LTR case) and the base case are shown in Figure 21.6-41-1. To address this point, a sensitivity case has been run with an additional core ring. [[  
]] Figure 21.6-41-2 shows the SLCS injection cells for the radial nodalization sensitivity case. [[

]]

Sensitivity studies have been performed with TRACG to address the issue.

[[

]]

**Renodalization**

The LTR case has [[

]]

The concern is that the SLCS injects into [[

]]

**Figure 21.6-41-1 LTR Case Vessel Model (3 Core Rings)  
(Red Regions Indicate the SLCS Injection cells for Vessel Level 5)**

[[

]]

The purpose of the renodalization study is to address potential boron smearing in the existing [[

]]

**Figure 21.6-41-2 Renodalized Case (4 Core Ring) Vessel Model, Red Regions Indicate the cells that boron inject into for Vessel Level 5**

[[

]]

**Results**

[[

]]

[[

]]

[[

]]

[[

]]

**Table 21.6-41-1 Main Parameters for 4-Ring vs. 3-Ring core Case**

Case 3	Shutdown Time (s)	Maximum Suppression Pool Temperature (°K)	Peak Dome Pressure (MPa)
[[			
			]]

**Reference**

21.6-41-1. NEDE 33083P Supplement 2, "Licensing Topical Report TRACG Application for ESBWR Anticipated Transient Without Scram Analysis," GE Energy Nuclear, January 2006.

**Affected Documents**

No changes to the ESBWR Tier 2 DCD will be made in response to this RAI.

The ATWS LTR (NEDE 33083P Supplement 2) will be revised to include discussion of the sensitivity studies that are described in this RAI response. The revision is scheduled for issue September 20, 2007.

**Appendix 21.6-41-A**

[[

]] This has been discussed separately in response to RAI 21.6-8.

[[

]] Figures 21.6-41-3 through 21.6-41-12 display the boron mass in the bypass region (Levels 4 and 5) and in the lower plenum region below the core (Level 3). Figures 21.6-41-3 through 21.6-41-6 show the mass of boron in [[ ]]. Figures 21.6-41-7 through 21.6-41-10 show the boron mass in [[ ]].

The base case (Figure 21.6-41-3) [[

]] This can be seen in Figures 21.6-41-7 and 21.6-41-8. In Figure 21.6-41-7, the base case, [[ ]], while in Figure 21.6-41-8, [[ ]]

[[

]]

[[

.  
. .  
. .

**Figure 21.6-41-3 Base Case**

]]

[[

]]

[[

]]

**Figure 21.6-41-4 Unblocked 3-Ring Core Case**

[[

]]

[[

]]

**Figure 21.6-41-5 Blocked 3-Ring Core Case with Small Sector Injection  
Boron Mass in Ring 3**

[[

]]

**Figure 21.6-41-6 Unblocked 3-Ring Core Case with Small Sector Injection  
Boron Mass in Ring 3**

[[ ]]

**Figure 21.6-41-7 Base Case (Blocked 3-Ring Core Case with Large Sector Injection)  
Boron Mass in Ring 2**

[[ ]]

**Figure 21.6-41-8 Unblocked 3-Ring Core Case with Large Sector Injection  
Boron Mass in Ring 2**

[[

]]

**Figure 21.6-41-9 Blocked 3-Ring Core Case with Small Sector Injection  
Boron Mass in Ring 2**

[[

]]

**Figure 21.6-41-10 Unblocked 3-Ring Core Case with Small Sector Injection  
Boron Mass in Ring 2**

NEDO-33083 Supplement 2-A Revision 2

**Attachment 1**

**NRC SAFETY EVALUATION**

**TRACG APPLICATION FOR  
ESBWR ANTICIPATED TRANSIENT WITHOUT SCRAM  
ANALYSES**

**Public Information Notice**

This is a public version of the NRC Safety Evaluation for NEDE-33083 Supplement 3P-A Revision 1 which was provided as enclosure 1 in the enclosed SER letter. Proprietary portions of the document that have been removed are indicated by white space within double square brackets, as shown here [[ ]]

October 20, 2010

Mr. Jerald G. Head  
Senior Vice President, Regulatory Affairs  
GE Hitachi Nuclear Energy  
3901 Castle Hayne Road MC A-18  
Wilmington, NC 28401

SUBJECT: FINAL SAFETY EVALUATION FOR GE HITACHI NUCLEAR ENERGY  
ADDENDUM TO THE SAFETY EVALUATION FOR LICENSING TOPICAL  
REPORT NEDE-33083P, SUPPLEMENT 2, REVISION 2, "TRACG  
APPLICATION FOR ESBWR ANTICIPATED TRANSIENT WITHOUT SCRAM  
ANALYSES"

Dear Mr. Head:

On August 24, 2005, GE Hitachi (GEH) Nuclear Energy submitted the Economic Simplified Boiling Water Reactor (ESBWR) design certification application to the staff of the U.S. Nuclear Regulatory Commission. Subsequently, in support of the design certification, GEH submitted license topical report (LTR) NEDE-33083P, Supplement 2, Revision 2, "TRACG Application for ESBWR Anticipated Transient Without Scram Analyses." The staff has now completed its review of NEDE-33083P.

The staff finds NEDE-33083P, Supplement 2, Revision 2, "TRACG Application for ESBWR Anticipated Transient Without Scram Analyses," acceptable for referencing for the ESBWR design certification to the extent specified and under the limitations delineated in the LTR and in the associated safety evaluation (SE). The SE, which is enclosed, defines the basis for acceptance of the LTR.

The staff requests that GEH publish the revised proprietary and non-proprietary versions of the LTR listed above within 1 month of receipt of this letter. The accepted version of the topical report shall incorporate this letter and the enclosed SE and add an "-A" (designated accepted) following the report identification number.

If NRC's criteria or regulations change, so that its conclusion that the LTR is acceptable is invalidated, GEH and/or the applicant referencing the LTR will be expected to revise and resubmit its respective documentation, or submit justification for continued applicability of the LTR without revision of the respective documentation.

Document transmitted herewith contains sensitive unclassified information. When separated from the enclosures, this document is "DECONTROLLED."

J. Head

- 2 -

Pursuant to 10 CFR 2.390, we have determined that the enclosed SE contains proprietary information. We will delay placing the non-proprietary version of this document in the public document room for a period of 10 working days from the date of this letter to provide you with the opportunity to comment on the proprietary aspects only. If you believe that any additional information in Enclosure 1 is proprietary, please identify such information line by line and define the basis pursuant to the criteria of 10 CFR 2.390.

The Advisory Committee on Reactor Safeguards (ACRS) subcommittee, having reviewed the subject LTR and supporting documentation, agreed with the staff's recommendation for approval following the August 16, 2010, ACRS subcommittee meeting.

Sincerely,

***/RA Frank Akstulewicz for:/***

David B. Matthews, Director  
Division of New Reactor Licensing  
Office of New Reactors

Docket No. 52-010

Enclosure:

1. Safety Evaluation (Non-Proprietary)
2. Safety Evaluation (Proprietary): Applicant only

cc: See next page

J. Head

- 2 -

Pursuant to 10 CFR 2.390, we have determined that the enclosed SE contains proprietary information. We will delay placing the non-proprietary version of this document in the public document room for a period of 10 working days from the date of this letter to provide you with the opportunity to comment on the proprietary aspects only. If you believe that any additional information in Enclosure 1 is proprietary, please identify such information line by line and define the basis pursuant to the criteria of 10 CFR 2.390.

The Advisory Committee on Reactor Safeguards (ACRS) subcommittee, having reviewed the subject LTR and supporting documentation, agreed with the staff's recommendation for approval following the August 16, 2010, ACRS subcommittee meeting.

Sincerely,

***/RA Frank Akstulewicz for:/***

David B. Matthews, Director  
Division of New Reactor Licensing  
Office of New Reactors

Docket No. 52-010

Enclosure:

1. Safety Evaluation (Non-Proprietary)
2. Safety Evaluation (Proprietary): Applicant only

cc: See next page

ADAMS ACCESSION NO. - ML102810123-Package

\*Via e-mail

NRO-002

OFFICE	BWR:PM	BWR:LA*	SRSB:BC*	BWR:LPM	BWR:BC	OGC/NLO*	DNRL:D
NAME	BBavol	SGreen	JDonoghue	ACubbage	MTonacci (B Bavol for)	SKirkwood	DMatthews
DATE	10/13/10	10/06/10	10/12/10	10/12/10	10/15/10	10/15/10	10/20/10

**OFFICIAL RECORD COPY**

SUBJECT: FINAL SAFETY EVALUATION FOR GE HITACHI NUCLEAR ENERGY  
ADDENDUM TO THE SAFETY EVALUATION FOR LICENSING TOPICAL REPORT NEDE-  
33083P, SUPPLEMENT 2, REVISION 2, "TRACG APPLICATION FOR ESBWR ANTICIPATED  
TRANSIENT WITHOUT SCRAM ANALYSES" DATED OCTOBER 20, 2010

Distribution:

Hard Copy:

NGE1 R/F

ACubbage

BBavol

Email:

RidsNroDnrINge1

NGE 1/2 Group

RidsAcrsAcnwMailCenter

RidsOgcMailCenter

JDonoghue

ACubbage

BBavol

DC GEH - ESBWR Mailing List

(Revised 08/11/2010)

cc:

Ms. Michele Boyd  
Legislative Director  
Energy Program  
Public Citizens Critical Mass Energy  
and Environmental Program  
215 Pennsylvania Avenue, SE  
Washington, DC 20003

Mr. Tom Sliva  
7207 IBM Drive  
Charlotte, NC 28262

## DC GEH - ESBWR Mailing List

### Email

aec@nrc.gov (Amy Cubbage)  
APH@NEI.org (Adrian Heymer)  
awc@nei.org (Anne W. Cottingham)  
bevans@enercon.com (Bob Evans)  
bgattoni@roe.com (William (Bill) Gattoni)  
BrinkmCB@westinghouse.com (Charles Brinkman)  
cberger@energetics.com (Carl Berger)  
charles.bagnal@ge.com  
charles@blackburncarter.com (Charles Irvine)  
chris.maslak@ge.com (Chris Maslak)  
CumminWE@Westinghouse.com (Edward W. Cummins)  
cwaltman@roe.com (C. Waltman)  
Daniel.Chalk@nuclear.energy.gov (Daniel Chalk)  
david.hinds@ge.com (David Hinds)  
david.lewis@pillsburylaw.com (David Lewis)  
David.piepmeyer@ge.com (David Piepmeyer)  
donaldf.taylor@ge.com (Don Taylor)  
erg-xl@cox.net (Eddie R. Grant)  
gcesare@enercon.com (Guy Cesare)  
GEH-NRC@hse.gsi.gov.uk (Geoff Grint)  
GovePA@BV.com (Patrick Gove)  
gzinke@entergy.com (George Alan Zinke)  
hickste@earthlink.net (Thomas Hicks)  
hugh.upton@ge.com (Hugh Upton)  
james.beard@gene.ge.com (James Beard)  
jerald.head@ge.com (Jerald G. Head)  
Jerold.Marks@ge.com (Jerold Marks)  
jgutierrez@morganlewis.com (Jay M. Gutierrez)  
Jim.Kinsey@inl.gov (James Kinsey)  
jim.riccio@wdc.greenpeace.org (James Riccio)  
joel.Friday@ge.com (Joel Friday)  
Joseph\_Hegner@dom.com (Joseph Hegner)  
junichi\_uchiyama@mnes-us.com (Junichi Uchiyama)  
kimberly.milchuck@ge.com (Kimberly Milchuck)  
KSutton@morganlewis.com (Kathryn M. Sutton)  
kwaugh@impact-net.org (Kenneth O. Waugh)  
lchandler@morganlewis.com (Lawrence J. Chandler)  
lee.dougherty@ge.com  
Marc.Brooks@dhs.gov (Marc Brooks)  
maria.webb@pillsburylaw.com (Maria Webb)  
mark.beaumont@wsms.com (Mark Beaumont)  
matias.travieso-diaz@pillsburylaw.com (Matias Travieso-Diaz)  
media@nei.org (Scott Peterson)  
mike\_moran@fpl.com (Mike Moran)

DC GEH - ESBWR Mailing List

MSF@nei.org (Marvin Fertel)  
mwetterhahn@winston.com (M. Wetterhahn)  
nirsnet@nirs.org (Michael Mariotte)  
Nuclaw@mindspring.com (Robert Temple)  
patriciaL.campbell@ge.com (Patricia L. Campbell)  
Paul@beyondnuclear.org (Paul Gunter)  
peter.yandow@ge.com (Peter Yandow)  
pshastings@duke-energy.com (Peter Hastings)  
rick.kingston@ge.com (Rick Kingston)  
RJB@NEI.org (Russell Bell)  
Russell.Wells@Areva.com (Russell Wells)  
sabinski@suddenlink.net (Steve A. Bennett)  
sandra.sloan@areva.com (Sandra Sloan)  
sara.andersen@ge.com (Sara Anderson)  
sfrantz@morganlewis.com (Stephen P. Frantz)  
stephan.moen@ge.com (Stephan Moen)  
steven.hucik@ge.com (Steven Hucik)  
strambgb@westinghouse.com (George Stramback)  
tdurkin@energetics.com (Tim Durkin)  
timothy1.enfinger@ge.com (Tim Enfinger)  
tom.miller@hq.doe.gov (Tom Miller)  
trsmith@winston.com (Tyson Smith)  
Vanessa.quinn@dhs.gov (Vanessa Quinn)  
Wanda.K.Marshall@dom.com (Wanda K. Marshall)  
wayne.marquino@ge.com (Wayne Marquino)  
whorin@winston.com (W. Horin)

**SAFETY EVALUATION BY THE OFFICE OF NEW REACTORS  
"TRACG APPLICATION FOR ESBWR  
ANTICIPATED TRANSIENT WITHOUT SCRAM ANALYSES,"  
NEDE-33083P, SUPPLEMENT 2, REVISION 2**

**1.0 INTRODUCTION**

GE-Hitachi Nuclear Energy (GEH) submitted for review topical report NEDE-33083P, Supplement 2, Revision 2, "TRACG Application for ESBWR Anticipated Transient Without Scram Analyses," issued September 2009 (Reference 1), in support of the economic simplified boiling-water reactor (ESBWR) advanced passive design. This safety evaluation report (SER) documents the staff's review of NEDE-33083P, Supplement 2, Revision 2, as it relates to the ability of TRACG04 to model ESBWR anticipated transients without scram (ATWS) analyses.

This SER builds on the conclusions and analyses of related reviews of the TRACG code, including the following:

- the generic applicability of TRACG for ESBWR analyses, NEDC-33083P-A (Reference 2)
- the applicability of TRACG to ATWS analyses for operating reactors, NEDE-32906P, Supplement 1,(References 3) and Supplement 3, (Reference 4)
- the applicability of TRACG to ESBWR stability analyses, NEDE-33083P, Supplement 1, (Reference 5)
- the applicability of TRACG to ESBWR anticipated operational occurrences (AOOs), NEDE-33083P, Supplement 3, (Reference 6)
- the applicability of TRACG to AOO transient analysis for operating reactors, NEDE-32906P-A, Revision 2, (Reference 7)
- a technical evaluation by a staff contractor of the applicability of TRACG to ESBWR ATWS events (Reference 8)

**2.0 REGULATORY BASIS**

As defined in NUREG-0800, "Standard Review Plan for the Review of Safety Analysis Reports for Nuclear Power Plants" (hereafter referred to as the SRP), Section 15.8, Revision 2, "Anticipated Transients Without Scram," issued March 2007 (Reference 9), the ATWS acceptance criteria are based on meeting the relevant requirements of the following Commission regulations:

Enclosure 1

- Title 10 of the *Code of Federal Regulations* (10 CFR) 50.62, "Requirements for Reduction of Risk from Anticipated Transients Without Scram (ATWS) Events for Light-Water-Cooled Nuclear Power Plants" (known as the ATWS rule), as it relates to the acceptable reduction of risk from ATWS events via (1) inclusion of prescribed design features and (2) demonstration of their adequacy
- 10 CFR 50.46, "Acceptance Criteria for Emergency Core Cooling Systems for Light-Water Nuclear Power Reactors," as it relates to maximum allowable peak cladding temperatures (PCTs), maximum cladding oxidation, and coolable geometry
- General Design Criterion (GDC) 12, "Suppression of Reactor Power Oscillations," as it relates to ensuring that oscillations are either not possible or can be reliably and readily detected and suppressed
- GDC 14, "Reactor Coolant Pressure Boundary," as it relates to ensuring an extremely low probability of failure of the coolant pressure boundary
- GDC 16, "Containment Design," as it relates to ensuring that containment design conditions important to safety are not exceeded as a result of postulated accidents
- GDC 35, "Emergency Core Cooling," as it relates to ensuring that fuel and clad damage, should it occur, will not interfere with continued effective core cooling and that clad metal-water reaction will be limited to negligible amounts
- GDC 38, "Containment Heat Removal," as it relates to ensuring that the containment pressure and temperature are maintained at acceptably low levels following any accident that deposits reactor coolant in the containment
- GDC 50, "Containment Design Basis," as it relates to ensuring that the containment does not exceed the design leakage rate when subjected to the calculated pressure and temperature conditions resulting from any accident that deposits reactor coolant in the containment

For boiling-water reactors (BWRs), the following specific criteria apply:

- Equipment shall be provided to initiate an automatic trip of the reactor coolant recirculation pumps under conditions indicative of an ATWS.
- An alternate rod injection system is provided that is independent and diverse from the reactor trip system sensor output to the final actuation device. The system shall have an independent scram air header exhaust valve.
- A standby liquid control system (SLCS) shall be provided that is capable of initiating reactivity control equivalent to injection of 326 liters per minute (or 86 gallons per minute) of 13 weight-percent sodium pentaborate decahydrate solution of boron-10 into a 638-centimeter (251-inch) inside diameter reactor pressure vessel (RPV) operating at a power density consistent with the original licensed thermal power.
- The SLCS initiation is automatic for the plants specified in 10 CFR 50.62(c)(4).

- For BWRs, reactor coolant system pressures should not exceed American Society of Mechanical Engineers (ASME) Service Level C limits (approximately 10.3 megapascals (MPa) (1,500 pounds per square inch (psig))).
- 10 CFR 50.34 (f), TMI-2 Action Item No. 1.C.9, requires a program which includes emergency procedures. Each plant emergency operating procedure or emergency operating instruction to implement the ATWS/stability mitigation actions, as described in References 8 and 10 of SRP Section 15.8. The two main mitigation actions are the following:
  - (1) Following a failure to scram, the reactor vessel water level must be lowered to a level below the feedwater spargers that will allow vessel steam to preheat the cold feedwater.
  - (2) If unstable power oscillations are detected following a failure to scram, boron injection through the SLCS must be initiated manually.

For evolutionary plants (e.g., the ESBWR), SRP Section 15.8 specifies that some of the equipment required to satisfy the rule may not apply. For example, passive BWRs do not have recirculation pumps; therefore, these designs cannot provide equipment to trip them, as required by the rule. For these designs, provision of an equivalent action, such as reducing the vessel water level, may be acceptable.

The ATWS rule (10 CFR 50.62) prescribes hardware requirements, rather than acceptance criteria because, during the rulemaking process, BWR performance with the required hardware was shown to meet specific acceptance criteria. SRP Section 15.8 specifies that, for evolutionary plants, the applicant's design shall ensure the following:

- Maintain coolable geometry for the reactor core. If fuel and clad damage were to occur following a failure to scram, GDC 35 requires that this condition should not interfere with continued effective core cooling. The regulation in 10 CFR 50.46 defines three specific core-coolability criteria: (1) PCT shall not exceed 2,200 degrees Fahrenheit (F), (2) the calculated total oxidation of the cladding shall nowhere exceed 0.17 times the total cladding thickness before oxidation, and (3) the calculated total amount of hydrogen generated from the chemical reaction with water or steam shall not exceed 0.01 times the hypothetical amount that would be generated if all of the metal in the cladding cylinders surrounding the plenum volume, were to react.
- Maintain reactor coolant pressure boundary integrity. The calculated reactor coolant system transient pressure should be limited such that the maximum primary stress anywhere in the system boundary is less than that of the "emergency conditions" as defined in the ASME Nuclear Power Plant Components Code, Section III. The acceptance criterion for reactor coolant pressure, based on the ASME Service Level C limits, is 10.3 MPa (1,500 pounds per square inch gauge (psig)).
- Maintain containment integrity. Following a failure to scram, the containment pressure and temperature must be maintained at acceptably low levels based on GDC 16 and 38. The containment pressure and temperature limits are design dependent, but to satisfy GDC 50, those limits must ensure that containment design values are not exceeded

when the containment is subjected to the calculated pressure and temperature conditions resulting from any ATWS event.

In the design control document (DCD) application, GEH used the TRACG04 code to ensure that acceptance criteria are met during an ATWS event. This SER documents the staff evaluation of the ability of the TRACG04 code to perform ATWS calculations to ensure ESBWR compliance with the above regulatory requirements.

### **3.0 TECHNICAL EVALUATION**

In the following sections, the staff addresses the scope of the review; the technical evaluation based on the code scaling, applicability, and uncertainty (CSAU) methodology; and confirmatory calculations performed in support of this review.

#### **3.1 SCOPE OF REVIEW**

The scope of this SER is limited to the capability of the TRACG04 code to perform ATWS analyses for the ESBWR. Section 15.5.4 of the SER on ESBWR design certification (Ref. 38) discusses the adequacy of the ESBWR ATWS systems (e.g., SLCS) and evaluation of the ATWS event as it pertains to regulatory criteria. This review builds on the evaluation of the ability of TRACG to perform AOO analysis for the ESBWR (Reference 6) and on the evaluation of the ability of TRACG to perform ATWS analyses in operating reactors (Reference 4).

#### **3.2 TECHNICAL EVALUATION BASED ON THE CODE SCALING, APPLICABILITY, AND UNCERTAINTY APPROACH**

GEH has chosen to follow the basic CSAU approach outlined in NUREG/CR-5249, "Quantifying Reactor Safety Margins: Application of Code Scaling, Applicability, and Uncertainty Evaluation Methodology to a Large-Break, Loss-of-Coolant Accident," issued December 1989 (Reference 10), for evaluating total model and plant parameter uncertainty in ESBWR ATWS calculations. [[

]] The staff review has also followed the methodology described in Reference 10, and the staff conclusions are organized based on the steps required in the CSAU methodology and the ability of TRACG04 to implement them.

The CSAU methodology consists of 14 steps contained within 3 elements (Reference 10). The first element includes Steps 1 through 6 and determines the requirements and code capabilities. The scenario modeling requirements are identified and compared against code capabilities to determine the applicability of the code to the specific plant and accident scenario. Element 1 notes code limitations.

The second element in the methodology includes Steps 7 through 10 and assesses the capabilities of the code by comparison of calculations against experimental data to determine code accuracy and scaleup capability and to determine appropriate ranges over which parameter variations must be considered in sensitivity studies.

The third element in the methodology consists of Steps 11 through 14, in which individual contributors to uncertainty, such as plant input parameters, states, and sensitivities, are calculated, collected, and combined with biases and uncertainties into a total uncertainty.

### 3.2.1 Element 1—Requirements and Code Capability

#### 3.2.1.1 Step 1—Scenario Selection

The processes and phenomena that can occur during an accident or transient vary considerably depending on the specific event being analyzed. GEH has identified the ATWS scenarios applicable to the ESBWR that can be analyzed using TRACG and the associated methodology described in Reference 3. These correspond to SRP Section 15.8.

More detail on the specific events for which this methodology is applicable appears in Section 2.0 of "Technical Evaluation Review of TRACG Applications to ESBWR ATWS," issued January 2007 (Reference 8).

GEH is consistent with Step 1 in the CSAU approach.

#### 3.2.1.2 Step 2—Nuclear Power Plant Selection

The dominant phenomena and timing for an event can vary significantly from one nuclear power plant design to another. GEH has specified that the methodology applies to the ESBWR natural circulation, passive design. The staff evaluated the methodology as it applies to the 4,500-megawatt thermal (MWt) ESBWR design described in the ESBWR DCD.

GEH is consistent with Step 2 in the CSAU approach.

#### 3.2.1.3 Step 3—Phenomena Identification and Ranking

All phenomena that occur during an accident or transient do not equally influence the behavior of the nuclear power plant undergoing the event. A determination must be made to establish those phenomena that are important for each event and various phases within an event. Development of a phenomena identification and ranking table (PIRT) establishes those phases and phenomena that are significant to the progress of the event being evaluated.

GEH identified important phenomena for ATWS events in the ESBWR in a PIRT, which appears in Table 3-1 of NEDE-33083P, Supplement 2, Revision 2, (Reference 1). NEDC-33079P, Revision 1, Supplement 1, "ESBWR Test and Analysis Program Description, Discussion of PIRT Parameters," issued March 2005 (Reference 11), discusses the parameters. The phenomena are identified as having an impact on three critical safety parameters: (1) suppression pool temperature, (2) vessel pressure, and (3) fuel clad temperature.

In ranking the phenomena, GEH divided the limiting scenarios into five phases:

- (1) short-term pressurization, neutron flux increase, and fuel heatup
- (2) feedwater runback and water level reduction
- (3) boron injection, mixing, and negative reactivity insertion
- (4) post shutdown suppression pool heatup
- (5) depressurization of the reactor

GEH states that emergency operating procedures may direct an operator to depressurize the reactor during an ATWS, but these procedures have not been established at this time. In Request for Additional Information (RAI) 21.6-4, the staff asked GEH to address depressurization during an ATWS event. In the RAI response (Reference 12), GEH described

its procedure for developing a PIRT for ATWS depressurization. This procedure was nearly identical to that used when developing the PIRT for loss-of-coolant accident (LOCA) events, with some differences noted by GEH. The staff finds that GEH has addressed the differences between a depressurization resulting from a LOCA and one resulting from a controlled depressurization during an ATWS. However, the staff noted in its supplemental RAI that GEH has not provided demonstration calculations or the procedures for depressurization during an ATWS, and therefore the staff cannot thoroughly review the application of TRACG to depressurization. In response to RAI 21.6-4 S01, the applicant provided TRACG depressurization analysis results for the limiting ATWS event with respect to suppression pool heatup, the main steam isolation valve closure (MSIVC) ATWS event. The results shown in Figure 21.6-4 S01-1 indicate that the final suppression pool temperature is consistent with containment pressure limits. This indicates that, as designed, the ESBWR suppression pool can adequately handle an operator-initiated depressurization during an ATWS event. In addition, this simulation shows that TRACG is capable of simulating the depressurization of the reactor in an ATWS MSIVC event. Based on the applicant's response, RAI 21.6-4 is resolved.

The following PIRT parameters were introduced specifically for ESBWR ATWS evaluation:

- ATW1—boron mixing/entrainment between the jets downstream of the injection nozzle
- ATW2—boron settling in the guide tubes or lower plenum
- ATW3—boron transport and distribution through the vessel, particularly in the core bypass region
- ATW5—boron reactivity

The staff concludes that this PIRT is comprehensive and gives the appropriate rating to ESBWR ATWS phenomena. GEH is consistent with Step 3 in the CSAU approach.

#### 3.2.1.4 Step 4—Frozen Code Version Selection

The version of a code, or codes, reviewed for acceptance must be "frozen" to ensure that after an evaluation has been completed, changes to the code do not impact the conclusions and that changes occur in an auditable and traceable manner. GEH has specified that the TRACG04 code be used for the ESBWR AOO applications. TRACG04 contains PANAC11 three-dimensional neutronic methods. PANAC11 and TGBLA06 are used to generate ESBWR cross section data for input into TRACG04.

On October 14 through 19, 2006, and October 30 through November 3, 2006, the staff performed an audit of PANAC11 and TGBLA06 as they are applied to the ESBWR. During the audit, the staff reviewed the most current versions of PANAC11 and TGBLA06 codes for their applicability to the ESBWR. Even though GEH regularly issues new versions of its code to correct errors, the staff considers these codes frozen, along with future revisions to the codes, as long as changes to the codes are within the conditions and limitations specified in its SER for NEDE-33239P, "GE14 for ESBWR Nuclear Design Report" (Reference 13).

The ATWS methodology documented in NEDE-33083P, Supplement 2, Revision 2, (Reference 1), restricts changes to the reference code (TRACG04). Thus, changes to the models documented in NEDE-32176P, Revision 3, "TRACG Model Description," issued

April 2006 (Reference 15), may not be made without NRC review and approval. However, the methodology does allow programming changes in numerical methods to improve code convergence or code enhancements or corrections of programming errors. These changes must be tested and auditable records kept in accordance with Appendix B, "Quality Assurance Criteria for Nuclear Power Plants and Fuel Reprocessing Plants," to 10 CFR Part 50. As part of the testing process, the calculated TRACG results must be compared against the results documented in the most recent version of the qualification test document NEDE-32177P, "TRACG Qualification" (References 16 and 17). If the differences are larger than the one-sigma uncertainty in that assessment, the methodology documented in NEDE-33083P, Supplement 2, Revision 2, (Reference 1), requires that GEH submit the changes for staff review. New models or features, other than input enhancements that do not affect calculated results significantly, may not be implemented without prior NRC review and approval.

In RAI 21.6-92, the staff asked GEH to provide the exact version and revision number for all analyses performed in the ESBWR DCD (Reference 18). In addition, GEH has two versions of the TRACG04 code—TRACG04A runs on an Alpha Virtual Memory System (VMS) platform, and TRACG04P runs on a Personal Computer (PC) platform. The staff asked GEH to state which of these two codes is used to perform the analyses for which this methodology will be applied. In its response, GEH provided a list of the code versions used for each calculation in the DCD, which the staff finds sufficient. Based on the applicant's response, RAI 21.6-92 is resolved.

GEH is consistent with Step 4 in the CSAU approach.

#### 3.2.1.5 Step 5—Provision of Complete Code Documentation

This step requires the applicant to provide documentation on the frozen code version such that evaluation of the code's applicability to postulated transient or accident scenarios for a specific plant design can be performed through a traceable record. GEH has provided the documentation through the submittal of ESBWR ATWS specific documentation in References 1, 11, and 19, and code documentation in References 11 and 15.

The staff concludes that the code documentation is adequate, and GEH is consistent with Step 5 in the CSAU approach.

#### 3.2.1.6 Step 6—Determination of Code Applicability

TRACG04 is based on two-fluid models capable of one-dimensional and three-dimensional thermal-hydraulic representation, along with three-dimensional neutronic representation. The code is designed to simulate reactor transients as best estimates. Conservatism is added, where appropriate, via input specifications. An analysis code used to calculate a transient scenario in a nuclear power plant should use many models to represent the thermal-hydraulics and components. These models should include the following four elements:

- (1) field equations—provide code capability to address global processes
- (2) closure equations—provide code capability to model and scale particular processes
- (3) numerics—provide code capability to perform efficient and reliable calculations

- (4) structure and nodalization—address code capability to model plant geometry and perform efficient and accurate plant calculations

The staff performed an extensive review of the thermal-hydraulics models and their applicability to the ESBWR for LOCA events and containment analysis (Reference 20) and the application to AOO and ATWS overpressure events in BWR/2–6 as described in the staff evaluation report included in the topical report (Reference 3). The staff also reviewed TRACG as applied to ESBWR AOO/infrequent event analysis (Reference 4). The current safety evaluation (SE) of the TRACG applicability for ATWS builds on these previous reviews.

#### 3.2.1.6.1 Thermal-Hydraulic Modeling

The SER for NEDE-33083P, Supplement 3, (Reference 6), contains a review of the TRACG thermal-hydraulic modeling as applied to ESBWR AOOs. In addition, Reference 8 documents a technical evaluation by a staff contractor of the TRACG thermal-hydraulic models related to ATWS phenomena. Some of the phenomena unique to ATWS events include those related to high heat flux and boron mixing and transport. The following sections in this SER discuss other phenomena that are unique to modeling ESBWR ATWS events.

#### 3.2.1.6.2 Minimum Stable Film Boiling Temperature

For the minimum stable film boiling temperature, GEH uses the Iloeje correlation for ESBWR applications. TRACG has the option of using the Shumway correlation, which, according to GEH, better captures the flow and pressure dependence. The staff has not reviewed the Shumway correlation, which was an option provided by GEH, and finds the use of the Iloeje correlation acceptable for ESBWR ATWS applications. For ATWS events where the core does go into film boiling, the minimum stable film boiling temperature is used to determine when the core will quench and has no effect on the value of the maximum PCT.

#### 3.2.1.6.3 Standby Liquid Control System Modeling

GEH modeled the SLCS using a [[ ]] component. In RAI 21.6-12 (Reference 21), the staff asked GEH to justify its selection of the velocity for this component. GEH responded to this RAI in Reference 12. The velocity profile assumed in TRACG04 is based on a simple model of adiabatic expansion of the standby liquid control (SLC) accumulator nitrogen gas, and it assumes a constant reactor pressure of 8.72 MPa (1260 psi). The adiabatic assumption is conservative because, in real life, some heat will be transferred from the environment to the nitrogen gas, resulting in increased SLC velocity. The constant reactor pressure assumption is conservative because 8.72 MPa (1260 psi) is higher than the safety/relief valve actuation pressure; thus, the reactor pressure is expected to be reduced when the safety/relief valves actuate. Since both assumptions are conservative, the TRACG model results in slower boron injection rates than in the real case. In addition, GEH performed a sensitivity calculation assuming 90 percent of the injection velocity table. The results indicate that this 10-percent reduction in SLC injection velocity had [[ ]].

The staff concludes that the SLC injection models documented in NEDE-33083P, Supplement 2, Revision 2 (Reference 1), are conservative. Based on the applicant's response, RAI 21.6-12 is resolved.

#### 3.2.1.6.4 Boron Mixing and Transport

The ESBWR uses the SLCS to shut down the reactor in the event of an ATWS. This system injects soluble boron, a strong neutron absorber, into the peripheral bypass of the core. GEH has included a mass-continuity equation in TRACG for boron transport, in a method similar to that for the treatment of noncondensable gas, which assumes that all noncondensable gases are in thermal equilibrium with the liquid that is present and move with the same velocity as the liquid. GEH has also incorporated single- and two-phase fluid mixing models to account for mixing resulting from molecular and turbulent diffusion. GEH made the following assumptions in modeling turbulent mixing and molecular diffusion:

- Equal volumes of two-phase mixture are exchanged among adjacent regions.
- In each computational cell, the properties of the incoming fluid volume and the resident fluids are perfectly mixed.
- Both vapor and liquid travel with the same lateral mixing velocity.

Even though the boron model is simplistic, it has produced sufficient results for a number of applications. However, empirical confirmation is still required at different scales. As a result of the assumption that there is perfect mixing in each computational cell in the boron mixing model, the model is highly dependent on nodalization because the boron is transported instantaneously to the whole node; very large nodes would result in nonconservative fast boron transport. Section 3.2.2.2 of this report discusses the adequacy of the GEH TRACG nodalization for performing ATWS evaluations. In RAI 21.6-41 (Reference 32), the staff requested that GEH justify its position that the uniform mixing assumption of the boron in the bypass will be conservative. The information requested in RAI 21.6-41 was also listed in RAI 21.6-44, which included a request for GEH to address computational fluid dynamics (CFD) calculations. The response to RAIs 21.6-44 and RAI 21.6-44 S01 are documented in References 39, 40 which shows a comparison of TRACG-predicted boron concentrations against experimental data from NEDE-22267, "Test Report Three-Dimensional Boron Mixing Model," issued October 1982 (Reference 23). The results of this benchmark indicate that TRACG calculations [[

]]. The staff performed CFD confirmatory calculations (see Section 3.3.2 of this report) and reached similar conclusions. Thus, the staff concludes that the overall TRACG boron mixing models result in a lower reactivity worth and, thus, are conservative.

[[

]] The ESBWR ATWS analysis does not use this model; therefore, the staff did not review it. Based on the applicant's response, RAI 21.6-41 is resolved.

#### 3.2.1.6.5 Boron Settling

Boron may be lost to the system because of settling in the control rod guide tubes and the lower plenum. Since TRACG assumes that boron is uniformly mixed in each cell, TRACG is not able to calculate the effects of boron settling. Therefore, the effects of potential removal of boron from the system because of settling can be controlled using nodalization and input assumptions. GEH did not adjust the nodalization to account for this settling. In Reference 1 (Section 5.0), by calculating a critical velocity based on a critical Froude number, GEH concluded that the boron

will not settle. GEH estimated that the critical velocity is much less than the velocity being calculated by TRACG, and thus, settling will not occur. In RAIs 21.6-9 (Ref. 24), 21.6-27, and 21.6-28 (Reference 12), the staff asked GEH to justify the assumptions about the settling of boron. In response to RAI 21.6-27 (Reference 12), GEH provided the velocity calculated by TRACG for the duration of the transient to demonstrate that it is mostly upward and that boron is not likely to settle in the guide tubes. During some time periods, the velocity is slightly negative, and in response to RAI 21.6-9 (Reference 24) and 21.6-28 (Reference 12), GEH performed sensitivity studies on the amount of boron settling in the guide tubes and found its effect on maximum suppression pool temperature to be negligible. The staff technical evaluation in Reference 8 discusses this issue and reaches similar conclusions. Based on the applicant's responses, RAIs 21.6-9, 21.6-27, and 21.6-28 are resolved.

The sensitivity studies performed by GEH are based on the MSIVC ATWS. The results may be different for different ATWS events since the flow field will be different. In a supplement to RAI 21.6-39, the staff asked GEH to address the flow field for ATWS events that may be different than MSIVC. In addition, the results of the CFD analyses discussed in Section 3.3.1 have provided additional insight into the settling of the boron. The staff evaluation of RAI 21.6-39 is included in Section 3.2.2.2 of this report.

#### 3.2.1.6.6 Channel Leakage Model

Following SLCS activation, the injected boron will fill or settle in the bottom of the bypass region and enter the channels through the leakage paths because the bypass flow is downwards during ATWS events. The staff reviewed the channel leakage model in TRACG. The staff issued RAI 21.6-100 (Reference 25) requesting justification for the applicability to ATWS of the TRACG channel leakage correlations. In response to RAI 21.6-100 S02 (Reference 27), the applicant stated that the hardware used to design the ESBWR core, including lower tie-plate and fuel bundle leakage path geometry, is similar to that of the operating BWRs. Therefore, the staff agreed that using the same forward and reverse channel leakage flow coefficients as for the current operating BWRs is appropriate for the ESBWR. Based on the applicant's response, RAI 21.6-100 is resolved.

#### 3.2.1.6.7 Fuel Thermal Conductivity and Gap Conductance

During the review of NEDE-33083P, Supplement 3 (Reference 6), the staff found a number of inconsistencies in the TRACG04 treatment of fuel thermal conductivity and gap conductance. These inconsistencies are also covered by a related 10 CFR Part 21, "Reporting of Defects and Notification". Sensitivity analyses were performed in the response to RAI 6.3-54 (Reference 28) and showed [ [ ]]. The AOO and ATWS sensitivity study results documented in the response to RAI 6.3-54 S01 provide the staff with reasonable assurance that the transient event analyses shown in NEDE-33083P do not exceed acceptance criteria, and therefore, RAI 6.3-54 is resolved. The fact remains that the inconsistencies in the TRACG04 thermal conductivity model have not been submitted for ESBWR application with the supporting empirical data. Therefore, the staff SER for NEDE-33083P, Supplement 3 (Reference 6), imposes a condition to use consistent pellet and gap models for future calculations. This condition is also outlined as Condition 10 as identified in Section 4 of this report as it applies to the AOO and ATWS calculations.

#### 3.2.1.6.8 Hot Rod Model

GEH has implemented a hot rod model in its one-dimensional thermal-hydraulic model of the

channel component in TRACG04. As described in Section 8.1.1 of NEDE-33083P Supplement 2, Rev 2, GEH calculated a PCT during ATWS events, for the limiting bundle. The hot rod model option is activated for the limiting PCT channels, where the rods are presumed to be near boiling transition or uncovered (as in the case of conventional BWR reflood during LOCA calculations prior to quenching). The model allows for accurate modeling of the peak cladding temperature (PCT) in conditions where the rods may dry out. In addition, a bundle power peaking is applied to one of the hot channels to operate at a Critical Power Ratio (CPR) lower than the expected Operating Limit CPR (which results in earlier dryout of the fuel bundle).

A detailed description of the hot rod model option is provided in Section 7.5.7 of the TRACG Model Description Topical Report, NEDE-32176P (Reference 15). Reference 31, NEDE-32177P, provides qualification of the hot rod model option by comparison to separate effects tests at several LOCA test facilities. The Core Spray Heat Transfer Test (CSHT) data indicate close agreement between measured PCT values and the TRACG hot rod model-predicted PCT for a core spray reflood test. The Two-Loop Test Apparatus (TLTA) data was also compared against TRACG predictions using the hot rod model, with good agreement. The Thermal Hydraulic Test Facility (THTF) PCT data was also generally well-predicted by TRACG, [[ ]], as noted in Section 3.2.1.3 of Reference 31.

In general, the LOCA tests show that TRACG, with the hot rod model option implemented, adequately predicts PCT based on average hydraulic conditions. However, localized variations in the test hydraulic conditions could lead to underprediction of PCT, considering measurement uncertainty, at some rod locations. This is particularly the case for transients with significant radial or azimuthal variation in void fraction from the bundle average value. Since the ESBWR core is never uncovered during LOCA, the hot rod model option is not utilized for LOCA analyses.

In Reference 41, GEH provided supplemental supporting information for ATWS application of the hot rod model option. As indicated in the reference, the above LOCA tests' comparisons are not fully representative of the rod conditions which would exist for ATWS scenarios, [[ ]]

]] These tests are described in Section 3.6.1 of Reference 31, the TRACG Qualification Report. [[ ]]

]] The TRACG-calculated and measured cladding surface temperatures are compared for two of the ATLAS tests (Figures 3.6-5 and 3.6-6). The calculated temperatures conservatively overpredict the test measurements by [[ ]].

GEH noted in Reference 41 that the hot rod model option was not used for the ATLAS qualification benchmarks, [[ ]]

]]. The staff agrees with the applicant's explanation that, for the ATLAS tests, as well as for expected ATWS scenarios, [[ ]]

]].

NEDE-33083P, Supplement 2, identifies the Main Steam Line Isolation Valve Closure (MSIVC), Loss of Feedwater Heating, and Loss of Condenser Vacuum as limiting scenarios for ATWS

overpressure and PCT. The supplemental information provided in Reference 41 further states that the results for the ESBWR ATWS bounding MSIVC calculation in NEDE-33083, Supplement 2 included a hot channel rod in which the hot rod model option was applied, and [[

]] Only the maximum PCT of all rods is reported. [[

]]

The staff reviewed the limiting cases for ATWS PCT presented in NEDE-33083P, Supplement 2, and all ATWS cases presented in DCD, Tier 2, Chapter 15. In all cases, substantial margin to the 10CFR 50.46 limit (2200°F or 1204°C) is calculated. The TRACG hot rod model option was utilized for all of the ATWS analyses. Therefore, the staff finds the TRACG hot rod model option acceptable for use in ESBWR design and reload ATWS applications with GE14E fuel.

GEH stated, and the staff agrees, that it is not expected that incremental design differences in replacement ESBWR fuel would significantly alter the PCT margin. However, it is possible that a shift in timing for prediction of the occurrence of boiling transition beyond the statistical uncertainty could result. For this reason, if replacement fuel different from GE14E is utilized, the limiting ATWS analyses should be submitted for staff review. This would already be necessary if any fuel design parameters specified in the fuel design topical reports designated as Tier 2\* documents are altered.

#### 3.2.1.6.9 Three-Dimensional Neutron Kinetics Modeling

The SER for NEDE-33083P, Supplement 3 (Reference 6), discusses the staff's review of the three-dimensional neutron kinetics in TRACG. In addition, Reference 8 provides a technical evaluation of the three-dimensional neutronic models in TRACG.

GEH has successfully benchmarked TRACG three-dimensional neutronic capabilities against experimental data, including the following:

- Peach Bottom turbine trip tests
- Hatch MSIVC tests
- Nine Mile Point pump upshift tests
- Leibstadt loss of feedwater with high-pressure core spray (HPCS) unavailable tests

Even though these operating BWR events are not expected to be the same as the AOOs in the ESBWR, similar phenomena must be modeled accurately to simulate the three-dimensional neutron fluxes during these transients in operating plants as well as in the ESBWR (i.e., power response to void collapse, pressure response to Turbine Control Valve (TCV) closure or MSIVC, among others). Therefore, the staff concludes that the three-dimensional neutronic models in TRACG04 are adequate to model ATWS events in the ESBWR.

#### 3.2.1.6.10 Xenon Reactivity

TRACG accounts for negative reactivity from xenon by adjusting the thermal absorption cross section at each node. The PANAC11 wrapup file includes the xenon number density and the microscopic absorption cross section. For TRACG calculations, the xenon concentrations are

held constant throughout the transient. Since the timeframe of concern for ATWS is on the order of seconds or minutes, and xenon concentrations change over the course of hours, the staff finds that the constant xenon assumption is reasonable.

#### 3.2.1.6.11 Boron Reactivity

Section 9.5 of References 13 and 15 describes the boron reactivity model in TRACG04. TRACG04 models the negative reactivity from boron by adjusting the absorption cross section for other preexisting neutron removal mechanisms already modeled in TRACG04. The SLCS shutdown margin is evaluated with PANACEA; therefore, cross sections could be provided for TRACG through PANACEA. However, GEH considers this method to result in cumbersome calculations and instead used the absorption cross section adjustment.

Since the boron is introduced into the core only during the ATWS event, there are no direct exposure effects on the boron or the reactivity. The reactivity worth of the boron can be accurately captured if the absorption cross section is increased to account for the neutron absorption in boron. This is most accurately done when the thermal cross section is adjusted. The boron absorption cross section depends on the local flux spectrum. The thermal spectrum is precollapsed in one group by TGBLA before being included in the PANACEA wrapup file; therefore, the GEH methodology adjusts the boron microscopic cross section to account for local perturbations to the thermal spectrum using a  $1/v$  (velocity) energy dependence of the boron cross section.

In RAIs 21.6-34 and 21.6-35 (Reference 29), the staff asked GEH to provide additional information on the boron reactivity model and justify some of the assumptions used in the development of the model. GEH provided these details in Reference 29 by propagating the lattice values into PANAC11 for purposes of model development and testing.

In the responses to RAIs 21.6-34 and 21.6-35 (Reference 29), GEH showed the PANAC11 lattice evaluations of the boron reactivity model as a function of exposure for a large number of lattice types and lattice conditions, such as void fraction, boron concentration, and gadolinium content. The trends with exposure depend on factors such as enrichment, gadolinium content, and lattice design. GEH did not explicitly account for the change in neutron spectrum resulting from exposure of the fuel in its boron cross section model; however, it did explain that the TRACG model accounts for the trends seen with features via the  $1/v$  dependence of the cross section and the exposure-dependent PANAC11 reference values provided to TRACG by the wrapup file. For two representative lattices, GEH showed that the boron cross section values as a function of exposure calculated by TRACG and PANAC11 are comparable.

TRACG also has an empirical correction for moderator temperature. GEH provided in Reference 29 a comparison of the TRACG model to PANAC11 for different moderator temperatures and demonstrated that they are comparable and that the trend in the cross section with moderator temperature is appropriate.

The analyses provided in Reference 29 did not account for the effect of void history on the boron cross section. Void history may have an effect through the neutron spectrum of the lattice. However, GEH showed through PANAC11 lattice evaluations that the effect of void history on the boron cross section is [[ ]]. The GEH evaluation indicates that at the higher void history, the TRACG model [[ ]], which is nonconservative. However, the [[ ]]

]]; therefore, the overall error in boron reactivity is expected to be significantly lower when realistic exposures and core-average void levels are used.

GEH accounted for self-shielding by reducing the boron cross section by empirically determined factors as the boron number density increases. GEH showed the self-shielding effect based on PANAC11 lattice evaluations and then stated that TRACG calculates a comparable reduction in the boron cross section for the same conditions.

GEH showed comparisons of the calculated eigenvalue versus boron concentration for PANAC11 and TRACG04. Since PANAC11 interpolates using boron concentrations of [[ ]], the two codes did not match exactly but did match where expected at the midpoint of the PANAC11 interpolation and for larger boron concentrations.

Since GEH uses empirical models to develop the boron reactivity model, the staff asked GEH to justify this model when applying it to other fuel designs not encompassed by those on page 5-15 of Reference 3 (or page 9-40 in Section 9.5.2 of Reference 15).

Even though the only validation available for staff review is a code-to-code comparison to PANAC11, the staff believes that GEH stated all of the factors affecting boron reactivity in the development and testing of its empirical model. Based on the applicant's responses, RAIs 21.6-34 and 21.6-35 are resolved.

To confirm GEH's assertions, the staff performed confirmatory calculations using the Monte Carlo MCNP code (Reference 30). Input decks representative of the ESBWR lattices were developed to support steady-state physics calculations. The staff added boron to these lattices to compare the resulting cross sections with the ones used in TRACG using the theoretical  $1/v$  boron model. The results of these analyses are documented in a technical evaluation report (Reference 29). The results of the staff technical evaluation confirmed the validity of the TRACG boron model.

The staff finds that GEH is consistent with Step 6 in the CSAU approach, and each step in Element 1 is consistent with the CSAU approach and, therefore, acceptable.

### 3.2.2 Element 2—Assessment and Ranging of Parameters

#### 3.2.2.1 Step 7—Establish Assessment Matrix

The staff's review of the assessment of TRACG as applied to ESBWR AOs appears in Reference 6. This review is also applicable to ESBWR ATWS events. In Table 4.2-1 of Reference 1, GEH identified the qualification basis for each of the high-ranked phenomena identified in the ATWS PIRT by citing the quantitative assessment performed for separate effects qualification, component performance qualification, integral system qualification, and plant data. The assessment descriptions cover the test facility, where applicable, the test results, TRACG sensitivity studies, and nodalization studies, where applicable. All high-ranked phenomena have been assessed.

In RAI 21.6-75, the staff asked GEH to provide an update to the TRACG qualification report (Reference 16) that is consistent with the current version of TRACG used in ESBWR licensing analyses (TRACG04). In response, GEH submitted Revision 3 of the TRACG qualification

report, NEDE-32177P (Reference 30), in August 2007, and this RAI and the associated concern are resolved.

GEH is consistent with Step 7 in the CSAU approach.

### 3.2.2.2 Step 8—Nuclear Power Plant Nodalization Definition

The nodalization for ATWS events is similar to that used for ESBWR AOO and stability analysis. Reference 6 discusses the adequacy of this nodalization for simulating transient thermal-hydraulic neutronic behavior in an ESBWR. The only ATWS-specific nodalization issue relates to the bypass region nodalization because it affects the boron transport.

As stated in Section 3.2.1.6.4 of this report, boron mixing is highly dependent on the nodalization scheme, especially in the bypass region. Section 5.1 of NEDE-33083P, Supplement 2, Revision 2 (Reference 1), presents the GEH justification for its vessel bypass nodalization in relation to boron mixing and transport. This justification is based on the qualitative discussion of postulated jet and plume characteristics of the SLCS liquid after injection. In addition, in RAI 21.6-42 staff requested (Reference 12) that GEH provide the boron concentrations and mass flow rates through the core bypass and channels for the MSIVC transient. In response, GEH provided the boron concentrations and mass flow rates in support of staff's review. Therefore, RAI 21.6-42 is resolved.

GEH also performed CFD calculations to help justify the selected TRACG nodalization. Separately, the NRC staff has completed independent confirmatory CFD calculations.

In addition to the CFD calculations, the staff requested in RAI 21.6-8 that GEH perform nodalization studies of the vessel to illustrate the sensitivity of the TRACG-calculated safety parameters to nodalization. [[

]] GEH submitted the results of its radial and azimuthal sensitivity studies in the response to RAI 21.6-8 (Reference 32). GEH performed a series of sensitivity studies that [[

]]

GEH showed that, when it injects boron into the two smaller sectors versus the four large sectors, the shutdown time [[

]]

GEH repeated this study with the blocking removed. The results for both the small- and large-sector injection cases [[

]]

GEH compared the results of just the large-sector injection cases (with and without blocking) to demonstrate that the case with blocking has a [[

]]. Despite the more conservative results, GEH proposed to maintain the size of the third outer ring and inject the boron into this ring [[

]]

The staff was concerned that, in the current GEH modeling approach, the outer ring into which boron is injected is the largest ring in the TRACG model and contains several rows of bundles. The staff was concerned that this is nonconservative because these bundles, which constitute a substantial portion of the bundles in the core [[ ], would see boron immediately. To resolve this problem, the staff requested that GEH perform CFD calculations of boron mixing in the bypass. In addition, the staff performed its own confirmatory calculations. Both the staff and GEH CFD calculations appear to indicate that the SLCS injection of boron into the core bypass region is effective in getting boron to the inner parts of the core. Penetration of the boron into the inner bundles is more effective than the TRACG modeling approach which puts an [[

]] radial boron mixing. Based on the staff's confirmatory CFD calculations, RAI 21.6-8 is resolved.

In RAI 21.6-83 (Reference 33), the staff requested that GEH perform sensitivity studies for the axial nodalization of the bypass. In the response to RAI 21.6-83 (Reference 33), GEH supplied a study of boron mixing under different axial nodalization schemes. The staff concurred that key ATWS figures of merit like peak suppression pool temperature and shutdown time were not affected significantly by changes in the nodalization, which indicates that the reference solution is sufficiently converged. Based on the applicant's response, RAI 21.6-83 is resolved.

The staff was also concerned that the nodalization studies by GEH and the CFD analyses were performed for the limiting ATWS event (MSIVC), where the core flow and associated core pressure drop are reduced significantly, resulting in reverse (downward) flow in the bypass region. In RAI 21.6-39, the staff requested that GEH evaluate the adequacy of this nodalization for nonisolation ATWS events, where the core flow and associated core pressure drop may remain high enough to maintain upward flow in the bypass during the boron injection time. In the response to RAI 21.6-39 S01 (Reference 24), GEH performed calculations for nonisolation ATWS events where the initial bypass flow was upwards. The calculations show that the shutdown time is achieved only a few seconds later than in the isolation ATWS event (with downwards bypass flow), and key ATWS parameters do not change significantly. The primary reason for these results is that, even for nonisolation ATWS events, the ESBWR initiates a feedwater flow runback to lower the downcomer water level and reduce the core flow and power. This feedwater flow runback eventually forces flow reversal on the bypass region, which enhances the core boron concentration.

The staff concludes that the bypass region nodalization documented in NEDE-33083P, Supplement 2, Revision 2, (Reference 1), is adequate to model the boron mixing effect in ESBWR ATWS events. Therefore, GEH is consistent with Step 8 in the CSAU approach, and RAI 21.6-39 is resolved.

### 3.2.2.3 Step 9—Definition of Code and Experimental Accuracy

Simulation of experiments developed from Step 7 (discussed in Section 3.2.2.1); using the nuclear power plant nodalization from Step 8 (discussed in Section 3.2.2.2), provides checks to determine code accuracy. The differences between the code-calculated results and the test data provide bias and deviation information. Code scaleup capability can also be evaluated from

separate effects data, full-scale component tests data, plant test data, and plant operating data where available. Overall code capabilities are assessed from integral systems test data and plant operational data. References 16 and 34 document the assessments of TRACG. Since the ESBWR is a new design, no operating plant data are available. However, many of the key parameters and phenomena for analyzing ATWS in the ESBWR are not significantly different from those in operating reactors.

GEH used TRACG to simulate separate effects tests, component performance tests, integral systems tests, and operating BWR plant data. GEH was able to determine an uncertainty between the code-calculated results and the test data. Sections 4.0 and 5.0 of Reference 8 include discussion of the uncertainties associated with various qualification tests.

### 3.2.2.3.1 Boron Mixing Qualification

To qualify and determine the uncertainty in the boron mixing model, GEH used data from three-dimensional boron mixing tests (Reference 23) conducted in a [[ ]] (BWR/5 and BWR/6), RPV using the HPCS spargers as the primary location for injection of the simulated boron solution. In the response to RAI 21.6-44 (References 39 and 40), GEH provided additional details of the boron mixing and transport tests used to qualify the TRACG boron model and its applicability to the ESBWR given its unique injection location (in the core bypass). GEH provided additional information about the test used to qualify the boron mixing model in Reference 22. The test used to qualify TRACG for ESBWR ATWS applications has simulated boron injection through the HPCS spargers. GEH stated that it expects the behavior of the boron to be similar to that of the ESBWR SLCS injection in the core bypass because of the downward flow conditions.

GEH defined a figure of merit, the boron "mixing coefficient," as the ratio of the local concentration of boron to the global average concentration of boron. With this definition, large mixing coefficient values indicate bad or incomplete mixing. GEH showed plots of the mixing coefficient in various elevations in the core and bypass for three tests. GEH also provided the conditions of the three tests. These three tests indicate that the mixing coefficient is [[ ]].

GEH developed scale factors between the test model and the ESBWR based on the dimensions of the ESBWR for the radial and axial directions. Using these scale factors, GEH then compared the mixing coefficients calculated by TRACG during the ESBWR MSIVC ATWS simulation and that of the test for various locations in the vessel. [[ ]]

]] and therefore is conservative.

During the review, the staff was concerned about the applicability of a direct comparison between the BWR tests (Reference 23) and ESBWR TRACG results because the boron injection points are different. Boron injection in BWR is through the HPCS. Boron injection for the ESBWR design is by direct injection to the lower bypass region. However, in one of the tests (Case 345), the bypass water level was held at approximately [[ ]], so that the HPCS boron injection would flow freely down to the bypass region and the boron flow paths would propagate from that level, which is similar to the ESBWR case. In addition, the TRACG mixing models are conservative by a significant factor, and TRACG predicts significantly higher mixing coefficients (greater than 200 percent in most cases) than in the experiment. Based on these two observations, the staff concludes that the TRACG boron mixing models with the input parameters recommended in NEDE-33083P, Supplement 2,

Revision 2, (Reference 1), are conservative and result in conservative shutdown times. Based on the applicant's response, RAI 21.6-44 is resolved.

The staff concludes that GEH is consistent with Step 9 in the CSAU approach.

#### 3.2.2.4 Step 10—Determination of Effect of Scale

Various physical processes may give different results as components or facilities vary in scale from small to full size. The effect of scale must be included in the quantification of bias and deviation to determine the potential for scaleup effects. The key parameters and phenomena for analyzing ATWS events in the ESBWR do not have significantly different scales than in operating reactors. The staff discusses scaling of tests performed to qualify TRACG for ESBWR-specific components in Section 21.5 of the SER for ESBWR design certification (Ref. 38).

The staff concludes that GEH is consistent with Step 10 in the CSAU approach.

The staff finds each step in Element 2 to be consistent with the CSAU approach and therefore acceptable.

### 3.2.3 Element 3—Sensitivity and Uncertainty Analysis

#### 3.2.3.1 Step 11—Determination of the Effect of Reactor Input Parameters and States

The purpose of this step is to determine the effect that variations in the plant operating parameters have on the uncertainty analysis. This evaluation has been performed in the SER for TRACG ESBWR AOOs (Reference 6), and it applies to ATWS calculations. The application methodology described in Section 2.7.2 in Reference 1 controls changes to the uncertainty values used for the model inputs. New data with which the specific model uncertainties may be reassessed may become available. If the reassessment results in a need to change specific model uncertainty, the specific model uncertainty may be revised for ESBWR ATWS licensing calculations without NRC review and approval as long as the process for determining the uncertainty is unchanged. In all cases, changes made to model uncertainties without review and approval will be transmitted to the NRC to keep the agency informed.

The treatment of initial conditions is slightly different for the TRACG ESBWR ATWS analyses than for the TRACG ESBWR AOO analyses discussed in Reference 6. The ATWS events will be initiated from the limiting point in the allowed operating domain. Initial conditions will not be adjusted to account for instrumentation and simulation uncertainties. Section 8.2.1.1 in Reference 1 describes the sensitivity studies on initial conditions performed by GEH. Since ATWS is a low-probability event, the NRC has accepted this approach in the past for TRACG ATWS analyses as applied to BWR/2-6 (Reference 3). The staff finds this approach acceptable for ESBWR ATWS analyses.

The treatment of plant parameters is slightly different for the TRACG ESBWR ATWS analyses than for the TRACG ESBWR AOO analyses discussed in Reference 6. GEH applied the analytical limit (often the same as the technical specification limit) for the plant parameters unless it determined that the safety parameters are not sensitive to that plant parameter. GEH performed a study investigating the effect of plant parameters on the MSIVC ATWS event. Section 8.2.2.1 in Reference 1 describes this study. Since ATWS is a low-probability event, the

NRC has accepted this approach in the past for TRACG ATWS analyses as applied to BWR/2-6 (Reference 3). The staff finds this approach acceptable for ESBWR ATWS analyses.

GEH is consistent with Step 11 in the CSAU approach.

### 3.2.3.2 Step 12—Performance of Nuclear Power Plant Sensitivity Calculations

Sensitivity calculations are performed to evaluate methodology sensitivity to various operating conditions that arise from uncertainties in the reactor state at the initiation of the transient, in addition to sensitivity to plant configuration. The safety-related quantities of importance in the ATWS analysis are peak vessel pressure, PCT, peak suppression pool temperature, and peak power. In RAI 21.6-77 (Reference 35) staff requested that the applicant provide additional information to support the staff's CFD modeling of the boron flow paths during an ATWS event. Using TRACG, GEH's response calculated representative ATWS events to demonstrate ESBWR plant behavior. In a subsequent supplement to its response to RAI 21.6-77, GEH identified and corrected an error associated with the channel leakage flow rates in its ATWS analysis that could affect the safety analysis results in this topical report. Staff was satisfied with GEH's response as compared to its CFD modeling and therefore, RAI 21.6-77 is resolved.

GEH is consistent with Step 12 in the CSAU approach.

### 3.2.3.3 Step 13—Determination of Combined Bias and Uncertainty

GEH chose the [[

]]

GEH is consistent with Step 13 in the CSAU approach.

### 3.2.3.4 Step 14—Determination of Total Uncertainty

GEH provides the uncertainty analysis in Section 8.0 of Reference 1. GEH provided clarifying information on this process in Reference 12 in response to RAI 21.6-36. GEH set each of the initial conditions and the highly ranked parameters in the PIRT at both the +1 sigma and the -1 sigma level and performed analyses to determine the impact on the calculated safety parameters.

[[

]] Following the uncertainty analysis, GEH added another set of conservatisms in the initial condition uncertainties, listed in Table 8.3-1 of Reference 1.

GEH provided the calculated peak RPV pressure, peak power, PCT, and peak suppression pool temperature for the nominal and bounding cases, and the uncertainty associated with each, in Tables 8.3-2 and 8.3-3 of Reference 1. Section 3.2.2.1 of this report discusses this issue.

The staff finds the GEH total uncertainty analysis acceptable, and GEH is consistent with Step 14 in the CSAU approach. Based on the applicant's response, RAI 21.6-36 is resolved. The staff finds each step in Element 3 to be consistent with the CSAU approach and therefore acceptable.

### 3.3 STAFF CONFIRMATORY CALCULATIONS

The staff performed independent CFD calculations using the FLUENT code to verify the GEH boron mixing and transport models and vessel bypass nodalization. In addition, the staff used MCNP to verify the TRACG04 boron reactivity models. The following sections discuss each modeled event.

#### 3.3.1 Computational Fluid Dynamics Calculations of Boron Mixing and Transport

The NRC staff conducted confirmatory CFD calculations to confirm the boron mixing and transport models used by GEH and then issued a technical evaluation report summarizing the analyses and major conclusions (Reference 36). The major conclusions from this report are described below.

The NRC has completed a confirmatory set of CFD predictions to judge the applicability of a set of GEH CFD predictions used to support the TRACG predictions of the ESBWR ATWS scenarios. The GEH CFD predictions indicate that the SLCS injection of boron into the core bypass region is effective in moving boron to the inner parts of the core. Penetration of the boron into the inner bundles is more effective than the TRACG modeling approach, which puts [[  
]].

The series of steady-state predictions that were completed to look for potential sensitivities to boundary conditions or other non-conservative modeling assumptions uncovered no significant issues. Variations in the upper surface mass inlet condition had little or no impact on the movement of boron into the inner regions of the core. The neglect of the increased specific gravity of the injected solution was also not a significant factor. The only factors that impacted the amount of boron penetrating into and building up in the core bypass were direct changes in the incoming boron mass flow or the exit mass flows from the bypass. These results are not unexpected.

The transient CFD predictions completed by the NRC agree reasonably well with the GEH predictions even though the approaches were quite different. The NRC CFD model used different material properties, geometry, turbulence modeling, wall treatments, and computational mesh along with a completely different code. The NRC predictions indicate a similar penetration rate for boron into the inner regions of the core bypass and differ only in the rate of boron accumulation and the rate of boron leakage from the GEH CFD predictions. These differences can be attributed partially to the geometric differences between the models and are not significant in light of the differences between the CFD and TRACG results, which are the ultimate subject of the GEH analyses. The principal conclusion is that the GEH CFD model is appropriate for demonstrating that the TRACG modeling approach, with the [[

]], is conservative with respect to boron mixing and penetration from the SLCS into the core bypass region.

### 3.3.2 Boron Reactivity Calculations

The staff developed MCNP input decks representative of the ESBWR lattices in support of steady-state physics calculations. The staff added boron to these lattices to compare the resulting cross sections with the ones used in TRACG using the theoretical  $1/v$  boron model. The results of these analyses are documented in a technical evaluation report (Reference 29). The results of the staff technical evaluation confirm the validity of the TRACG boron model.

The technical evaluation (Reference 29) performed a series of MCNP calculations as an independent check of the TRACG boron model by calculating the effective microscopic boron-10 cross section and the average neutron velocity for several configurations. These calculations were carried out for the appropriate assembly type (depending on axial height), for the void fraction and boron concentrations, and for four burnup levels. This resulted in a total of sixty combinations of assembly type, burnup, void fraction, and boron concentration. Based on the relationships between cross section and velocity, it is clear that the microscopic cross section should decrease with increasing average velocity. This decrease should vary inversely with velocity, but it could be modified by non- $1/v$  effects. This dependence might be closer to linear, since any variation of the boron cross section will be small compared to the variation in boron number density for this particular transient.

The average cross section and velocity were calculated over both (1) the thermal range (less than 0.625 electronvolts (eV)), and (2) the total range (0–20.0 megaelectronvolts (MeV)). The results show that, for all cases, at each height, the thermal range microscopic cross section is essentially linearly proportional to the average neutron velocity, regardless of burnup level, boron concentration, or height (implies assembly type). However, this was not the case for the cross sections averaged over the entire energy range. In this case, there were four distinct “straight” lines for each burnup level at each height. The correlation is still largely linear, but there are burnup effects that separate the lines. In addition, an effect due to height (neutron spectral effect) is evident in the cross section magnitude. The staff noted that these conclusions are valid only for the conditions encountered in the evaluated transient; thus, any possible self-shielding effects caused by significantly higher boron concentrations were not explored because they are not likely in an ESBWR ATWS event. The fast range (above 0.625 eV) microscopic cross section has essentially no correlation with average neutron velocity. The cross section values group themselves into distinct groups (as a function of burnup) with no easily identifiable correlation.

Furthermore, the average macroscopic thermal range cross section can be determined by multiplying the microscopic cross section by the boron number density at the time of interest. The variation of the macroscopic cross section with average velocity for the thermal range shows an increasing cross section with increasing boron concentration (and time into the transient), regardless of height or burnup. The increase is essentially linear, with a slightly different slope, depending on burnup.

## 4.0 **CONDITIONS AND LIMITATIONS**

The staff has identified the following specific conditions that will be applied to NEDE-33083P, Supplement 2, Revision 2, (Reference 1):



ESBWR TRACG ATWS analyses (including the 350-psi (2413 Kilopascal) critical pressure penalty) contained in the NRC staff evaluation of GEH's 10 CFR Part 21 report (Appendix F to the SE for NEDC-33173P (Agencywide Documents Access and Management System (ADAMS) Accession No. ML073340214) are applicable to this SE. The NRC must approve the use of other methods or analysis strategies for the ESBWR design.

## 5.0 CONCLUSIONS

The staff concludes that the ATWS analysis methodology documented in NEDE-33083P, Supplement 2, Revision 2, (Reference 1), is an acceptable way to employ the TRACG04 code to demonstrate compliance with the regulatory requirements for ESBWR ATWS events. The staff finds that the ATWS methodology and the TRACG04 code comply with all three elements of the CSAU methodology to calculate best-estimate results and estimate their uncertainty.

## 6.0 REFERENCES

1. NEDE-33083P, Supplement 2, Revision 2, "TRACG Application for ESBWR Anticipated Transient Without Scram Analyses," September 2009. (ADAMS Accession No. ML092750618)
2. NEDC-33083P-A, MFN 05-017, "TRACG Application for ESBWR," March 2005. (ADAMS Accession No. ML051390265)
3. NEDE-32906P, Supplement 1-A, "TRACG Application for Anticipated Transient Without Scram Overpressure Transient Analysis," November 2003. (ADAMS Accession No. ML033381102)
4. Final Safety Evaluation Report By the Office of NRR Licensing Topical Report NEDE-32906P, Supplement 3, "Migration To TRACG04/PANAC11 From TRACG02/PANAC10 For TRACG AOO And ATWS Overpressure Transients General Electric Hitachi Nuclear Energy Americas, LLC, July 10, 2009(ADAMS Accession No. ML0917511021), GE Hitachi Letter MFN 10-137, Add NEDE-32906P, Supplement 3, "Migration To TRACG04/PANAC11 From TRACG02/PANAC10 For TRACG AOO And ATWS Overpressure Transients," to ESBWR Docket, dated March 31, 2010 (ADAMS Accession No. ML100900085)
5. NEDE-33083P, Supplement 1, "Safety Evaluation Report Regarding the Application of General Electric's Topical Report, 'TRACG Application for ESBWR Stability Analysis'" (TAC MC3288). (ADAMS Accession Nos. ML060890075 and ML061000463)
6. Safety Evaluation Report for NEDE-33083P, Supplement 3, "Application of the TRACG Computer Code to the Transient Analysis for the Economic Simplified Boiling Water Reactor Design", July 2010. (ADAMS Accession No. ML100270024)
7. NEDE-32906P-A, Revision 2, MFN 06-046, "TRACG Application for Anticipated Operational Occurrences (AOO) Transient Analysis," February 28, 2006. (ADAMS Accession Nos. ML060530571 and ML060530575)

8. J. Spore (ISL), Information Systems Lab (ISL), ISL-NSAD-TR-07-02, "Technical Evaluation Review of TRACG Applications to ESBWR ATWS," January 2007 (ADAMS Accession No. ML080040449).
9. NUREG-0800, Revision 2 "Standard Review Plan for the Review of Safety Analysis Reports for Nuclear Power Plants, LWR Edition," Section 15.8, March 2007 (ADAMS Accession No. ML070570008).
10. NUREG/CR-5249, "Quantifying Reactor Safety Margins: Application of Code Scaling, Applicability, and Uncertainty Evaluation Methodology to a Large-Break, Loss-of-Coolant Accident," December 1989. (ADAMS Accession No. ML070310119)
11. NEDC-33079P, Revision 1, Supplement 1, "ESBWR Test and Analysis Program Description, Discussion of PIRT Parameters," March 2005. (ADAMS Accession No. ML051390233)
12. Letter from D.H. Hinds (GE) to NRC, MFN 06-301, "Response to Portion of NRC Request for Additional Information Letter No. 31 and NRC Letter No. 57 Related to ESBWR Design Certification Application—TRACG Application for ESBWR ATWS—RAI Numbers 21.6-4, 21.6-12, 21.6-27 through 21.6-29, 21.6-36 through 21.6-38, 21.6-42, 21.6-45, 21.6-46, and 21.6-52," September 6, 2006. (ADAMS Accession No. ML062650237)
13. Safety Evaluation Report for Global Nuclear Fuel, Licensing Topical Report NEDC-33239P, "GE14 for ESBWR Nuclear Design Report." July 2010 (ADAMS Accession No. ML101650747)
14. NEDO-32176P, Revision 1, "TRACG Model Description," March 1996. (ADAMS Legacy No. 9604220045)
15. NEDE-32176P, Revision 3, "TRACG Model Description," April 2006. (ADAMS Accession No. ML061160238)
16. NEDE-32177P, Revision 2, "TRACG Qualification," January 2000. (ADAMS Accession No. ML003683162)
17. MFN 04-059, "Update of ESBWR TRACG Qualification for NEDC-32725P and NEDC-33080P Using the 9-Apr-2004 Program Library Version of TRACG04," June 6, 2004. (ADAMS Accession No. ML041610037)
18. Letter from D.H. Hinds (GE) to NRC, "General Electric Company—ESBWR Standard Plant Design Revision 2 to Design Control Document Tier 2, Chapters 2 through 5, 7 through 15, 17, and 18," October 31, 2006. (ADAMS Accession No. ML063100233)
19. NEDC-33079P, Revision 1, "ESBWR Test and Analysis Program Description," March 2005. (ADAMS Accession No. ML051390233)
20. Addendum to the Safety Report for NEDC-33083P, "Application of the TRACG Computer Code to the ECCS and Containment LOCA Analysis for the ESBWR Design," December 2, 2009. (ADAMS Accession No. ML093380597)

21. Letter from M.C. Barillas (NRC) to D.H. Hinds (GE), "Request for Additional Information Letter No. 31 Related to ESBWR Design Certification Application," June 23, 2006. (ADAMS Accession No. ML061740028)
22. Letter from D.H. Hinds (GE) to NRC, MFN 06-324, "Response to Portion of NRC Request for Additional Information Letter No. 31 Related to ESBWR Design Certification Application—TRACG Application for ESBWR ATWS—RAI Numbers 21.6-4 and 21.6-50, September 18, 2006. (ADAMS Accession No. ML062720032)
23. NEDE-22267, Class III, "Test Report Three-Dimensional Boron Mixing Model," Proprietary Information, General Electric Co., October 1982. (ADAMS Accession No. ML101120970)
24. Letter from D.H. Hinds (GE) to NRC, MFN 06-232, "Response to Portion of NRC Request for Additional Information Letter No. 31 Related to ESBWR Design Certification Application—TRACG Application for ESBWR ATWS—RAI Numbers 21.5-1, 21.6-5, 21.6-6, 21.6-9, 21.6-33, 21.6-39, 21.6-40, and 21.6-47," July 24, 2006. (ADAMS Accession No. ML062230247)
25. Letter from D.H. Hinds (GE) to NRC, MFN 06-301, "Response to Portion of NRC Request for Additional Information Letter No. 31 and NRC Letter No. 57 Related to ESBWR Design Certification Application -TRACG Application for ESBWVR ATWS RAI Numbers 21.6-4,21.6-12,21.6-27 through 21.6-29,21.6-36 through 21.6-38,21.6-42,21.6-45,21.6-46 and 21.6-52," September 6, 2006. (ADAMS Accession Nos. ML062650246, ML062650248, ML070810043, ML073130588)
26. Letter from S.A. Williams (NRC) to D.H. Hinds (GE), "Request for Additional Information Letter No. 85 related to ESBWR Design Certification Application," January 17, 2007. (ADAMS Accession No. ML070080448)
27. Letter from R.E. Kingston to NRC, MFN 08-698, "Response to Portion of NRC Request of Additional Information Letter No. 225, Related to ESBWR Design Certification Application RAI Number 21.6-100 S02," September 24, 2008. (ADAMS Accession No. ML082700557)
28. Letter from R.E. Kingston to NRC, MFN 08-713, "Response to Portion of NRC Request for Additional Information Letter No. 156 Related to ESBWR Design Certification Application—Emergency Core Cooling Systems—RAI Number 6.3-54 S01," September 22, 2008. (ADAMS Accession Nos. ML082680145 and ML082680144)
29. Letter from D.H. Hinds (GE) to NRC, MFN 06-408, "Response to Portion of NRC Request for Additional Information Letter No. 31 Related to ESBWR Design Certification Application—TRACG Application for ESBWR ATWS—RAI Numbers 21.6-34, 21.6-35, 21.6-43, and 21.6-48," October 19, 2006. (ADAMS Accession No. ML063200120)
30. H. Ludewig, A. Aronson, and A. Mallen, "MCNP Validation of the TRACG Boron Reactivity Model for the ESBWR," Brookhaven National Laboratory, July 2010 (See Appendix C of SER for LTRs NEDC-33239P and NEDC-33197P). (ADAMS Accession Nos. ML101670068, ML101720671, ML101670050)

31. NEDE-32177P, Revision 3, "TRACG Qualification," August 2007. (ADAMS Accession Nos. ML072480083 and ML072480089)
32. Letter from J.C. Kinsey (GE) to NRC, MFN 07-255, "Response to Portion of NRC Request for Additional Information Letter No. 31—RAI Numbers 21.6-8 and 21.6-41," May 21, 2007. (ADAMS Accession No. ML071770364)
33. Letter from J.C. Kinsey (GE) to NRC, MFN 07-448, "Response to Portion of NRC Request for Additional Information Letter No. 66 Related to ESBWR Design Certification Application RAI Numbers 2 1.6-63, 2 1.6-78, 2 1.6-81, 2 1.6-83," August 20, 2007. (ADAMS Accession Nos. ML072350147 and ML072350152)
34. NEDC-32725P, Revision 1, "TRACG Qualification for SBWR," August 30, 2002. (ADAMS Accession Nos. ML022560558 and ML022560559)
35. Letter from J.C. Kinsey (GE) to NRC, MFN 06-339/S2, "Response to Portion of NRC Request for Additional Information Letter No. 56—ATWS—RAI Number 21.6-77S02," March 22, 2007. (ADAMS Accession No. ML070860260)
36. Christopher F. Boyd, Office of Nuclear Regulatory Research, Nuclear Regulatory Commission, "Boron Mixing in Core Bypass Region of ESBWR during ATWS: Confirmatory CFD Predictions," Technical Evaluation Report, April 2008. (ADAMS Accession No. ML081080311)
37. Final Safety Evaluation Report for GEH Topical Reports NEDC-33239P, Revision 4, 'GE14 for ESBWR Nuclear Design Report' and NEDE-33197P, Revision 4, 'Gamma Thermometer System for LPRM Calibration and Power Shape Monitoring,'" July 2010. (ADAMS Accession Nos. ML101670068, ML101720671, ML101670050)
38. ESBWR Final Evaluation Report (FSER) Chapter 15, June 2010 (ADAMS Accession No. ML101650500)
39. Letter from David H Hinds (GE) to NRC, MFN 06-324, "Response to NRC Request for Additional Information Related to ESBWR DC Application, RAI Number 21.6-44," September 18, 2006(ADAMS Accession No. ML0627200342)
40. Letter from Richard E. Kingston to NRC, MFN 08-659, "Response to NRC Request for Additional Information Related to ESBWR DC Application, RAI Number 21.6-44, S01," September 4, 2008(ADAMS Accession No. ML0825304511)
41. Letter from Richard E. Kingston to NRC, MFN 10-295, "Transmittal of Additional Information Regarding the Hot Rod Model in ESBWR ATWS Analyses – "TRACG Application for ESBWR Anticipated Transient Without Scram Analyses," NEDE-33083P, Supplement 2, Revision 2, September 30, 2010 (ADAMS Accession No. ML102770396)